AIRCRAFT ENGINE: DESIGN AND ANALYSIS



Haifa El-Sadi

Wentworth Institute of Technology



Jet Engine: Design and Analysis

Haifa El-Sadi

Wentworth Institute of Technology

This text is disseminated via the Open Education Resource (OER) LibreTexts Project (https://LibreTexts.org) and like the thousands of other texts available within this powerful platform, it is freely available for reading, printing, and "consuming."

The LibreTexts mission is to bring together students, faculty, and scholars in a collaborative effort to provide an accessible, and comprehensive platform that empowers our community to develop, curate, adapt, and adopt openly licensed resources and technologies; through these efforts we can reduce the financial burden borne from traditional educational resource costs, ensuring education is more accessible for students and communities worldwide.

Most, but not all, pages in the library have licenses that may allow individuals to make changes, save, and print this book. Carefully consult the applicable license(s) before pursuing such effects. Instructors can adopt existing LibreTexts texts or Remix them to quickly build course-specific resources to meet the needs of their students. Unlike traditional textbooks, LibreTexts' web based origins allow powerful integration of advanced features and new technologies to support learning.



LibreTexts is the adaptable, user-friendly non-profit open education resource platform that educators trust for creating, customizing, and sharing accessible, interactive textbooks, adaptive homework, and ancillary materials. We collaborate with individuals and organizations to champion open education initiatives, support institutional publishing programs, drive curriculum development projects, and more.

The LibreTexts libraries are Powered by NICE CXone Expert and were supported by the Department of Education Open Textbook Pilot Project, the California Education Learning Lab, the UC Davis Office of the Provost, the UC Davis Library, the California State University Affordable Learning Solutions Program, and Merlot. This material is based upon work supported by the National Science Foundation under Grant No. 1246120, 1525057, and 1413739.

Any opinions, findings, and conclusions or recommendations expressed in this material are those of the author(s) and do not necessarily reflect the views of the National Science Foundation nor the US Department of Education.

Have questions or comments? For information about adoptions or adaptions contact info@LibreTexts.org or visit our main website at https://LibreTexts.org.

The LibreTexts name, logo, and book covers are trademarked by LibreTexts, Inc. (a 501(c)(3) not-for-profit organization) and protected against unauthorized use.

This text was compiled on 11/18/2026

TABLE OF CONTENTS

Licensing

1: Introduction to Compressible Flow

1.0: Fundamentals of Compressible Flow

1.1: Ideal Gas Relations

1.2: Thermodynamic Entropy Relations (Tds Equations)

1.3: Isentropic Relations

1.4: Integral Formulations via Reynolds Transport Theorem (RTT)

1.5: Compressible Flow Relationships

1.6: Problems and References

2: Compressible Flow With Heat Addition

2.0: Introduction

2.1: Subsonic, sonic and supersonic flow

2.2: Rayleigh flow

2.3: Problems and References

3: Aircraft Engines- Reciprocating Engine

3.0: Introduction

3.1: Aircraft Piston Engine

3.2: Volumetric Efficiency

3.3: Problems and References

4: Aircraft Engine- Gas Turbine Engine

4.0: Introduction

4.1: Gas Generator Components

4.2: On/Off Design Analysis

4.3: Turbojet

4.4: Turbofan Engine

4.5: Turboprop Engine

4.6: Problems and References

5: Compressor and Turbines

5.0: Introduction

5.1: Axial-Flow Turbomachinery

5.2: Radial / Centrifugal Turbomachinery

5.4: Problems and References

6: Combustor- Working Fluid and Models of Engine Cycles

6.0: Working Fluid Dynamics

6.1: Thermodynamic and Chemical Evolution of Working Fluids

6.2: Thermodynamics Relations for Engine Process

6.3: Problems and References

7: Engine Heat Transfer

7.0: Introduction

7.1: Heat transfer and Engine energy balance

7.2: Convective heat transfer

7.3: Radiative Heat Transfer

7.4: Problems and References

Index

Glossary

Detailed Licensing

This page titled Aircraft Engine: Design and Analysis is shared under a CC BY 4.0 license and was authored, remixed, and/or curated by Haifa El-Sadi.

Licensing

A detailed breakdown of this resource's licensing can be found in ***Back Matter/Detailed Licensing***.

This page titled Licensing is shared under a CC BY 4.0 license and was authored, remixed, and/or curated by Haifa El-Sadi.

1: INTRODUCTION TO COMPRESSIBLE FLOW

1.0: Fundamentals of Compressible Flow
1.1: Ideal Gas Relations
1.2: Thermodynamic Entropy Relations (Tds Equations)
1.3: Isentropic Relations
1.4: Integral Formulations via Reynolds Transport Theorem (RTT)
1.5: Compressible Flow Relationships
1.6: Problems and References

This page titled 1: Introduction to Compressible Flow is shared under a CC BY 4.0 license and was authored, remixed, and/or curated by Haifa El-Sadi.

1.0: Fundamentals of Compressible Flow

In fluid mechanics, a flow is treated as compressible when variations in fluid mass density significantly alter system dynamics. These density fluctuations generally become non-negligible when local flow velocities represent a notable fraction of the speed of sound (a). This motion is non-dimensionalized by the Mach number (Ma):

$$Ma = \frac{V}{a}$$

By standard convention, density changes must be explicitly calculated whenever the Mach number exceeds 0.3 ($Ma > 0.3$).

As a rule of thumb, when the Mach number exceeds **0.3** ($\mathrm{Ma} > 0.3$), the flow can no longer be treated as incompressible, and density changes must be explicitly accounted for.

To keep analytical formulations tractable while preserving key physical behavior, the following primary assumptions are routinely adopted:

1. Time-invariant state (steady state): Fluid properties at a given spatial location do not change over time ($\partial/\partial t = 0$).
2. One-dimensional transport: State variables vary along a single spatial dimension.
3. Uniform viscosity: Dynamic fluid viscosity remains constant across the domain.
4. Ideal gas behavior: The working medium adheres to the classical ideal gas thermodynamic state relations

This page titled 1.0: Fundamentals of Compressible Flow is shared under a CC BY 4.0 license and was authored, remixed, and/or curated by Haifa El-Sadi.

1.1: Ideal Gas Relations

The state of an ideal gas is governed by the ideal gas equation of state:

$$PV = nR_uT$$

Where $n = \frac{m}{M}$ represents the number of moles (mass m divided by molecular weight M), and R_u is the universal gas constant. Defining the specific gas constant as $R = \frac{R_u}{M}$, the equation simplifies to:

$$PV = mRT \qquad \Longrightarrow \qquad Pv = RT$$

Where $v = \frac{V}{m}$ is the specific volume, P is absolute pressure, and T is absolute temperature.

For an ideal gas, internal energy (u) is purely a function of temperature. The specific heat at constant volume (C_v) is defined as:

$$C_v = \frac{du}{dT} \qquad \Longrightarrow \qquad u_2 - u_1 = C_v\,(T_2 - T_1)$$

Similarly, specific enthalpy (h) is related to temperature via specific heat at constant pressure (C_p):

$$dh = C_p dT$$

By definition, specific enthalpy is given by:

$$h = u + Pv = u + RT$$

Differentiating both sides with respect to temperature (T):

$$\frac{dh}{dT} = \frac{du}{dT} + R\frac{dT}{dT} \qquad \Longrightarrow \qquad C_p = C_v + R$$

The ratio of specific heats, denoted as k (or γ), plays a fundamental role in gas dynamics:

$$k = \frac{C_p}{C_v}$$

This page titled 1.1: Ideal Gas Relations is shared under a CC BY 4.0 license and was authored, remixed, and/or curated by Haifa El-Sadi.

1.2: Thermodynamic Entropy Relations (Tds Equations)

Applying the First Law of Thermodynamics to a reversible process yields the first canonical Tds relationship:

$$Tds = du + Pdv$$

Since enthalpy is defined as $h = u + Pv$, taking its differential yields $dh = du + Pdv + vdP$. Rearranging gives:

$$du = dh - vdP$$

Substituting du back into the first Tds relation provides the second alternative form:

$$Tds = dh - vdP$$

Expressing these equations in terms of temperature, pressure, and volume using $du = C_v dT$, $dh = C_p dT$, and $Pv = RT$, integration between two thermodynamic states (1 and 2) yields:

$$s_2 - s_1 = C_v \ln\left(\frac{T_2}{T_1}\right) + R \ln\left(\frac{v_2}{v_1}\right)$$

$$s_2 - s_1 = C_p \ln\left(\frac{T_2}{T_1}\right) - R \ln\left(\frac{P_2}{P_1}\right)$$

This page titled 1.2: Thermodynamic Entropy Relations (Tds Equations) is shared under a CC BY 4.0 license and was authored, remixed, and/or curated by Haifa El-Sadi.

1.3: Isentropic Relations

If a flow process is both **adiabatic** ($q = 0$) and **frictionless** (reversible), it is defined as **isentropic** ($s_2 - s_1 = 0$).

Setting entropy change to zero in the Tds equations give:

$$0 = C_v \ln\left(\frac{T_2}{T_1}\right) + R \ln\left(\frac{v_2}{v_1}\right)$$

$$0 = C_p \ln\left(\frac{T_2}{T_1}\right) - R \ln\left(\frac{P_2}{P_1}\right)$$

Manipulating these expressions through the relations $R = C_p - C_v$ and $k = C_p/C_v$ leads directly to the standard isentropic state relations:

$$\frac{P_2}{P_1} = \left(\frac{T_2}{T_1}\right)^{\frac{k}{k-1}}$$

$$\frac{T_2}{T_1} = \left(\frac{\rho_2}{\rho_1}\right)^{k-1}$$

Where $\rho = \frac{1}{v}$ is the fluid density.

This page titled 1.3: Isentropic Relations is shared under a CC BY 4.0 license and was authored, remixed, and/or curated by Haifa El-Sadi.

1.4: Integral Formulations via Reynolds Transport Theorem (RTT)

To evaluate fluid mechanics within a fixed spatial boundary (Eulerian viewpoint) rather than tracking fixed fluid masses (Lagrangian viewpoint), we utilize the Reynolds Transport Theorem. For any extensive property B and its corresponding intensive property $\beta = \frac{dB}{dm}$, RTT states:

$$\frac{dB_{\text{sys}}}{dt} = \frac{\partial}{\partial t}\int_{\text{CV}} \rho\beta dV + \int_{\text{CS}} \rho\beta\left(\vec{V}\cdot\hat{n}\right)dA$$

where:

- CV represents the Control Volume.
- CS represents the Control Surface.
- $\hat{n}$ is the outward pointing unit normal vector to control surface.
- $\vec{V}$ is the fluid velocity vector relative to the control surface.

1.5.1 Continuity Equation (Conservation of Mass)

Setting $B = m$ (mass) means $\beta = 1$. Since system mass is conserved ($\frac{dm_{\text{sys}}}{dt} = 0$):

Mass is conserved within a closed system:

$$\frac{dm_{\text{sys}}}{dt} = 0$$

Applying RTT with $B = m$ and $\beta = 1$:

$$\frac{dm_{\text{sys}}}{dt} = \frac{\partial}{\partial t}\int_{\text{CV}} \rho dV + \int_{\text{CS}} \rho\left(\vec{V}\cdot\hat{n}\right)dA = 0$$

1. For a steady, one-dimensional stream with a single entrance [GrindEQ__1_] and exit [GrindEQ__2_]: $\frac{\partial}{\partial t}\int_{\text{CV}} \rho dV = 0$
2. $-\rho_1 A_1 V_1 + \rho_2 A_2 V_2 = 0$

1.5.2 Linear Momentum Balance

Setting $B = \mathbf{P} = m\mathbf{V}$ (linear momentum) means $\beta = \mathbf{V}$. By Newton's Second Law ($\frac{d\mathbf{P}_{\text{sys}}}{dt} = \mathbf{F}_{\text{net}}$):

The rate of change of linear momentum equals the sum of external forces acting on the system:$\frac{d\vec{P}_{\text{sys}}}{dt} = \sum \vec{F}$

Applying RTT with $B = \vec{P}$ and $\beta = \vec{V}$:

$$\sum \vec{F} = \frac{\partial}{\partial t}\int_{\text{CV}} \rho\vec{V} dV + \int_{\text{CS}} \rho\vec{V}\left(\vec{V}\cdot\hat{n}\right)dA$$

For steady ($\frac{\partial}{\partial t} = 0$) and 1D entry/exit:

$$\sum \vec{F} = \dot{m}\left(\vec{V}_2 - \vec{V}_1\right)$$

Accounting for pressure and wall shear forces along the primary flow axis:

$$P_1 A_1 - P_2 A_2 + F_{\text{net, wall}} = \dot{m}\,(V_2 - V_1)$$

1.5.3 Conservation of Energy

Setting $B = E$ (total energy) means $\beta = e = u + \frac{V^2}{2} + gz$. By the First Law of Thermodynamics ($\frac{dE_{\text{sys}}}{dt} = \dot{Q} - \dot{W}$):

Applying RTT with $B = E$ and $\beta = e$:

$$\dot{Q} - \dot{W} = \frac{\partial}{\partial t}\int_{\text{CV}} \rho e dV + \int_{\text{CS}} \rho e \left(\vec{V}\cdot\hat{n}\right) dA$$

Splitting work into shaft work (W ̇_"shaft") and pressure flow work (W ̇_"flow"), and using specific enthalpy h=u+P/\rhoup:

$$\dot{W}_{\text{flow}} = \int_{\text{CS}} P\left(\vec{V}\cdot\hat{n}\right) dA$$

$$\dot{Q} - \dot{W}_{\text{shaft}} = \frac{\partial}{\partial t}\int_{\text{CV}} \rho e dV + \int_{\text{CS}} \left(e + \frac{P}{\rho}\right)\rho\left(\vec{V}\cdot\hat{n}\right) dA$$

Replacing $e = u + \frac{V^2}{2} + gz$ and using specific enthalpy $h = u + \frac{P}{\rho} = u + Pv$:

$$\dot{Q} - \dot{W}_{\text{shaft}} = \frac{\partial}{\partial t}\int_{\text{CV}} \rho e dV + \int_{\text{CS}} \left(h + \frac{V^2}{2} + gz\right)\rho\left(\vec{V}\cdot\hat{n}\right) dA$$

For steady, adiabatic ($\dot{Q} = 0$), no shaft work ($\dot{W}_{\text{shaft}} = 0$), and negligible elevation changes ($\Delta z \approx 0$):

$$0 = \dot{m}\left(h_2 + \frac{V_2^2}{2}\right) - \dot{m}\left(h_1 + \frac{V_1^2}{2}\right)$$

$$h_1 + \frac{V_1^2}{2} = h_2 + \frac{V_2^2}{2} = h_0 = \text{constant}$$

Where h_0 is defined as the total enthalpy or stagnation enthalpy of the flow.

This page titled 1.4: Integral Formulations via Reynolds Transport Theorem (RTT) is shared under a CC BY 4.0 license and was authored, remixed, and/or curated by Haifa El-Sadi.

1.5: Compressible Flow Relationships

Six primary analytical relations govern compressible flow evaluations. These equations evaluate local state properties at a specific cross-section, rather than comparing states across two locations.

1.6.1 Total or Stagnation Temperature

The stagnation temperature Tt represents the fluid temperature attained when a stream at Mach number (Ma) is brought to rest adiabatically:

Extra \left or missing \right

The bracketed term $\frac{k-1}{2}Ma^2$ represents the ratio of dynamic kinetic energy to internal thermal energy in the moving stream.

1.6.2 Total or Stagnation Pressure

The stagnation pressure $P\mathrm{t}$ is the pressure achieved if the flow is decelerated to rest isentropically:

Extra \left or missing \right

This illustrates that flow decelerations raise pressure without mechanical compressors. Aircraft engines like ramjets and scramjets rely entirely on this freestream deceleration to achieve operating compression ratios.

1.6.3 Total Pressure Mass Flow Parameter (MFP)

Combining continuity with ideal gas laws, speed of sound, and stagnation relations yields the total pressure mass flow parameter:

MFP = $\frac{\dot{m}\sqrt{Tt}}{PtA}$

MFP help to calculate throat areas required for flow choking ($Ma = 1$). Because MFP depends exclusively on local Mach number and gas properties, it is widely tabulated. Note that a given MFP value corresponds to two distinct Mach numbers (one subsonic and one supersonic), reaching its theoretical maximum at $Ma = 1$ at which the flow is choked or sonic and the flow per unit area is the greatest.

1.6.4Static Pressure Mass Flow Parameter

Expressed using local static pressure, the static mass flow parameter is given by:

$$\mathrm{MF}_p = \frac{\dot{m}\sqrt{Tt}}{PA}$$

This form is preferred in experimental setups where static pressure measurements are more accessible. Unlike MFP, each MF_p value maps uniquely to a single Mach number, allowing direct algebraic resolution

1.6.5 Impulse Function (I)

The impulse function quantifies total axial momentum flux and pressure forces:

$$I = PA + \dot{m}V = PA(1 + kMa^2)$$

Net force calculations across propulsion components simplify to the change in impulse function across the control volume $\Delta I = I_{exit} - I_{entry}$, avoiding complex surface integrations over engine geometry.

1.6.6 Dynamic Pressure

Dynamic pressure scales fluid inertial forces relative to static pressures. The dynamic pressure q is given by the expression:

$$P = \frac{1}{2}\rho V^2$$

It serves as the reference dynamic pressure across incompressible, compressible, and hypersonic regimes.

1.6.7 Ratio of Specific Heats

Engineers must select the specific heat ratio carefully so mathematical models align with real-world gas dynamics. In practice, two widely accepted estimates are k = 1.33 for temperatures from 2500 to 3000° R, and k = 1.30 for 3000 to 3500° R.

This page titled 1.5: Compressible Flow Relationships is shared under a CC BY 4.0 license and was authored, remixed, and/or curated by Haifa El-Sadi.

1.6: Problems and References

Problem Statement:

A liquid rocket combustion chamber receives continuous mass inputs of $\dot{m}_{\mathrm{H2}} = 4.5\ \mathrm{kg/s}$ of liquid hydrogen and $\dot{m}_{\mathrm{O2}} = 36.0\ \mathrm{kg/s}$ of liquid oxygen are continuously injected into the combustion chamber Exhaust products discharge uniformly through an exit nozzle with diameter $D_e = 0.42\ \mathrm{m}$. Write the mass conservation equation for the combustion chamber.

Assuming an exhaust gas density of $\rho_e = 0.28\ \mathrm{kg/m^3}$ at the exit section, compute the exit velocity V_e.

Problem 2

Problem Statement:

A rocket engine undergoing static bench testing exhausts combustion gases at $\dot{m} = 15\ \mathrm{kg/s}$ with a uniform exit velocity of $V_e = 1200\ \mathrm{m/s}$ and exit area $A_e = 0.018\ \mathrm{m^2}$. Static exit pressure is measured at $P_e = 35\ \mathrm{kPa}$ relative to an ambient pressure $P_{\mathrm{atm}} = 101.3\ \mathrm{kPa}$. Determine the total axial thrust F_{thrust} registered by the test mount.

Problem 3

Problem Statement:

A turbojet engine flies at an altitude of $10,000\ \mathrm{m}$ ($\rho_1 = 0.413\ \mathrm{kg/m^3}$). Air enters the intake ($D_1 = 0.95\ \mathrm{m}$) at $V_1 = 220\ \mathrm{m/s}$. Exhaust gases exit ($D_2 = 0.45\ \mathrm{m}$) at $V_2 = 680\ \mathrm{m/s}$ with a density $\rho_2 = 0.510\ \mathrm{kg/m^3}$. Assuming steady, uniform state conditions, determine the required fuel mass flow rate $\dot{m}_{\mathrm{fuel}}$ in $\mathrm{kg/s}$.

Problem 4

Problem Statement:

Air ($R = 0.287\ \mathrm{kJ/kg \cdot K}, C_p = 1.005\ \mathrm{kJ/kg \cdot K}$) enters a steady compressor at $P_1 = 1.2\ \mathrm{bar}$, $T_1 = 290\ \mathrm{K}$, and $V_1 = 25\ \mathrm{m/s}$ through an inlet area $A_1 = 0.85\ \mathrm{m^2}$. At the outlet, velocity drops to $V_2 = 12\ \mathrm{m/s}$ and enthalpy increase to $h_2 = 490\ \mathrm{kJ/kg}$. Heat dissipates to the environment at $\dot{Q}_{\mathrm{loss}} = 350\ \mathrm{kJ/min}$. Calculate the required power input $\dot{W}_{\mathrm{in}}$ in kW.

Problem 5

Problem Statement:

Hydrogen gas expands adiabatically from a large stagnant reservoir ($P_0 = 650\ \mathrm{kPa}$, $T_0 = 480\ \mathrm{K}$, $V_0 \approx 0$) through a convergent-divergent nozzle. Static pressure at the exit plane is $P_e = 120\ \mathrm{kPa}$ with exit area $A_e = 350\ \mathrm{cm^2}$. Taking $C_p = 14.307\ \mathrm{kJ/kg \cdot K}$ and $k = 1.41$:

1. Calculate the exhaust velocity V_e.
2. Compute the total mass flow rate $\dot{m}$.

This page titled 1.6: Problems and References is shared under a CC BY 4.0 license and was authored, remixed, and/or curated by Haifa El-Sadi.

2: COMPRESSIBLE FLOW WITH HEAT ADDITION

2.0: Introduction
2.1: Subsonic, sonic and supersonic flow
2.2: Rayleigh flow
2.3: Problems and References

This page titled 2: Compressible Flow With Heat Addition is shared under a CC BY 4.0 license and was authored, remixed, and/or curated by Haifa El-Sadi.

2.0: Introduction

Rayleigh flow is named after John Strutt, 3rd Baron Rayleigh, an English physicist who formulated the foundations of 1D compressible wave propagation in the late 19th century. While ideal Rayleigh flow relies on simplifying assumptions (such as a constant-area duct), it serves as a baseline tool in high-speed propulsion. It is used in jet engine combustion chambers to model the baseline pressure drop and temperature rise of air as fuel burns. It is also applied to analyze afterburners—specifically the secondary injection and burning of fuel in supersonic military aircraft engines—to calculate maximum extra thrust and prevent choking. Additionally, it is crucial for evaluating thermal choking limits and the maximum critical fuel-to-air ratio at high supersonic and hypersonic speeds in ramjet and scramjet combustors. Finally, Rayleigh flow helps estimate compressible flow characteristics and fundamental pressure losses in industrial heat exchangers and process piping.

In fluid mechanics, the behavior of a moving gas depends strongly on how fast it moves relative to the speed of sound. This ratio is the Mach number, $Ma = V/a$, where V is the flow velocity and $a = \sqrt{kRT}$ is the local speed of sound. When Ma is above roughly 0.3, density changes become significant and the flow must be treated as compressible.

This page titled 2.0: Introduction is shared under a CC BY 4.0 license and was authored, remixed, and/or curated by Haifa El-Sadi.

2.1: Subsonic, sonic and supersonic flow

The Mach number divides compressible flow into three regimes as shown in Figure 1, each with different behavior:

1. **Subsonic flow (Ma $<$ 1):** Pressure disturbances travel faster than the flow, so they propagate upstream and the fluid "senses" obstacles ahead of it. In a converging duct the flow accelerates and its pressure drops, as in incompressible flow.
2. **Sonic flow (Ma = 1):** The flow speed equals the local speed of sound. This is the boundary between the two regimes and often occurs at the throat of a nozzle, where the flow is said to be *choked*. Further downstream conditions can no longer change the mass flow rate.
3. **Supersonic flow (Ma $>$ 1):** The flow outruns pressure disturbances, so information cannot travel upstream. Abrupt changes occur through shock waves, and the flow behaves opposite to the subsonic case. A diverging duct accelerates it and a converging duct decelerates it.

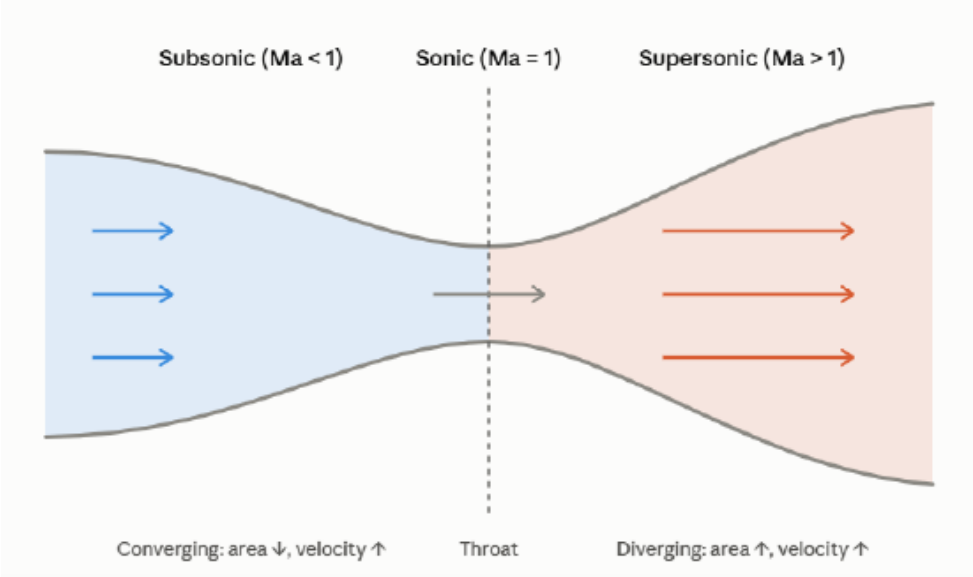


Figure 1. converging–diverging (de Laval) nozzle

For $Ma < 1$ the flow speeds up as the area shrinks. For $Ma > 1$ it speeds up as the area grows. This is why a rocket nozzle converges to a throat and then diverges. To calculate the mass flow rate, we need to know the local flow area A, the local Mach number Ma, the local total pressure pt and total temperature Tt, and the gas properties k and R. Total temperature stays constant in adiabatic flow with no shaft work, and total pressure stays constant in isentropic flow with no shaft work. In steady flow the mass flow rate must be the same at every section of a duct. We express this as a dimensionless area ratio, using the sonic flow area A^*, which is the area where $Ma = 1$:

$$\frac{A}{A^*} = \frac{1}{Ma}\left[\frac{1+\frac{k-1}{2}Ma^2}{\frac{k+1}{2}}\right]^{\frac{k+1}{2\,(k-1)}}$$

This page titled 2.1: Subsonic, sonic and supersonic flow is shared under a CC BY 4.0 license and was authored, remixed, and/or curated by Haifa El-Sadi.

2.2: Rayleigh flow

Rayleigh flow describes steady, one-dimensional, frictionless flow of a perfect gas through a constant-area duct with heat transfer as shown in Figure 2. It is a model for combustion chambers, afterburners and ramjet combustors, where the dominant effect is heat addition rather than area change or friction.

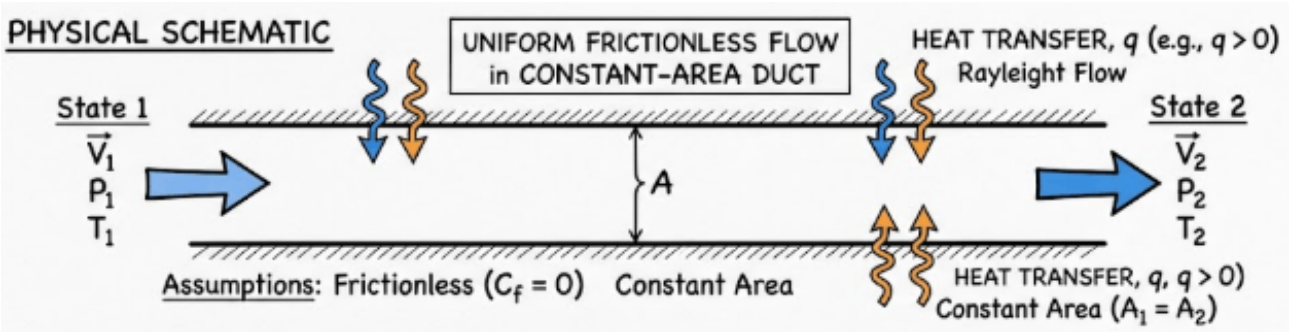


Figure 2. schematic of Rayleigh flow

Its main features are:

- Heat addition drives the flow toward $Ma = 1$ adding heat to a subsonic flow accelerates it. Adding heat to a supersonic flow decelerates it. Either way the Mach number approaches 1.
- Thermal choking, once $Ma = 1$ is reached, no more heat can be added without changing the upstream conditions. This sets the maximum heat input for a given inlet state.
- Cooling has the opposite effect; it moves the flow away from $Ma = 1$.
- Adding heat to a flowing fluid causes a irreversible drop in total (stagnation) pressure (p_0), often referred to as fundamental pressure loss or Rayleigh loss, even in the complete absence of wall friction.

2.2.1 Governing Conservation Equations

For uniform, frictionless flow of a perfect gas in a constant-area duct with heat transfer rate $\dot{Q}$:

1. Continuity Equation:

$$\rho_1 u_1 = \rho_2 u_2$$

2. Momentum Equation:

$$p_1 + \rho_1 u_1^2 = p_2 + \rho_2 u_2^2 \Longrightarrow I_1 = I_2$$

In Rayleigh flow, the fluid impulse function I remains constant along the flow direction due to the frictionless assumption. Accounting for heat transfer across the duct boundary, the energy balance for the fluid is expressed as:

$$\dot{m}\,(h_{t2} - h_{t1}) = \dot{Q}$$

Because mass flow rate ($\dot{m}$) acts as a scaling parameter, dividing the equation by $\dot{m}$ yields the heat input per unit mass, defined as $q = \dot{Q}/\dot{m}$:

$$h_{t2} = h_{t1} + q$$

Thus, given the entry total enthalpy h_{t1} and the specific heat addition q, the exit total enthalpy h_{t2} can be determined directly. Rayleigh flow shares identical conservation of mass and momentum relations with standard normal shock waves; it differs solely through the addition of the thermal energy term in the energy equation.

Relating static pressures across the region using the momentum equation gives:

$$\frac{p_2}{p_1} = \frac{1 + kMa_1^2}{1 + kMa_2^2}$$

From mass conservation, the density ratio can be expressed in terms of Mach numbers and static temperatures:

$$\frac{\rho_2}{\rho_1} = \frac{u_1}{u_2} = \frac{Ma_1 a_1}{Ma_2 a_2} = \frac{Ma_1}{Ma_2}\sqrt{\frac{T_1}{T_2}}$$

Applying the ideal gas state equation ($\rho = p/RT$) allows the density ratio to be replaced by pressure and temperature ratios:

$$\frac{p_2}{p_1}\left(\frac{T_1}{T_2}\right) = \left(\frac{1 + kMa_1^2}{1 + kMa_2^2}\right)\left(\frac{T_1}{T_2}\right) = \frac{Ma_1}{Ma_2}\sqrt{\frac{T_1}{T_2}}$$

Rearranging this relationship yields the static temperature ratio across the state change:

$$\frac{T_2}{T_1} = \left(\frac{Ma_2}{Ma_1}\right)^2\left(\frac{1 + kMa_1^2}{1 + kMa_2^2}\right)^2$$

Since density is proportional to pressure divided by temperature, combining the pressure and temperature ratio expressions yields the density ratio:

$$\frac{\rho_2}{\rho_1} = \frac{p_2/p_1}{T_2/T_1} = \left(\frac{Ma_1}{Ma_2}\right)^2\left(\frac{1 + kMa_2^2}{1 + kMa_1^2}\right)$$

This formulation links all downstream thermodynamic properties directly to the upstream conditions and the inlet and outlet Mach numbers. The unknown exit Mach number can then be evaluated using the energy relation.

Thermodynamic Relations & Gibbs Equation

Next, we can evaluate the thermodynamic behavior of the flow along a T-s diagram (Figure 3), commonly referred to as the Rayleigh line. We begin with the Gibbs equation in differential form:

$$ds = c_p\frac{dT}{T} - R\frac{dp}{p}$$

From conservation of momentum, the relationship between static pressure and Mach number remains constant across the process:

$$p\left(1 + kMa^2\right) = \text{constant}$$

Taking the logarithmic derivative of this momentum expression yields a differential relation between relative pressure changes and variations in Mach number:

$$\frac{dp}{p} + \frac{2kMa\ dMa}{1 + kMa^2} = 0$$

By replacing the incremental pressure ratio as a function of dMa/Ma into the differential entropy equation, we obtain:

$$ds = c_p\frac{dT}{T} + R\left(\frac{2kMa^2}{1 + kMa^2}\right)\frac{dMa}{Ma} \tag{2.2.1}$$

Next, consider the differential form of the mass conservation (continuity) equation:

$$\frac{d\rho}{\rho} + \frac{du}{u} = 0$$

Applying the ideal gas law ($p = \rho RT$) along with the Mach number relation ($u = Ma\sqrt{kRT}$), we can rewrite the density variation in terms of pressure, temperature, and Mach number:

$$\frac{dp}{p} - \frac{dT}{T} + \frac{dMa}{Ma} + \frac{dT}{2T} = \frac{dp}{p} - \frac{dT}{2T} + \frac{dMa}{Ma} = 0$$

Integrating the momentum differential equation allows us to link changes in static temperature (dT) directly to Mach number variations:

$$\frac{dMa}{Ma} = \frac{1}{2}\frac{dT}{T} + \left(\frac{2kMa^2}{1+kMa^2}\right)\frac{dMa}{Ma}$$

Rearranging terms yields a direct relationship between dMa/Ma and dT/T:

$$\frac{dMa}{Ma} = \left(\frac{dT}{2T}\right)\left(\frac{1+kMa^2}{1-kMa^2}\right) \tag{2.2.2}$$

Substituting Equation 2.2.2 back into the entropy relation Equation 2.2.1 produces:

$$ds = c_p\frac{dT}{T} + R\left(\frac{2kMa^2}{1+kMa^2}\right)\left[\frac{1}{2}\frac{dT}{T}\left(\frac{1+kMa^2}{1-kMa^2}\right)\right] = c_p\frac{dT}{T}\left[1+(k-1)\left(\frac{Ma^2}{1-kMa^2}\right)\right]$$

Factoring out the temperature gradient gives the final expression for entropy variation along a Rayleigh line as a function of T and local Mach number Ma:

$$ds = c_p\left(\frac{1-Ma^2}{1-kMa^2}\right)\frac{dT}{T}$$

The $T-s$ Rayleigh curve as indicated in Figure 3:

- Setting $\frac{ds}{dT} = 0$ identifies the state of maximum entropy (occurring at $Ma = 1$).
- Setting $\frac{dT}{ds} = 0$ locates the state of maximum static temperature (occurring at $Ma = 1/\sqrt{k}$).

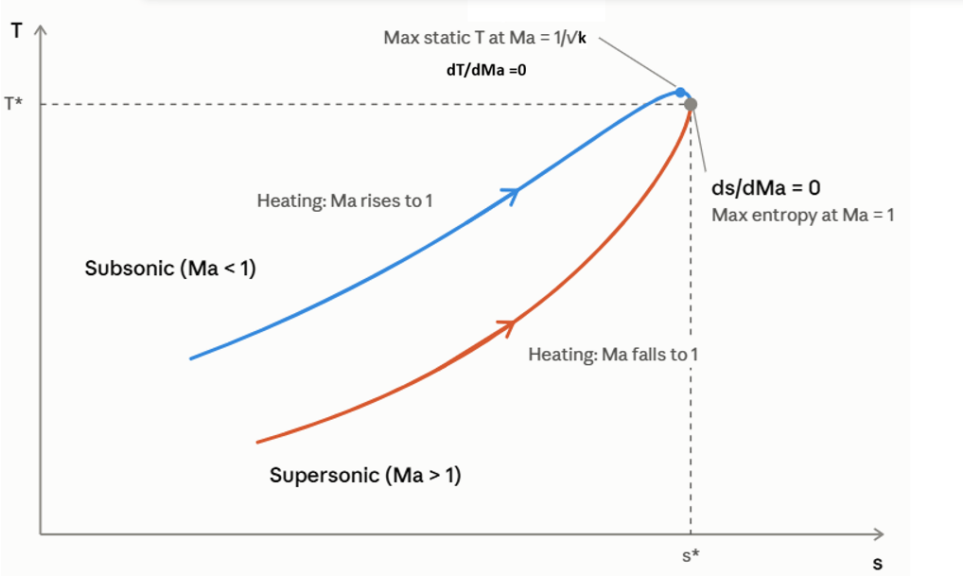


Figure 3: T-s diagram-supersonic Rayleigh flow

The Rayleigh curve comprises subsonic and supersonic branches that converge at the sonic point ($Ma = 1$). Energy addition pushes both speed regimes toward thermal choking, whereas heat extraction shifts the flow away from $Ma = 1$—reducing velocity in subsonic regimes and increasing it in supersonic ones. Static temperature peaks prior to sonic conditions, occurring specifically at $Ma = 1/\sqrt{k}$. Past this threshold, further heat input decreases static temperature even as the flow continues accelerating toward $Ma = 1$; total (stagnation) temperature, however, increases monotonically with heat addition. The maximum heat input required to choke the exit ($Ma_e = 1$) is defined as the critical thermal input, q^*. Because maximum entropy aligns precisely with $Ma = 1$, sonic flow can only be attained at the duct's exit boundary.

Graphically, the Rayleigh line represents all thermodynamic states sharing a constant mass flux ($\dot{m}/A = \rho u$). Because the energy equation is omitted when constructing the T-s diagram for Rayleigh flow, its governing momentum balance matches that of a normal shock wave—meaning a normal shock transition connects two points along the same Rayleigh curve. Because wall friction is neglected, heat transfer processes along the Rayleigh line are internally reversible. Consequently, the area beneath the curve on a T-s diagram, as seen in Figure 4, directly quantifies heat transfer per unit mass ($\int T\ ds$). Heating a subsonic entry state drives it along the lower branch toward higher entropy and Mach numbers, eventually reaching the limiting sonic state.

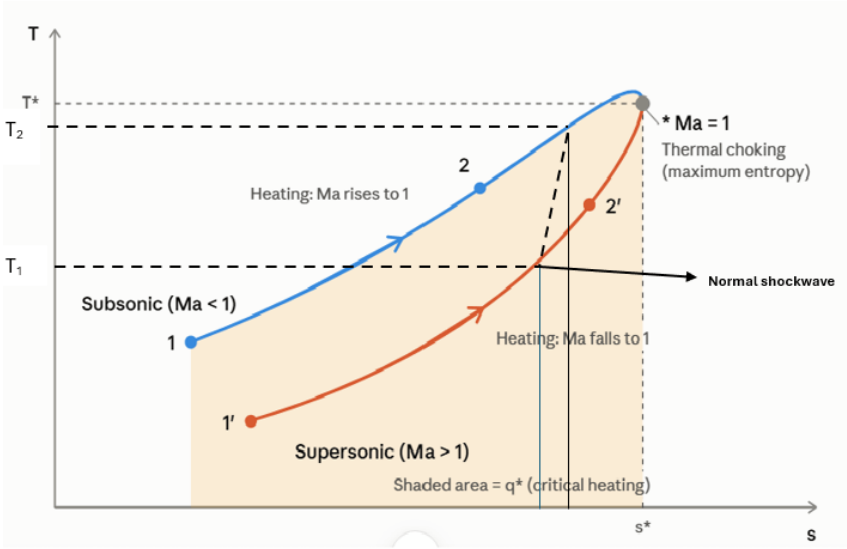


Figure 4. T-s diagram- critical heating area

- Subsonic Branch ($Ma < 1$): Adding heat accelerates the flow toward $Ma = 1$. Between $Ma = 1/\sqrt{k}$ and $Ma = 1$, heating causes static temperature T to decrease while total temperature T_t continues to rise.
- Supersonic Branch ($Ma > 1$): Adding heat decelerates the flow toward $Ma = 1$.
- Thermal Choking: Heating a flow to the point where the exit reaches $Ma = 1$ defines the maximum allowable heat addition, termed the critical heating rate (q^*). Any heat input exceeding q^* alters the inlet conditions (reducing inlet mass flow rate or causing flow spillage).

Adding the maximum allowable thermal energy, q^*, drives the duct exit to a choked condition ($Ma = 1$). Because adding heat to a supersonic stream reduces its velocity, scramjet combustors face an operational threshold: exceeding a specific fuel delivery rate will force the combustion chamber exit to choke. Additional details on supersonic burning processes are discussed later in this text. The magnitude of this critical heat input q^* depends directly on the initial state of the incoming gas. If thermal addition exceeds q^*, the system can no longer maintain its original inlet conditions and must adjust by throttling the incoming mass flow. This behavior is represented on a T-s diagram by a set of Rayleigh curves corresponding to progressively lower mass flux values.

This page titled 2.2: Rayleigh flow is shared under a CC BY 4.0 license and was authored, remixed, and/or curated by Haifa El-Sadi.

2.3: Problems and References

Problem#1

Air flows through a circular duct of uniform cross-sectional area with an inner diameter of $D = 0.5$ ft. At the duct inlet, the flow parameters are recorded as Mach number $Ma_1 = 0.35$, static pressure $p_1 = 15$ psia, and static temperature $T_1 = 520$ °R. Thermal energy is added to the air stream at a rate of $\dot{Q} = 200$ BTU/s. Assuming frictionless, one-dimensional Rayleigh flow with $k = 1.4$, $c_p = 0.24$ BTU/(lbm · °R), and gas constant $R = 1716$ ft · lbf/(slug · °R) (or 53.34 ft · lbf/(lbm · °R)), determine:

a. Mass flow rate through the channel, $\dot{m}$ (lbm/s)
b. The threshold thermal addition rate, $\dot{Q}^*$, required to choke the exit ($Ma_2 = 1$) for these inlet conditions
c. Exit Mach number, Ma_2
d. Percentage reduction in total pressure, $\Delta p_t/p_{t1} \times 100\%$
e. Change in specific entropy, Δs (BTU/(lbm · °R))
f. Total static pressure change, $\Delta p = p_1 - p_2$ (psi)
g. Sketch and label the inlet (State 1) and exit (State 2) conditions along a Rayleigh line on a Temperature–entropy ($T - -s$) diagram.

Problem#2

Find the maximum specific heat input, q^*, that can be added to a uniform, frictionless duct flow before reaching thermal choking at the exit. The air enters the channel at a supersonic Mach number of $Ma_1 = 2.4$ with an inlet static temperature of $T_1 = -20°\text{C}$ (253.15 K).

Assume the working fluid is air with:

- Specific heat ratio, $k = 1.4$
- Specific heat at constant pressure, $c_p = 1005$ J/(kg · K)

Project#1

Rayleigh Flow & Thermal Choking Limits in Scramjet Combustors

Objective: Model the 1D Rayleigh flow through a constant-area combustion chamber with variable heat release profiles.

Core Tasks:

1. Critical Heat Input (q^*)

- The total temperature as a function of Mach number

$$\frac{T_t}{T_t^*} = \frac{2(k+1)Ma^2\left(1+\frac{k-1}{2}Ma^2\right)}{\left(1+kMa^2\right)^2}$$

where

$$\dot{m}\left(h_{t2}-h_{t1}\right) = \dot{Q} \Longrightarrow h_{t2} - h_{t1} = q.$$

Assuming constant specific heat ($h = c_pT$), this becomes:

$$q = c_p\left(T_{t2} - T_{t1}\right)$$

Then $q^* = c_p\left(T_t^* - T_{t1}\right)$ Therefore, the critical heat input:

$$q^* = c_p T_{t1} \left[\frac{\left(1 + k Ma_1^2\right)^2}{2\left(k+1\right) Ma_1^2 \left(1 + \frac{k-1}{2} Ma_1^2\right)} - 1 \right]$$

2. Maximum Fuel-to-Air Ratio (Φ_{crit})

- Assuming complete combustion of a standard hydrocarbon fuel (e.g., Jet-A or Kerosene with lower heating value $LHV \approx 43\ \text{MJ/kg}$ and stoichiometric ratio $f_{\text{stoich}} \approx 0.068$):

  $$q^* = \frac{f \cdot LHV}{1+f} \approx f_{\text{crit}} \cdot LHV \Longrightarrow f_{\text{crit}} = \frac{q^*}{LHV - q^*}$$

  The equivalence ratio Φ_{crit} is:

  $$\Phi_{\text{crit}} = \frac{f_{\text{crit}}}{f_{\text{stoich}}}$$

- **Benchmark Calculations Across Varying Inlet Mach Numbers (Ma_1)**
- Assumed flow parameters: $T_1 = 300\ \text{K}$, $\gamma = 1.4$, $c_p = 1005\ \text{J/(kg} \cdot \text{K)}$, $LHV = 43\ \text{MJ/kg}$, $f_{\text{stoich}} = 0.068$.

Using EES (parametric tables) to determine the maximum allowable fuel-to-air ratio (Φ_{crit}) and critical heat input (q^*) before thermal choking ($Ma = 1$) occurs at the exit for varying inlet Mach numbers ($Ma_1 = \text{from } 2.0 \text{ to } 3 \text{ and the increment is } 0.2$.

References

Anderson, J. D. (2003). *Modern Compressible Flow: With Historical Perspective* (3rd ed.). McGraw-Hill Education.

Shapiro, A. H. (1953). *The Dynamics and Thermodynamics of Compressible Fluid Flow* (Vol. 1). Ronald Press.

Mattingly, J. D. (1996). *Elements of Gas Turbine Propulsion*. McGraw-Hill.

Oates, G. C. (1988). *Aerothermodynamics of Gas Turbine and Rocket Propulsion*. AIAA Education Series

This page titled 2.3: Problems and References is shared under a CC BY 4.0 license and was authored, remixed, and/or curated by Haifa El-Sadi.

3: AIRCRAFT ENGINES- RECIPROCATING ENGINE

3.0: Introduction
3.1: Aircraft Piston Engine
3.2: Volumetric Efficiency
3.3: Problems and References

This page titled 3: Aircraft Engines- Reciprocating Engine is shared under a CC BY 4.0 license and was authored, remixed, and/or curated by Haifa El-Sadi.

3.0: Introduction

Aircraft engines fall into two primary mechanical classifications: Piston (Reciprocating) Engines and Gas Turbine Engines (along with non-air-breathing Rocket Engines). Piston Engines operate on an internal combustion four-stroke cycle (Otto or Diesel) where pistons turn into crankshaft to drive a propeller. Piston engines are extremely efficient at low speeds and low altitudes; limited in total power output and high-altitude performance. Piston engines are used in small general aviation aircraft (e.g., Cessna 172, Piper Cherokee). Gas turbine engines generate thrust using continuous flow thermodynamics (Brayton Cycle): intake, compression, combustion, expansion through a turbine, and exhaust. Gas turbine engine such as a **turbojet** draws in air, compresses it, burns it with fuel, and expands it through a turbine, discharging all exhaust gases through a nozzle to produce pure reaction thrust—a design that operates efficiently at supersonic speeds (e.g., Concorde, F-104), though it is loud and fuel-inefficient at subsonic cruise. To improve efficiency, the other example of gas turbine engine is **turbofan** which combines a core gas turbine with a large front fan, splitting incoming air between core combustion and an outer bypass stream; this lower average exhaust velocity provides superior fuel economy and noise reduction at high subsonic cruise speeds ($Ma \approx 0.7 - -0.85$), making it the standard for modern commercial jetliners and military aircraft. For low-to-medium speed regimes ($Ma < 0.6$) and regional routes. However, the **turboprop** uses its gas turbine to drive a reduction gearbox and external propeller, offering exceptional fuel economy for aircraft like the ATR 72 and C-130. Operating on a similar mechanical principle, the **turboshaft** extracts nearly all fluid power through the turbine to drive an external shaft rather than a propeller, delivering high power-to-weight ratios for helicopters, tank propulsion (M1 Abrams), and auxiliary power units.

Moving beyond mechanical compressors, high-speed non-turbine air-breathing engines leverage forward momentum for axial compression: the **ramjet** relies on high supersonic flight speeds ($Ma > 3$) to compress intake air before combustion and nozzle expansion, whereas the **scramjet** (supersonic combustion ramjet) bypasses thermal choking by maintaining supersonic airflow throughout the combustion chamber for hypersonic operations ($Ma > 5$).

This page titled 3.0: Introduction is shared under a CC BY 4.0 license and was authored, remixed, and/or curated by Haifa El-Sadi.

3.1: Aircraft Piston Engine

Aircraft Piston (Reciprocating) Engines operate on internal combustion principles, converting the chemical energy of fuel into kinetic energy through the linear movement of pistons, which is then transformed into rotational movement by a crankshaft to drive a propeller.

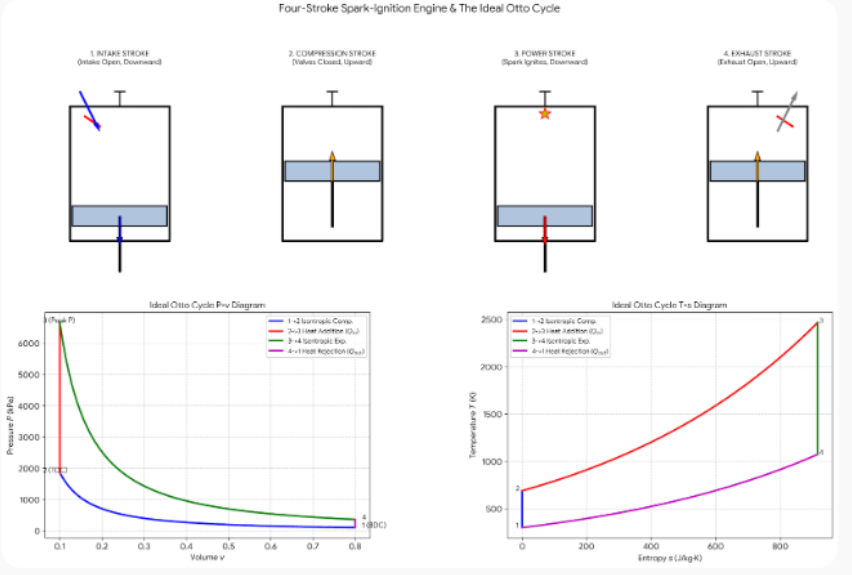


Figure 1. Four strokes piston engine

Most aviation piston engines operate on the Four-Stroke (Otto) Cycle as shown in Figure 1, completing four distinct strokes over two full revolutions (720°) of the crankshaft:

Intake Stroke ($0^\circ - 180^\circ$):

- The intake valve opens as the piston moves downward from Top Dead Center (TDC) to Bottom Dead Center (BDC).
- A low-pressure area is created, drawing in a vaporized fuel-air mixture from the induction system.

Compression Stroke ($180^\circ - 360^\circ$):

- Both valves close. The piston moves upward from BDC to TDC, compressing the fuel-air mixture.
- Just before TDC, twin spark plugs ignite the mixture.

Power (Expansion) Stroke ($360^\circ - 540^\circ$):

- The burning air-fuel mixture expands rapidly, driving the piston downward from TDC to BDC.
- This force delivers mechanical work to the crankshaft via the connecting rod.

Exhaust Stroke ($540^\circ - 720^\circ$):

- The exhaust valve opens. The piston moves back up from BDC to TDC, forcing burned combustion gases out through the exhaust manifold.

The compression ratio, r, is defined as the ratio of the maximum cylinder volume when the piston is at Bottom Dead Center (BDC) to the minimum cylinder volume when the piston is at Top Dead Center (TDC), expressed mathematically as $r = \left(\frac{V_d}{V_c}\right) + 1$, where V_d is the displacement volume per cylinder and V_c is the clearance combustion chamber volume. For an engine with N_c cylinders, the total engine displacement V_D is calculated as $V_D = N_c \cdot \left(\frac{\pi}{4} {D_B}^2 L\right)$, where D_B represents the cylinder bore diameter and L denotes the piston stroke length and N_c is the number of cylinders. In the ideal air-standard Otto cycle, the thermal efficiency

η_{thermal} depends directly on this compression ratio and the specific heat ratio of air k through the relationship $\eta_{\text{thermal}} = 1 - \frac{1}{r^{k-1}}$.

Although higher compression ratios yield higher thermodynamic efficiency, they are typically limited in aircraft engines to a range of $7:1$ to $9:1$ to prevent violent autoignition, also known as knocking or detonation. Furthermore, the work performed during this process can be quantified by the Indicated Mean Effective Pressure (IMEP), which represents the theoretical average pressure acting on the piston across the power stroke ($\text{IMEP} = W_{\text{net,cycle}}/V_d$). BMEP is the brake mean effective pressure, BMEP = $\eta_m IMEP$

The Indicated Power (P_i) is the total theoretical work rate generated inside the combustion chambers:

$$P_i = \text{IMEP} \cdot V_D \cdot \left(\frac{N}{2 \cdot 60}\right)$$

where:

1. N = Engine speed in Rotational Speed (RPM)
2. The factor of 2 accounts for power stroke occurring once every 2 crankshaft revolution.

The Brake Power (P_b) is the actual usable power delivered at the propeller shaft after overcoming internal friction and accessory losses:

$$P_b = \eta_m \cdot P_i = \tau \cdot \omega = \frac{2\pi \cdot \tau \cdot N}{60}$$

where:

1. η_m = Mechanical efficiency ($\approx 80\% - 90\%$)
2. τ = Shaft torque ($\text{N} \cdot \text{m}$)
3. ω = Shaft angular speed (rad/s)

Engine fuel performance can be evaluated using Brake Specific Fuel Consumption (BSFC), which measures how effectively the engine converts fuel mass into usable mechanical work.

$$\text{BSFC} = \frac{\dot{m}_f}{P_b}$$

where:

1. $\dot{m}_f$ = Fuel mass flow rate, cruise (kg/s or lb/hr)
2. P_b = Brake Power (kW or hp)

Thrust power is the power delivered by the propeller, THP,

$$THP = (T \times \backslash) V \backslash (\infty \backslash)) / 550 or \backslash (\text{THP} = P_b \times \eta_p$$

where: T: thrust, $IbfV\backslash(\infty$ = aircraft speed, ft/s Friction horsepower is the power loss due to friction and supercharger, FP, $FP = P_i$ - P_{b}\)

Modern aircraft piston engines incorporate several key operational features to ensure reliability, performance, and efficiency at high altitudes. Most aviation engines, such as the Lycoming O-360 and Continental IO-550, utilize air-cooled, horizontally opposed configurations to minimize overall system weight and reduce aerodynamic drag compared to liquid-cooling systems. To maximize safety and performance, these engines employ dual ignition systems featuring two independent magnetos that power two spark plugs per cylinder; this design provides critical redundancy while ensuring a more uniform combustion flame front. Finally, to combat the loss of manifold pressure and air density at higher altitudes, many systems incorporate turbochargers that compress ambient intake air, allowing naturally aspirated engines to maintain sea-level power output up to high critical altitudes.

The Otto cycle is a thermodynamic cycle (constant-volume heat addition, spark ignition). A spark-ignition (SI) engine can use either a carburetor (way of mixing fuel and air) or fuel injection.

3.2.1 Otto Cycle Engine: Carburetor

Carburetors govern fuel metering through fluid dynamics and pressure differentials created across a venturi tube. It is used for light aircraft like the Cessna 150/172

A. Air Mass Flow Rate ($\dot{m}_a$)

Assuming incompressible flow for low-speed intake air across the venturi throat (Bernoulli's Principle):

$$P_1 + \frac{1}{2}\rho_a V_1^2 = P_2 + \frac{1}{2}\rho_a V_2^2$$

$$\Delta P = P_1 - P_2 = \frac{1}{2}\rho_a \left(V_2^2 - V_1^2\right)$$

Applying continuity ($\dot{m}_a = \rho_a A_t V_t$) and incorporating the discharge coefficient C_{da} to account for fluid friction:

$$\dot{m}_a = C_{da} A_t \sqrt{\frac{2\rho_a \Delta P}{1 - (A_t/A_1)^2}} \approx C_{da} A_t \sqrt{2\rho_a \Delta P}$$

1. P_1, P_2: Inlet atmospheric pressure and venturi throat pressure (Pa)
2. ρ_a: Density of intake air ($\mathrm{kg/m^3}$)
3. A_1, A_t: Cross-sectional area of inlet and venturi throat ($\mathrm{m^2}$)
4. C_{da}: Discharge coefficient of the air throat ($\sim 0.85 - -0.95$)

The intake air mass flow rate $\dot{m}_a$ using the simplified venturi relation

$$\dot{m}_a = C_{da} A_t \sqrt{2\rho_a \Delta P}$$

B. Fuel Mass Flow Rate ($\dot{m}_f$)

Fuel is drawn from the float chamber through the main jet orifice. Considering the fuel lip height (h) above the float level to prevent spillage at rest:

$$\dot{m}_f = C_{df} A_f \sqrt{2\rho_f \left(\Delta P - \rho_f g h\right)}$$

1. C_{df}: Discharge coefficient of the fuel jet ($\sim 0.60 - -0.75$)
2. A_f: Area of the fuel jet metering orifice ($\mathrm{m^2}$)
3. ρ_f: Density of liquid fuel ($\mathrm{kg/m^3}$)
4. h: Fuel nozzle lip height above the float bowl fuel level (m)
5. g: Acceleration due to gravity ($9.81 \mathrm{m/s^2}$)

C. Delivered Air-Fuel Ratio (AFR)

$$\mathrm{AFR} = \frac{\dot{m}_a}{\dot{m}_f} = \frac{C_{da} A_t}{C_{df} A_f} \sqrt{\frac{\rho_a}{\rho_f} \left(\frac{\Delta P}{\Delta P - \rho_f g h}\right)}$$

Note: At high airflows ($\Delta P \gg \rho_f g h$), the pressure drop terms cancel out, leaving the air-fuel ratio governed purely by geometric areas ($\frac{A_t}{A_f}$) and fluid densities.

3.2.2 Otto Cycle Engine: Fuel Injection Equations

Electronic fuel injection calculates the required fuel mass per stroke using sensor inputs (e.g., MAP sensor, MAF sensor, engine RPM) and actuates solenoid or piezoelectric valves. It comes in two main forms: Port Fuel Injection (PFI), in which fuel is sprayed into the intake port just upstream of the intake valve and mixes with air before entering the cylinder, and Gasoline Direct Injection (GDI), in which fuel is sprayed at high pressure directly into the combustion chamber, allowing finer control of timing and mixture

but requiring much higher injection pressures.

A. Air Mass per Cylinder per Cycle (m_a)

Calculated using volumetric efficiency (η_v) and engine displacement volume (V_d):

$$m_a = \eta_v \cdot \rho_{a,\text{manifold}} \cdot \left(\frac{V_d}{n_{\text{cyl}}} \right)$$

1. η_v: Volumetric efficiency of the engine (ratio of actual air mass to theoretical cylinder volume)
2. V_d: Total engine displacement volume (m^3)
3. n_{cyl}: Number of cylinders

B. Required Fuel Mass per Injection Event (m_f)

\[m_f=\dfrac{m_a}

ParseError: invalid DekiScript (click for details)

```
Callstack:
    at (Bookshelves/Aerospace_Engineering/Aircraft_Engine:_Design_and_Analysis/
03:_Aircraft_Engines-_Reciprocating_Engine/3.02:_Aircraft_Piston_Engine), /content/body/
div[2]/div[2]/p/span, line 1, column 1
```

\nonumber \]

C. Fuel Injector Flow Rate ($\dot{m}_{f,\text{inj}}$)

Modeled via the orifice flow equation across the injector nozzle tip:

$$\dot{m}_{f,\text{inj}} = C_d A_{\text{orif}} \sqrt{2\rho_f \left(P_{\text{fuel}} - P_{\text{manifold}} \right)}$$

1. $P_{\text{fuel}} - P_{\text{manifold}}$: Differential injection pressure across the nozzle (ΔP_{inj})
2. For PFI: $P_{\text{fuel}} - P_{\text{manifold}} \approx 3 - -6 mathrm bar$
3. For GDI: $P_{\text{fuel}} - P_{\text{cylinder}} \approx 150 - -350 + mathrm bar$

D. The duration the injector orifice must be fully open to deliver m_f is (t_{inj}):

\[t_{\mathrm{inj}}=\dfrac{m_f}

ParseError: invalid DekiScript (click for details)

```
Callstack:
    at (Bookshelves/Aerospace_Engineering/Aircraft_Engine:_Design_and_Analysis/
03:_Aircraft_Engines-_Reciprocating_Engine/3.02:_Aircraft_Piston_Engine), /content/body/
div[2]/div[3]/div/p[1]/span, line 1, column 1
```

\nonumber \]

$t_{total} = t_{\text{inj}} + t_{\text{dead}}$

1. t_{dead}: Electrical dead time / latency (delay for solenoid coil energization and needle lift, typically $0.5 - -1.5 mathrm ms$) where ms is milliseconds

3.2.3 Ignition system

The battery supplies 12 V through the ignition switch to the coil's primary winding, and current builds up a magnetic field in the coil. The crank sensor (or the cam in a points system) reports piston position, so the control unit knows when to fire. At the right moment, the interrupter (breaker points in older engines, a transistor or ECU in modern ones) cuts the primary current. The magnetic field collapses, which induces a very high voltage, typically 20-40 kV, in the coil's secondary winding. The distributor routes that pulse to the correct cylinder, and the spark plug sparks across its gap (Figure 2), igniting the compressed fuel-air mixture shortly before TDC as indicated in Figure 3.

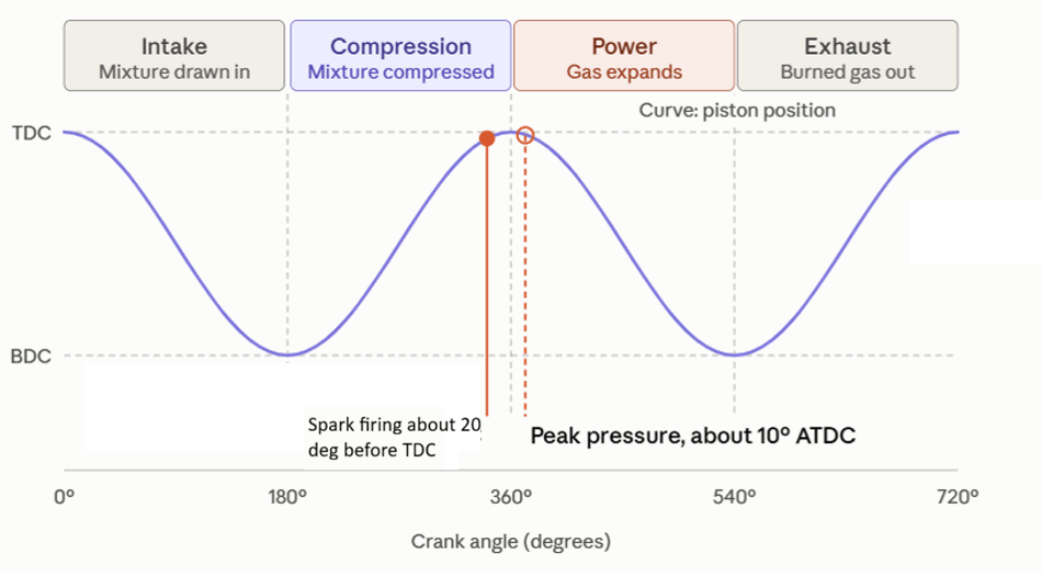


Figure 2. The spark fires before TDC

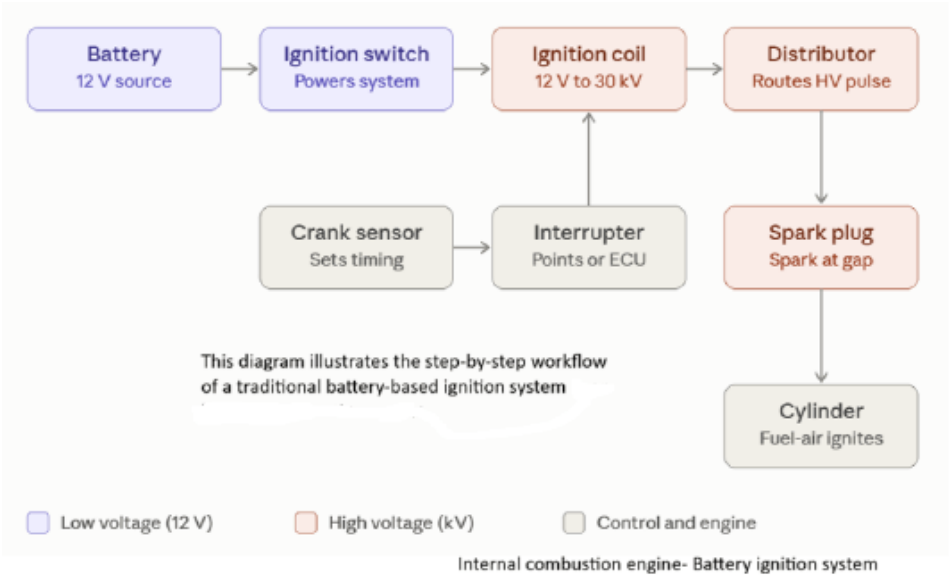


Figure 3. The spark from the 12 V battery, through the coil, to the plug.

Modern engines with coil-on-plug ignition have no distributor. Each cylinder has its own coil, and the ECU sends the pulses directly. A magneto system, as used in aircraft, combines the source, coil and interrupter in one self-powered unit, so it needs no battery or ignition switch in the power path

---

This page titled 3.1: Aircraft Piston Engine is shared under a CC BY 4.0 license and was authored, remixed, and/or curated by Haifa El-Sadi.

3.2: Volumetric Efficiency

Volumetric efficiency measures how effectively a four-stroke engine and its induction/exhaust systems act as an air pump. It is defined as:

$$\eta_v = \frac{m_a}{\rho_a V_d}$$

or

$$\eta_{\mathrm{v}} = \frac{2\dot{\mathrm{m}}_{\mathrm{a}}}{\rho_{\mathrm{a},0}\mathrm{V_d N}}$$

The air density $\rho_{\mathrm{a},0}$ can be estimated by using atmospheric conditions; η_{v} is the overall volumetric efficiency; $\mathrm{V_d}$ is displacement cylinder volume, N is crankshaft rotational speed; $\dot{m}_a$ is the mass flow rate of fresh air. A four-stroke engine takes in air only once every two crankshaft revolutions, so the intake rate is N/2 cycles per second.

The parameters that affect the volumetric efficiency (η_v) of a four-stroke internal combustion engine can be grouped into fuel/charge effects, flow & intake design, valve timing, and engine operating parameters:

- Fuel Type,
- Fuel-Air Ratio,
- The length and diameter of intake runners,
- Exhaust Backpressure: High exhaust backpressure prevents complete scavenging of burned gases, leaving higher residual gas mass in the cylinder and reducing space for the fresh air charge.
- Intake Valve Flow,
- Heat Transfer & Cylinder Wall Temperature. 6. Engine Speed (RPM).

This page titled 3.2: Volumetric Efficiency is shared under a CC BY 4.0 license and was authored, remixed, and/or curated by LibreTexts.

3.3: Problems and References

Problem#1

The following information is available for an aircraft four-stroke reciprocating engine:

- indicated mean effective pressure (IMEP) = 140 psi
- stroke = 4.5 in
- bore = 4.5 in
- engine rpm = 2700
- number of cylinders = 6
- cylinder clearance volume = 10 in^3 (per cylinder)
- engine mechanical efficiency = 90%
- propeller efficiency = 82%

Calculate (a) brake horsepower, (b) indicated horsepower, (c) thrust (hp), (d) compression ratio (is your answer reasonable for a spark ignition engine?)

Problem#2

A four-stroke piston aircraft engine delivers 180 brake horsepower while burning 13 gallons of aviation gasoline per hour. Determine

a. the brake specific fuel consumption of the engine. Is your answer reasonable for aircraft spark-ignition engines?
b. the brake thermal efficiency, of the engine. Is your answer reasonable for aircraft spark-ignition engines?

Note: Assume the heating value of the fuel is 19,500 Btu/lb and the nominal weight of avgas is 6 lb/gal.

Problem#3

A general aviation aircraft engine (such as on a Cessna 172) uses a venturi carburetor to meter intake air. The carburetor features an inlet diameter of $d_1 = 60\ \text{mm}$ and a narrowed throat diameter of $d_t = 38\ \text{mm}$. At full power, the static pressure drop from the inlet to the throat is $\Delta P = 4.5\ \text{kPa}$.

Assuming an ambient air density of $\rho_a = 1.15\ \text{kg/m}^3$, an air discharge coefficient of $C_{da} = 0.90$, and a local speed of sound of $a = 340\ \text{m/s}$:

1. Compute the intake air mass flow rate $\dot{m}_a$ using the simplified venturi relation:
2. Re-compute the mass flow rate using the exact incompressible flow equation accounting for inlet kinetic energy. Determine the percentage error of the approximate formula relative to the exact result.
3. Calculate the average velocity at the throat V_t. Evaluate whether the assumption of incompressible flow is physically justified.

Problem#4

A four-cylinder Lycoming O-320 aircraft engine (displacement $V_D = 320\ \text{in}^3$, brake power $P_b = 160\ \text{hp}$) operates at $2700\ \text{RPM}$ under full power. The induction system uses a venturi carburetor with the following operating parameters:

- Volumetric efficiency: $\eta_v = 0.75$
- Ambient air density: $\rho_a = 0.07491\ \text{lb/ft}^3 \quad \left(0.002328\ \text{slug/ft}^3\right)$
- Fuel density: $\rho_f = 44.95\ \text{lb/ft}^3 \quad \left(1.3970\ \text{slug/ft}^3\right)$
- Air discharge coefficient: $C_{da} = 0.90$
- Fuel discharge coefficient: $C_{df} = 0.70$
- Fuel nozzle lip height: $h = 0.3937\ \text{in} = 0.03281\ \text{ft}$

- Full-power pressure drop across venturi: $\Delta P = 83.54\ \mathrm{lbf/ft^2} = 0.5802\ \mathrm{psi}$

1. Calculate the engine air mass flow rate ($\dot{m}_a$) in $\mathrm{lb/s}$ and determine the required venturi throat diameter (d_t) in inches.
2. Determine the required fuel mass flow rate ($\dot{m}_f$) for a full-power air-fuel ratio of $\mathrm{AFR} = 12:1$, and compute the necessary main fuel jet diameter (d_f) in inches.
3. Convert the fuel mass flow rate to $\mathrm{lb/h}$ and calculate the Brake Specific Fuel Consumption (BSFC). Evaluate whether this value is reasonable for an aircraft spark-ignition engine.
4. Calculate the delivered AFR at a reduced throttle setting where $\Delta P = 8.354\ \mathrm{lbf/ft^2}$ $(0.05802\ \mathrm{psi})$, and explain the physical significance for engine operation at low airflow.

Problem#5

A 4-stroke aircraft piston engine produces a brake power (P_b) of $180\ \mathrm{hp}$ $(134.2\ \mathrm{kW})$ at an engine speed of $2700\ \mathrm{RPM}$ while consuming aviation gasoline at a rate of $m_f = 0.0105\ \mathrm{kg/s}$ $(83.3\ \mathrm{lb/hr})$. The engine's mechanical efficiency is $\eta_m = 85\%$ (0.85).

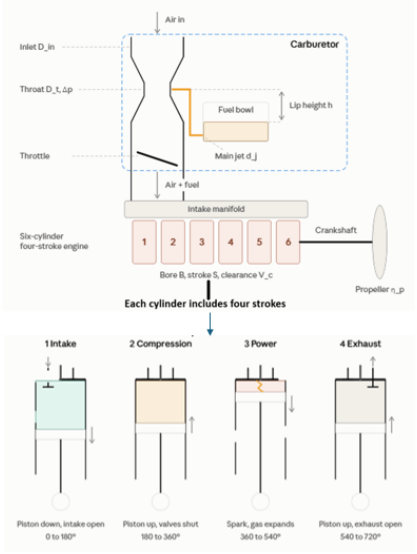
1. Friction Power: Determine the friction power loss (FP) in kilowatts (kW).
2. Brake Specific Fuel Consumption (BSFC): Calculate the BSFC in $\mathrm{kg/kW \cdot s}$

Problem#6

A four-cylinder, four-stroke gasoline engine with a swept volume of $122\ \mathrm{in^3}$ runs at $3000\ \mathrm{RPM}$. Under ambient atmospheric conditions of $14.7\ \mathrm{psia}$ and $77^\circ\mathrm{F}$ ($R = 53.35\ \mathrm{ft \cdot lbf/lbm \cdot R}$), an intake sensor records an induction air flow rate of $0.115\ \mathrm{lbm/s}$. Calculate the engine's volumetric efficiency.

Project#2:

Consider a 6-cylinder four-stroke aircraft piston engine operating at $N = 2700\ \mathrm{RPM}$ with a bore $B = 4.5\ \mathrm{in}$, stroke $S = 4.5\ \mathrm{in}$, clearance volume $V_c = 10\ \mathrm{in^3/cylinder}$, $\mathrm{IMEP} = 140\ \mathrm{psi}$, mechanical efficiency $\eta_m = 90\%$, and propeller efficiency $\eta_p = 82\%$. At a break power of $\mathrm{P}_b = 180\ \mathrm{hp}$ the engine consumes $\dot{m} = 13\ \mathrm{gal/hr}$ of Avgas (aviation gasoline) ($\mathrm{density} = 6\ \mathrm{lb/gal}$, heating value $= 19,500\ \mathrm{Btu/lb}$). The engine is fed by a general aviation carburetor with inlet diameter $\mathrm{d_1} = 2.36\ \mathrm{in}$, $throatdiameter \mathrm{d_t} = 1.50\ \mathrm{in}$, and venturi pressure drop $\Delta \mathrm{P} = 0.653\ \mathrm{psi}$, air density $\rho_\mathrm{a} = 0.0718\ \mathrm{lb/ft^3}$, $\mathrm{C_{da}} = 0.90$, speed of sound $\mathrm{a} = 1115.5\ \mathrm{ft/s}$). A four-cylinder Lycoming O-320 engine ($V_D = 320\ \mathrm{in^3}$, $P_b = 160\ \mathrm{hp}$ at $2700\ \mathrm{RPM}$) with parameters $\eta_v = 0.75$, $\rho_a = 0.07491\ \mathrm{lb/ft^3}$, $\rho_f = 44.95\ \mathrm{lb/ft^3}$, $C_{da} = 0.90$, $C_{df} = 0.70$, and fuel lip height $h = 0.3937\ \mathrm{in}$



Part#1: Mechanical Performance Analysis

1. Calculate the indicated horsepower (P_i), brake horsepower (P_b), thrust horsepower (THP), and friction horsepower (FP).
2. Compute the Brake Mean Effective Pressure (BMEP) and the engine compression ratio (r).
3. Evaluate whether the calculated compression ratio is reasonable for aviation spark-ignition engines and discuss the physical/knocking constraints that limit compression ratios in general aviation.

Part#2: Fuel Economy & Thermal Efficiency

1. Calculate the Brake Specific Fuel Consumption (BSFC) in $\mathrm{lb}/(\mathrm{bhp}\cdot\mathrm{hr})$.
2. Compute the brake thermal efficiency ($\eta_{th,b}$).
3. Compare your findings against standard general aviation benchmarks and comment on performance suitability.

Part# 3: Aerodynamic Modeling of Intake Carburetion

1. Calculate air mass flow rate m_a using both the simplified venturi relation and the exact incompressible flow equation accounting for inlet kinetic energy.
2. Determine the percentage error induced by using the simplified equation.
3. Calculate the throat velocity V_t and evaluate the throat Mach number to justify whether the incompressible flow assumption holds.

Part#4: Fuel Metering & Mixture Enrichment Behavior

1. Full-Power Condition ($\Delta P = 83.54\ \mathrm{lbf/ft^2}$):
    1. Compute air mass flow rate m_a ($\mathrm{lb/s}$) and required venturi throat diameter d_t (in).
    2. For a target full-power $\mathrm{AFR} = 12:1$, determine fuel mass flow rate m_f ($\mathrm{lb/s}$) and required main fuel jet diameter d_f (in).
    3. Calculate BSFC in $\mathrm{lb}/(\mathrm{hp}\cdot\mathrm{hr})$.
2. Reduced Throttle Condition ($\Delta P = 8.354\ \mathrm{lbf/ft^2}$):
    1. Compute the new delivered AFR.
    2. Explain the physical significance of the fuel lip height h on mixture leaning/enrichment at low airflow rates.

Part#5: Electronic Fuel Injection (EFI) System Comparative Study

Construct a comparative analysis between Port Fuel Injection (PFI) and Gasoline Direct Injection (GDI)

1. Explain how differential pressure (ΔP_{inj}), fuel density (ρ_f), orifice area (A_{orif}), and electrical dead time (t_{dead}) affect the injector pulse width duration (t_{total}).
2. Contrast the operating pressures ($3--6\ \mathrm{bar}$ vs. $150--350+\ \mathrm{bar}$) and list advantages and challenges of integrating GDI into air-cooled aircraft engines.

References

Heywood, J. B. (1988). *Internal Combustion Engine Fundamentals*. McGraw-Hill Education.

(Source for the four-stroke Otto cycle thermodynamics, volumetric efficiency parameters, and carburetor/injector fluid dynamics).

Taylor, C. F. (1985). *The Internal-Combustion Engine in Theory and Practice* (Vols. 1 & 2). MIT Press.

Mattingly, J. D. (1996). *Elements of Gas Turbine Propulsion / Aircraft Engine Design*. McGraw-Hill / AIAA.

Federal Aviation Administration (FAA). *Pilot's Handbook of Aeronautical Knowledge* (FAA-H-8083-25B) & *Aviation Maintenance Technician Handbook—Powerplant* (FAA-H-8083-32A).

This page titled 3.3: Problems and References is shared under a CC BY 4.0 license and was authored, remixed, and/or curated by Haifa El-Sadi.

4: AIRCRAFT ENGINE- GAS TURBINE ENGINE

4.0: Introduction

4.1: Gas Generator Components

4.2: On/Off Design Analysis

4.3: Turbojet

4.4: Turbofan Engine

4.5: Turboprop Engine

4.6: Problems and References

This page titled 4: Aircraft Engine- Gas Turbine Engine is shared under a CC BY 4.0 license and was authored, remixed, and/or curated by Haifa El-Sadi.

4.0: Introduction

A gas turbine engine is an internal combustion engine that converts the chemical energy in fuel into rotating shaft power or high-speed exhaust thrust. It works on a continuous flow of air, unlike a piston engine, which runs in discrete intake, compression, power, and exhaust strokes. That continuous flow lets it deliver a great deal of power from a compact, relatively lightweight machine, which is why it dominates aviation and plays a major role in electricity generation.

The thermodynamic cycle is the Brayton cycle, which has four stages handled by three main components. The working fluid of the Brayton cycle is air, which is drawn in and compressed by rows of rotating and stationary blades in the compressor. Modern engines reach overall pressure ratios of 30:1 or higher. Compression increases the air's temperature and pressure, which improves combustion performance. Fuel is then injected into the compressed air and burned continuously at roughly constant pressure. The temperature of the gases leaving the combustor can exceed 1,500 ° C in advanced engines, which is above the melting point of the metals used downstream. The hot, high-pressure gases expand through the turbine blades, rotating them. The turbine is connected to the compressor by a shaft, so the turbine extracts the energy required to drive the compressor, and any remaining energy is used either for thrust or for turning an output shaft. The remaining gases accelerate out of the nozzle to produce thrust.

There are different types of gas turbine engines. The turbojet produces all of its thrust from the exhaust jet; it is fast but noisy, and it is efficient at high speeds. The turbofan has a large front fan that bypasses much of the air around the core, giving better fuel efficiency and lower noise. Turboprop and turboshaft engines use the turbine to drive a propeller or rotor through a gearbox, and they are very common in regional aircraft and helicopters. The core of an aircraft gas turbine engine is the gas generator, which consists of three main components: a compressor, a burner, and a turbine. The compressor total pressure ratio, rp, is a design parameter. The flight Mach number is a key factor in choosing the number and type of compressor stages. As a general rule, the higher the flight Mach number, the lower the compressor pressure ratio the cycle needs to operate efficiently. At high supersonic speeds, the engine does not need mechanical compression at all, so the compressor can be removed. These engines rely on ram compression, in which the incoming air is compressed simply because the aircraft is moving fast, and they are called ramjets.

This page titled 4.0: Introduction is shared under a CC BY 4.0 license and was authored, remixed, and/or curated by Haifa El-Sadi.

4.1: Gas Generator Components

4.1.1 The Inlet

The *basic* function of the inlet is to transport the air to the compressor. The subsonic compressors are designed for an axial Mach number of Ma = 0.5–0.6. When the flight Mach number exceeds 0.5 or 0.6, as in commercial and military aircraft, the inlet is required to slow down the air efficiently. Because the main function of an inlet is to diffuse the flow, it is also called a diffuser. As the flow velocity decreases, static pressure increases. One of the main challenges facing an inlet designer is preventing boundary layer separation. This challenge is even greater for supersonic aircraft. At Mach 0.9, the inlet acts as a diffuser that slows the air to around Mach 0.5. However, at Mach 2 or higher, shock waves form and reduce total pressure, leaving only about 72% of the initial total pressure. At Mach 3, a strong normal shock wave retains only about 33% of the total pressure.

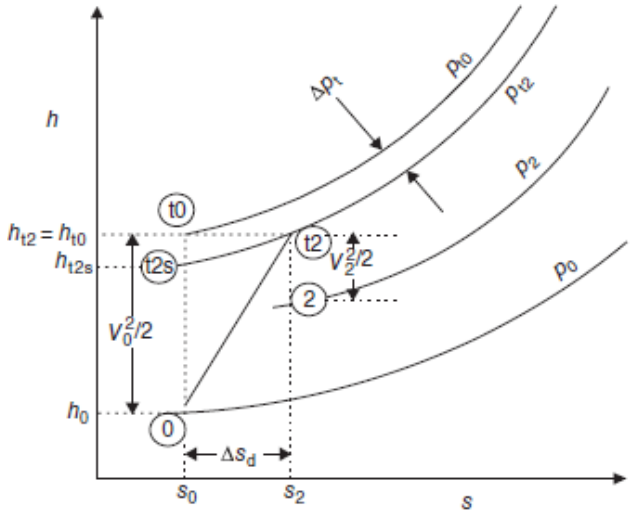


Figure 1. Mollier Diagram (h-s) for aircraft inlet/diffuser

From the h -s diagram, we observe that the freestream static state (0) and the freestream total state $(t0)$ are separated isentropically by the specific kinetic energy $\frac{V_0^2}{2}$, as defined by the relationship between static and stagnation states.

The fictitious total state $(t2s)$ is also separated isentropically from state (0) by an ideal kinetic energy amount, establishing p_{t2} as its stagnation pressure. The enthalpy gap between $(t0)$ and $(t2s)$ represents the portion of kinetic energy dissipated into heat through fluid friction, boundary layer growth, and shock wave losses. Consequently, a smaller gap between $(t2s)$ and $(t0)$ signifies a more efficient diffusion process.

Inlet Adiabatic Efficiency (η_d)

To quantify this performance, we define the **inlet adiabatic efficiency** (η_d) using the fictitious state $(t2s)$ as a Figure of merit:

\[\eta_d\equiv \dfrac{h_{t2s}-h_0}{h_{t0}-h_0} = \dfrac{\left(\dfrac{V^2_0}{2}\right)_\mathrm{ideal} \dfrac{V^2_0}{2} \nonumber \]

Dividing both the numerator and denominator by h_0 yields a practical form expressed in terms of thermodynamic property ratios:

$$\eta_d = \frac{\frac{h_{t2s}}{h_0} - 1}{\frac{h_{t0}}{h_0} - 1} = \frac{\frac{T_{t2s}}{T_0} - 1}{\frac{h_{t0}}{h_0} - 1}$$

Applying the isentropic temperature-pressure relation between states $(t2s)$ and (0), along with the temperature ratio parameter $\tau_r = \frac{T_{t0}}{T_0} = 1 + \frac{k-1}{2} Ma_0^2$:

$$\eta_d = \frac{\left(\frac{p_{t2}}{p_0}\right)^{\frac{k-1}{k}} - 1}{\frac{k-1}{2} Ma_0^2} = \frac{\left(\frac{p_{t2}}{p_0}\right)^{\frac{k-1}{k}} - 1}{\tau_r - 1}$$

Pressure Ratio Relations

For a given flight altitude (p_0), flight Mach number (Ma_0), and known inlet efficiency (η_d), the exit total pressure p_{t2} can be isolated directly:

$$\frac{p_{t2}}{p_0} = \left[1 + \eta_d \left(\frac{k-1}{2}\right) Ma_0^2\right]^{\frac{k}{k-1}}$$

Note: For an ideal, 100% efficient inlet ($\eta_d = 1.0$), this expression simplifies back to the standard isentropic stagnation pressure relation.

Total Pressure Recovery (π_d)

An alternative Figure of merit for evaluating inlet performance is the **inlet total pressure recovery** (π_d), defined as the total pressure ratio between the engine compressor face and the freestream flight condition:

$$\pi_d \equiv \frac{p_{t2}}{p_{t0}}$$

The relationship between adiabatic efficiency (η_d) and total pressure recovery (π_d) is derived by expanding the pressure ratio:

$$\frac{p_{t2}}{p_0} = \left(\frac{p_{t2}}{p_{t0}}\right)\left(\frac{p_{t0}}{p_0}\right) = \left[1 + \eta_d \left(\frac{k-1}{2}\right) Ma_0^2\right]^{\frac{k}{k-1}}$$

Solving for π_d:

Missing superscript or subscript argument

where $\pi_r = \left(1 + \frac{k-1}{2} Ma_0^2\right)^{\frac{k}{k-1}}$ is the ram pressure ratio.

Thus far, our analysis has focused on cruise conditions—the high-speed end of the flight envelope—where inlets function strictly as diffusers. However, under low-speed flight or takeoff conditions, the captured stream tube accelerates toward the engine face ($A_0 > A_2$) as seen in Figure 2, causing the inlet to operate as a nozzle rather than a diffuser.

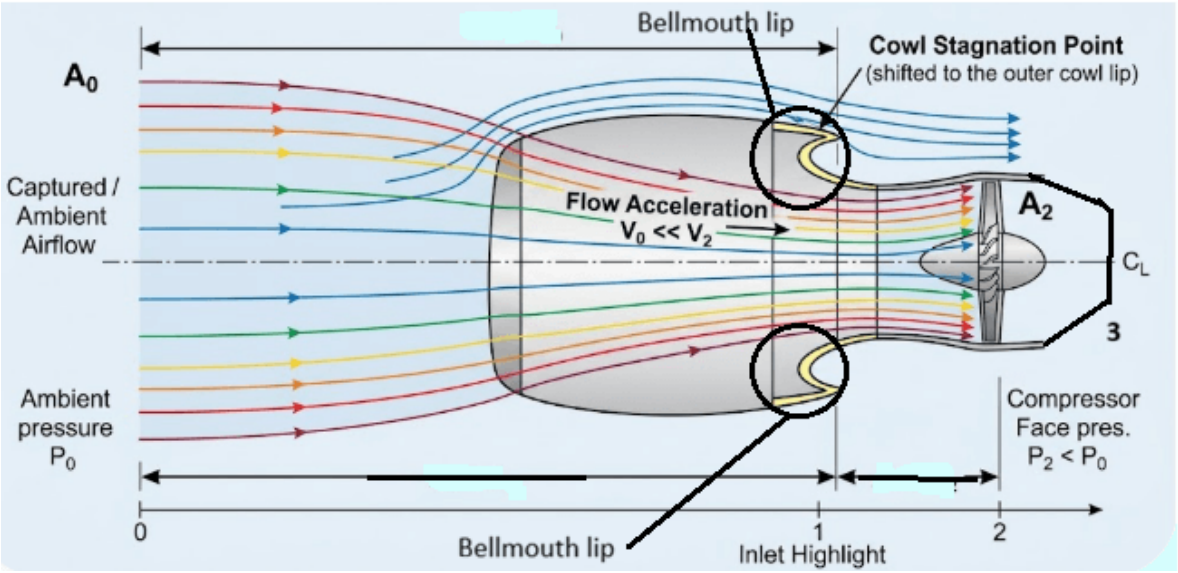


Figure 2. low speed/takeoff - $A_0 > A_2$

Under these low-speed conditions, the flow stagnation point shifts onto the outer cowl (is the smooth, curved outer skin and leading edge of the engine inlet housing) as indicated in Figure 3 While the aerodynamics of the external nacelle geometry strongly influence drag divergence and play a critical role in overall engine installation and propulsion system integration, standard cycle analysis typically focuses on internal propulsion performance and omits these external drag effects. At zero forward speed (static engine testing) or very low forward speeds, the incoming flow path must accelerate rapidly to feed the engine. This acceleration causes the static pressure along the streamlines to drop from the ambient pressure (p_0) down to the engine face static pressure (p_2), accompanied by a corresponding velocity increase from $V_0 \approx 0$ to V_2.

To guide this accelerating flow smoothly into the engine without boundary layer separation or severe flow distortion, static ground test rigs utilize a **bellmouth inlet**. The smooth, flared geometry of the bellmouth minimizes contraction losses and ensures uniform flow delivery across the compressor face during ground tests.

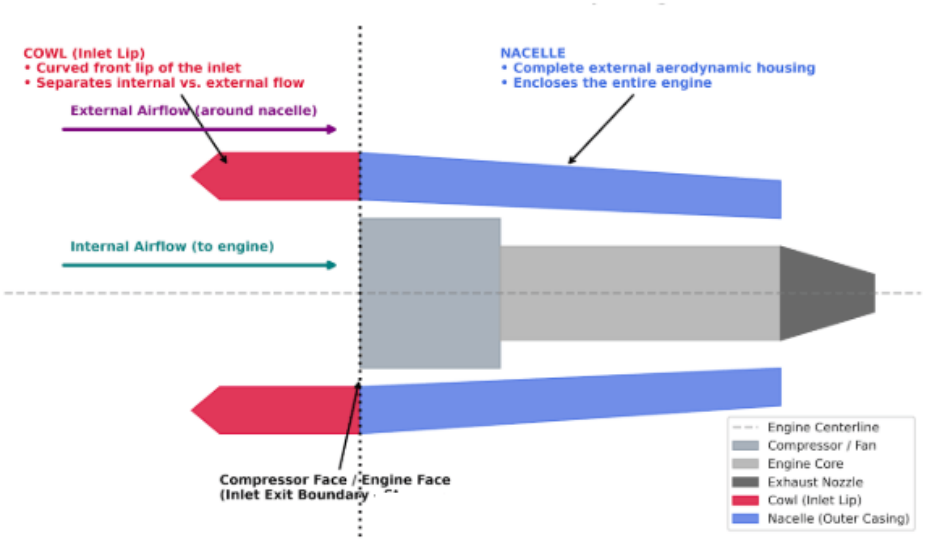


Figure 3. location of Cowl and Nacelle on jet engine

4.1.2 Compressor

The thermodynamic cycle of a gas generator begins with the mechanical compression of intake air. Because the compressed discharge air possesses a higher energy state, the compressor requires work input to operate. During steady-state operation, this

power is driven by the turbine via a connecting shaft. For engine startup, external power is supplied by auxiliary systems such as electric, or hydraulic starters. The air flowing through the compressor is modeled as an essentially adiabatic process, assuming negligible heat exchange between the internal fluid and the ambient environment. Consequently, even in a real compressor analysis, we treat the process as adiabatic while accounting for non-reversible thermodynamic losses. Power is transferred to the working fluid in a compressor through rows of rotating blades (rotors) mounted on one or more spinning shafts (spools). As each rotor blade alters the swirl of the fluid, it experiences an equal and opposite reaction torque. For a rotor spinning at angular velocity ω under a torque τ, the mechanical power $\mathcal{P}$ delivered to the fluid is given by:

$$\mathcal{P} = \tau \cdot \omega$$

A typical multi-stage axial-flow compressor contains hundreds of rotor blades operating under this mechanical principle. Consequently, the rate of mechanical energy transfer $\mathcal{P}_c$ in modern compressors larger than the rate of heat loss through the casing wall ($\dot{Q}_w$):

$$\mathcal{P}_c \gg \dot{Q}_w$$

Because heat transfer is negligible ($\dot{Q}_w \approx 0$), real compressor flows are modeled as adiabatic. For a steady-flow actual mass flow rate $\dot{m}_0$, the compressor power and performance parameters are defined as:

$$\mathcal{P}_c = \dot{m}_0 \left(h_{t3} - h_{t2}\right)$$

$$\pi_c \equiv \frac{p_{t3}}{p_{t2}}, \qquad \tau_c \equiv \frac{T_{t3}}{T_{t2}}$$

where π_c is the total pressure ratio, τ_c is the total temperature ratio, and h_{t2}, h_{t3} are the inlet and exit stagnation enthalpies as shown in Figure 2, respectively. Although assumed adiabatic, real compression processes are inherently irreversible. The principal sources of irreversibility are:

1. Viscous Boundary Layers: Wall friction along the blade surfaces and casing leads to boundary layer growth, wake formation, and vortex shedding.
2. Shock Waves**:** Passages with relative supersonic flow experience shock formation, creating sudden entropy jumps.

To quantify irreversibility, two efficiency metrics are commonly used, Compressor Adiabatic Efficiency (η_c) and Compressor Polytropic Efficiency (e_c).

Evaluating a real compression process on an enthalpy-entropy ($h - -s$) diagram demonstrates an entropy rise (Δs_c) from the actual inlet state $t2$ (p_{t2}, T_{t2}) to the exit state $t3$ (p_{t3}, T_{t3}). Because entropy increases during actual compression, the standard isentropic relationship does not apply directly to actual total states:

$$\tau_c \neq \pi_c^{\frac{k-1}{k}}$$

Due to irreversible losses, the actual temperature ratio τ_c is always greater than the ideal isentropic temperature ratio ($\tau_{c,s} = T_{t3s}/T_{t2}$).

The adiabatic efficiency η_c is defined as the ratio of ideal (isentropic) specific work input to actual specific work input:

$$\eta_c \equiv \frac{h_{t3s} - h_{t2}}{h_{t3} - h_{t2}} = \frac{\Delta h_{t,\text{isentropic}}}{\Delta h_{t,\text{actual}}}$$

Dividing the numerator and denominator by $h_{t2} = C_p T_{t2}$ yields:

$$\eta_c = \frac{\frac{T_{t3s}}{T_{t2}} - 1}{\frac{T_{t3}}{T_{t2}} - 1} = \frac{\left(\frac{T_{t3s}}{T_{t2}}\right) - 1}{\tau_c - 1}$$

Since states $t2$ and $t3s$ share the same isentrope, T_{t3s}/T_{t2} converts directly to the total pressure ratio π_c:

$$\frac{T_{t3s}}{T_{t2}} = \left(\frac{p_{t3s}}{p_{t2}}\right)^{\frac{k-1}{k}} = \left(\frac{p_{t3}}{p_{t2}}\right)^{\frac{k-1}{k}} = \pi_c^{\frac{k-1}{k}}$$

Substituting this into the efficiency expression yields the final form for compressor adiabatic efficiency:

$$\eta_c = \frac{\pi_c^{\frac{k-1}{k}} - 1}{\tau_c - 1}$$

4.1.3 Combustor

Within the combustor, fuel mixes with compressed air to initiate an exothermic chemical reaction that releases heat. An ideal combustor is modeled as a reversible heater, assuming frictionless wall flow and near-zero flow velocity. Under these ideal conditions, total pressure is fully conserved. However, In a real combustor, total pressure decreases due to wall friction, turbulent mixing, and chemical heat release occurring at a finite Mach number:

$$\pi_b = \frac{p_{t4}}{p_{t3}} < 1 \qquad \text{(Real Combustion Chamber)}$$

$$\pi_b = 1 \qquad \text{(Ideal Combustion Chamber)}$$

Kerrebrock provides an empirical approximation for the combustor total pressure ratio π_b as a function of the average burner Mach number Ma_b:

$$\pi_b \approx 1 - \varepsilon\left(\frac{k}{2}Ma_b^2\right) \qquad \text{where } 1 < \varepsilon < 2$$

This expression shows that total pressure loss is directly proportional to the average dynamic pressure ratio ($\frac{k}{2}Ma_b^2$) inside the burner, scaled by the coefficient ε. For example, for subsonic flow with an average Mach number $Ma_b = 0.2$, $\varepsilon = 2$, and $k \approx 1.33$, the pressure ratio is:

$$\pi_b \approx 1 - 2\left(\frac{1.33}{2}(0.2)^2\right) \approx 0.95$$

This demonstrates a $\sim$ 5% loss in total pressure. While this model is invalid for supersonic combustion, it highlights the thermodynamic advantage of maintaining low flow velocities in conventional combustors. A fuel's energy capacity is characterized by its heat of reaction (Q_R), which represents the thermal energy released per unit mass during complete chemical reaction. In practical combustion chambers, physical volume constraints prevent the complete theoretical heat release from being fully realized. The actual fraction of chemical energy converted into thermal energy is defined by the burner (or combustion) efficiency (η_b):

$$\eta_b \equiv \frac{Q_{R,\text{Actual}}}{Q_{R,\text{Ideal}}}$$

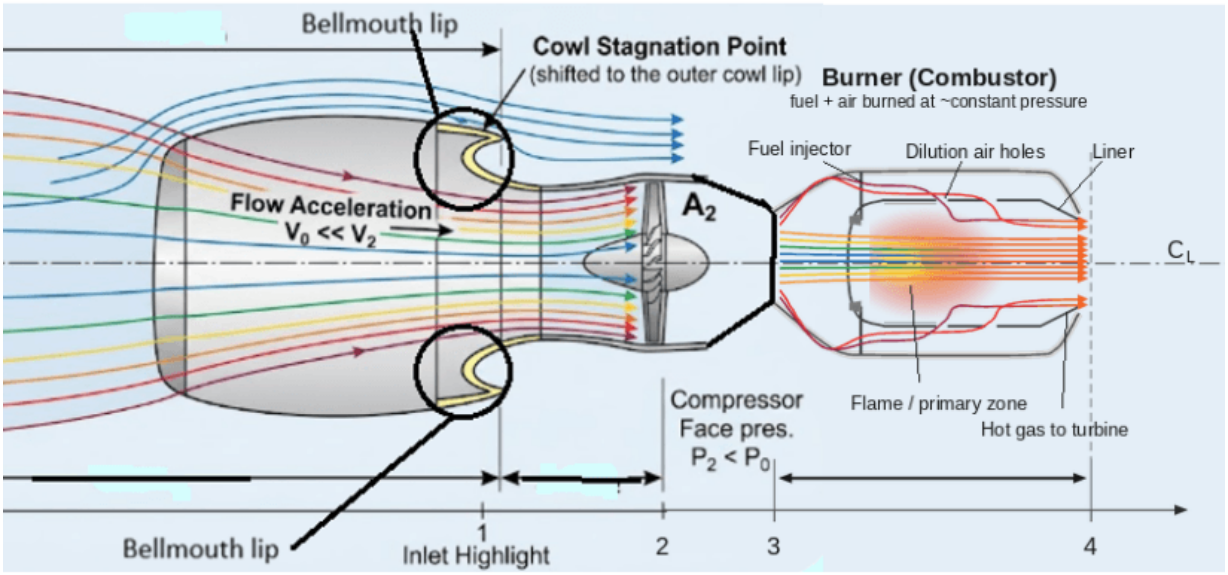


Figure 4. combustor (Burner)

Modern gas turbine engines achieve high combustion performance, with burner efficiencies typically reaching 99%. In thermodynamic cycle analysis, loss parameters across the combustor are accounted for using two non-ideal factors: the total pressure ratio ($\pi_b < 1$) and the burner efficiency ($\eta_b < 1$). Real combustors exhibit a drop in total pressure $\Delta p_{t,\text{burner}}$ from inlet to exit ($p_{t4} < p_{t3}$) as seen in Figure 4. The peak cycle temperature T_{t4} is strictly limited by turbine cooling technology, high-temperature material selection, and thermal barrier coatings. Current state-of-the-art values typically range from 3200–3600 ° R. The temperature rise $\Delta T_t = T_{t4} - T_{t3}$ directly reflects the thermal energy added by the fuel. The rate of heat input is approximately:

$$\dot{Q}_{\text{in}} \approx \dot{m}_0 C_p (\Delta T_t)_{\text{burner}}$$

Applying a steady-flow energy balance across the combustion chamber accounts for the incoming air enthalpy, added chemical fuel energy, and outgoing mixture enthalpy:

$$\dot{m}_0 h_{t3} + \dot{m}_f Q_R \eta_b = (\dot{m}_0 + \dot{m}_f)\, h_{t4}$$

Dividing by the air mass flow rate $\dot{m}_0$ and substituting the fuel-to-air ratio $f = \dfrac{\dot{m}_f}{\dot{m}_0}$ yields the fundamental governing equation:

$$h_{t3} + f Q_R \eta_b = (1 + f)\, h_{t4}$$

This equation allows for the direct determination of f given the target turbine inlet temperature T_{t4}. In an ideal combustor, heat addition occurs along a constant total pressure isobar ($p_{t3} = p_{t4}$). In a real combustor, viscous friction and heat release at finite velocities cause an entropy increase and a drop in total pressure, shifting the exit state to a lower isobar ($p_{t4} < p_{t3}$). By isolating the unknown parameter f from the combustor energy balance equation, the fuel-to-air ratio is explicitly written as:

$$f = \frac{h_{t4} - h_{t3}}{\eta_b Q_R - h_{t4}}$$

The denominator in this expression is completely specified when the fuel lower heating value (Q_R), burner efficiency (η_b), and target turbine inlet total temperature (T_{t4}) are given. Similarly, the compressor discharge enthalpy (h_{t3}) in the numerator is predetermined by the compressor pressure ratio, compressor isentropic efficiency, and inlet ambient conditions. Consequently, applying the energy balance across the burner serves as the primary method to calculate f.

In standard thermodynamic cycle analysis, it is customary to express this relation using non-dimensional temperature and enthalpy ratios. Dividing the numerator and denominator by the ambient free-stream static enthalpy (h_0) yields:

$$f = \frac{\dfrac{h_{t4}}{h_0} - \dfrac{h_{t3}}{h_0}}{\dfrac{\eta_b Q_R}{h_0} - \dfrac{h_{t4}}{h_0}} = \frac{\tau_\lambda - \tau_r \tau_c}{\dfrac{\eta_b Q_R}{h_0} - \tau_\lambda}$$

4.1.4 Turbine

Conceptually, the turbine acts as a primary flow-control boundary analogous to a valve—separating the high-pressure combustion zone from the low-pressure downstream components. In a gas turbine engine, the turbine represents the first throttling station; for supersonic aircraft, the throat of the exhaust nozzle serves as the second and final throttling station.

As the gas expands through the turbine and nozzle as shown in Figure 5, it undergoes a substantial drop in static pressure and static temperature. This continuous expansion process generates both the mechanical power required to drive the compressor and the overall propulsive thrust for the aircraft. The turbine transmits shaft power directly to the compressor via a shared connecting shaft. Functionally, this expansion is the continuous-flow equivalent of the power stroke in a reciprocating internal combustion engine.

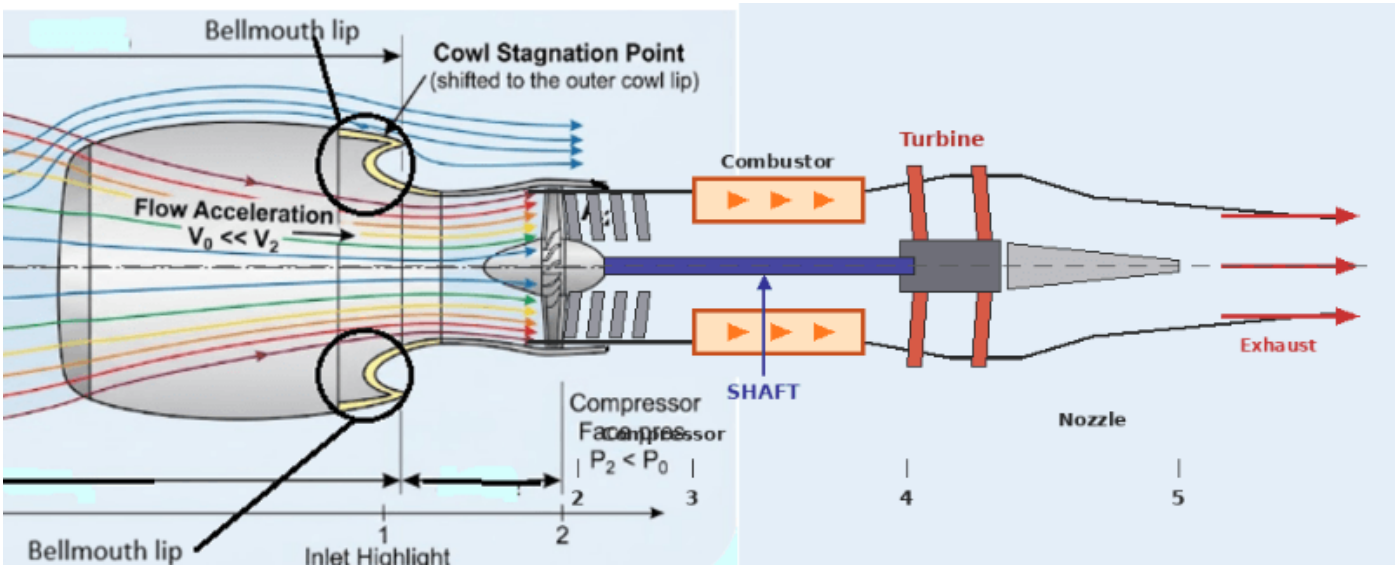


Figure 5. Turbine-Compressor Mechanical Coupling

The actual power $\mathcal{P}_{t,\text{actual}}$ produced in an uncooled turbine account for fluid friction and losses, whereas the ideal power $\mathcal{P}_{t,\text{ideal}}$ represents the maximum power output achieved via a reversible, isentropic expansion between the same total pressures:

$$\mathcal{P}_{t,\text{actual}} = \dot{m}_t \left(h_{t4} - h_{t5}\right) = \dot{m}_t \Delta h_{t,\text{actual}}$$

$$\mathcal{P}_{t,\text{ideal}} = \dot{m}_t \left(h_{t4} - h_{t5s}\right) = \dot{m}_t \Delta h_{t,\text{isentropic}}$$

The total working gas mass flow rate $\dot{m}_t$ includes both the entering air mass flow rate ($\dot{m}_0$) and the added fuel mass flow rate ($\dot{m}_f$):

$$\dot{m}_t = \dot{m}_0 + \dot{m}_f = (1 + f)\, \dot{m}_0$$

where $f = \dfrac{\dot{m}_f}{\dot{m}_0}$ is the fuel-to-air ratio.

The turbine adiabatic efficiency (η_t) is defined as the ratio of actual work output to ideal (isentropic) work output:

$$\eta_t \equiv \frac{h_{t4} - h_{t5}}{h_{t4} - h_{t5s}} = \frac{\Delta h_{t,\text{actual}}}{\Delta h_{t,\text{isentropic}}}$$

Dividing both the numerator and denominator by $h_{t4} = C_p T_{t4}$ yields:

$$\eta_t = \frac{1 - \dfrac{T_{t5}}{T_{t4}}}{1 - \dfrac{T_{t5s}}{T_{t4}}}$$

Because states $t4$ and $t5s$ lie on the same isentrope, their temperature ratio relates directly to the turbine total pressure ratio $\pi_t \equiv \frac{p_{t5}}{p_{t4}}$ via the isentropic relation:

$$\frac{T_{t5s}}{T_{t4}} = \left(\frac{p_{t5s}}{p_{t4}}\right)^{\frac{k-1}{k}} = \left(\frac{p_{t5}}{p_{t4}}\right)^{\frac{k-1}{k}} = \pi_t^{\frac{k-1}{k}}$$

Defining the actual total temperature ratio as $\tau_t \equiv \frac{T_{t5}}{T_{t4}}$, the turbine adiabatic efficiency simplifies to:

$$\eta_t = \frac{1-\tau_t}{1-\pi_t^{\frac{k-1}{k}}}$$

To evaluate individual turbine stages or small differential expansions, we define the turbine polytropic (small-stage) efficiency (e_t) as the ratio of differential actual enthalpy drop to differential isentropic enthalpy drop:

$$e_t \equiv \frac{dh_t}{dh_{ts}} = \frac{dh_t}{\left(\frac{dp_t}{\rho_t}\right)}$$

Assuming a perfect gas ($dh_t = C_p dT_t$) and integrating across the expansion stage relates the total temperature ratio τ_t and total pressure ratio π_t:

$$\tau_t = \pi_t^{\frac{(k-1)\,e_t}{k}} \qquad \text{or} \qquad \pi_t = \tau_t^{\frac{k}{(k-1)\,e_t}}$$

When $e_t = 1$, the expression reduces directly to the standard isentropic relationship between the temperature and pressure ratios. By substituting π_t from Equation 4.42 into Equation 4.40, we derive the relation connecting turbine adiabatic efficiency (η_t) and polytropic efficiency (e_t):

For a constant small-stage efficiency (e.g., $e_t = 0.90$), the turbine adiabatic efficiency η_t increases as the total expansion increases (i.e., as $\frac{1}{\tau_t}$ grows larger).

This behavior contrasts with compressor performance, where the overall adiabatic efficiency (η_c) decreases as pressure ratio increases. Fluid friction and inefficiencies generate heat that increases the gas temperature at subsequent stages. Because compressing a hotter fluid requires more work, each additional compressor stage increases the required power input. Fluid friction and internal losses dissipate energy as heat back into the expanding gas stream. This frictionally generated heat increases the enthalpy of the gas entering subsequent stages, allowing downstream turbine blades to recover a fraction of those thermal losses as additional shaft power. The total temperature ratio τ_t across the turbine is governed by an energy balance connecting the turbine, the compressor, and any auxiliary power extractions (such as an electrical generator) attached to the spool.

Assuming a simplified system where the turbine exclusively powers the compressor ($\mathcal{P}_t = \mathcal{P}_c$):

$$\mathcal{P}_t = \mathcal{P}_c$$

$$\dot{m}_0\,(1+f)\,(h_{t4} - h_{t5}) = \dot{m}_0\,(h_{t3} - h_{t2})$$

Dividing by the ambient static enthalpy (h_0) and simplifying yields the non-dimensional energy balance equation:

$$(1+f)\,\tau_\lambda\,(1-\tau_t) = \tau_r\,(\tau_c - 1)$$

where: τ_λ is temperature parameter representing maximum cycle energy (h_{t4}/h_0), τ_t is turbine total temperature ratio (T_{t5}/T_{t4}), τ_r is free-stream ram temperature ratio (T_{t0}/T_0), τ_c is Compressor total temperature ratio (T_{t3}/T_{t2}). Isolating the turbine expansion parameter τ_t yields:

$$\tau_t = 1 - \frac{\tau_r\,(\tau_c - 1)}{(1+f)\,\tau_\lambda}$$

4.1.5 Nozzle

The primary function of an aircraft engine exhaust nozzle (as shown in Figure 6) is to accelerate the expanding working fluid to produce propulsive force. The critical performance parameter for any exhaust system is the gross thrust (F_g), given by:

$$F_g = \dot{m}_9 V_9 + (p_9 - p_0)\, A_9$$

Momentum Thrust ($\dot{m}_9 V_9$) is the force generated by the change in fluid momentum. Where, Pressure Thrust ($(p_9 - p_0)\, A_9$) is the force resulting from any static pressure imbalance at the nozzle exit plane (A_9) relative to ambient pressure (p_0). Beyond propulsion requirements, modern exhaust systems are critical to aircraft stealth design (is a discipline in military engineering that reduces an aircraft's visibility). The exhaust flow leaves distinct operational "signatures" (are the physical traces an engine leaves behind) including thermal infrared emissions, visible exhaust plumes, smoke, and high acoustic noise levels that must be minimized in low-observable military platforms. As flow accelerates through a converging nozzle, the static pressure continuously decreases ($dp/dx < 0$). This establishes a favorable pressure gradient, which stabilizes boundary layer development and minimizes flow separation. Consequently, nozzle losses are significantly lower and easier to model than those in diffusers and inlets, which operate under adverse pressure gradients.

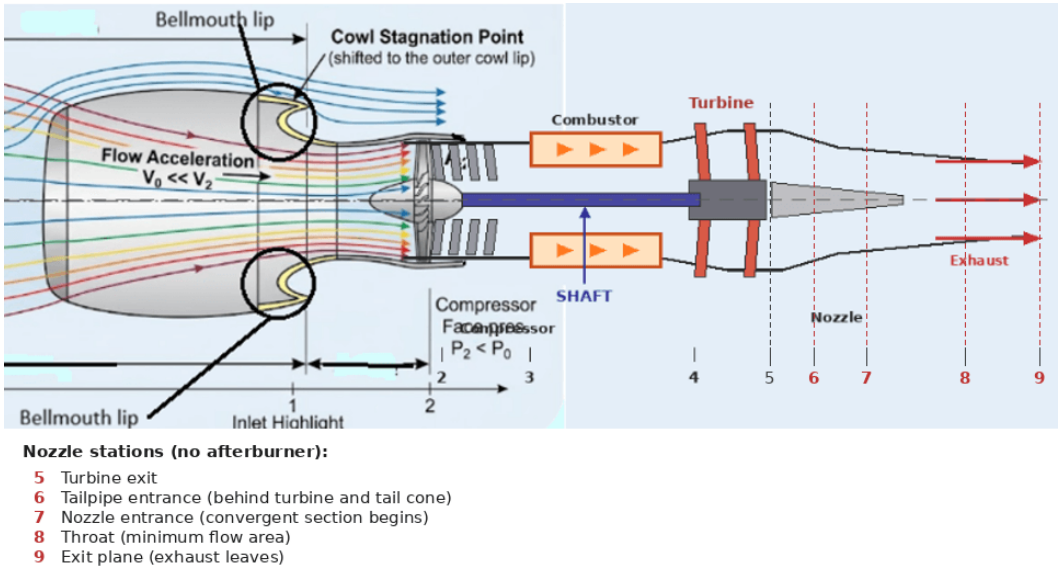


Figure 6. Gas turbine Engine- Nozzle and Exhaust

In subsonic compressible aerodynamics, a convergent duct accelerates a subsonic flow up to a maximum limit of $Ma = 1$, which can only occur at the duct's minimum cross-sectional area (the exit plane). For any subsonic exhaust jet ($Ma_9 < 1$), the static pressure at the exit plane (p_9) inherently equilibrates with the surrounding atmospheric pressure (p_0):

$$\text{If } Ma_9 = Ma_{\text{jet}} < 1, \qquad \text{then } p_{\text{jet}} = p_{\text{ambient}} \qquad (p_9 = p_0)$$

While mandatory for subsonic flows, expanding the exhaust fully to match ambient pressure is also achievable and highly desirable for sonic ($Ma_9 = 1$) and supersonic ($Ma_9 > 1$) exit flows. When an exhaust stream expands such that its exit static pressure precisely equals ambient pressure, the nozzle is operating in a perfectly expanded state which is if:

$$p_{\text{jet}} = p_{\text{ambient}} \qquad (p_9 = p_0)\,, \qquad \text{then the nozzle is perfectly expanded } \longrightarrow F_g = F_{g,\max}$$

Under this condition, the pressure thrust term $(p_9 - p_0)\, A_9$ drops to zero, and the nozzle achieves its maximum possible gross thrust ($F_{g,\max}$) for the given energy state. A real nozzle flow experiences total pressure losses due to boundary layer viscous dissipation and shock formation. Despite these non-ideal effects, a real nozzle can still achieve perfect expansion to ambient static pressure ($p_9 = p_0$). In compressible duct flow, the exit static pressure p_9 depends directly on the nozzle area ratio ($A_{\text{exit}}/A_{\text{throat}} \equiv A_9/A_8$) and the Nozzle Pressure Ratio (NPR):

$$\text{NPR} \equiv \frac{p_{t7}}{p_0}$$

This behavior is governed by two key aerodynamic principles for convergent and convergent-divergent (C–D) nozzles. When the

nozzle pressure ratio reaches or exceeds its critical threshold, the flow velocity at the nozzle throat reaches sonic speed ($Ma_8 = 1.0$). If:

$$\text{NPR} \geq (\text{NPR})_{\text{critical}}, \qquad \text{then } Ma_8 = 1.0 \qquad (\text{Throat is choked})$$

As a practical approximation, the nozzle throat chokes when the exit static pressure drops to roughly half of the upstream total pressure ($p_{\text{throat}} \approx \frac{1}{2} p_{t7}$), If:

$$\text{If } \frac{p_{t7}}{p_0} \geq\sim 2, \qquad \text{then } Ma_8 = 1.0 \qquad (\text{Throat can be choked})$$

Similar to the inlet section, the performance of an exhaust nozzle can be evaluated using the nozzle adiabatic efficiency (η_n). This metric compares the actual kinetic energy realized at the exit plane against the ideal kinetic energy from an isentropic expansion over the same total-to-static pressure ratio:

$$\eta_n \equiv \frac{h_{t7} - h_9}{h_{t7} - h_{9s}} = \frac{V_9^2/2}{V_{9s}^2/2}$$

where: h_{t7} is total enthalpy at the nozzle inlet (Station 7), h_9 is actual static enthalpy at the nozzle exit plane (Station 9), h_{9s} is ideal static enthalpy achieved via an isentropic expansion to ambient pressure, V_9 is actual gas velocity at the exit plane, V_{9s} is ideal exit velocity resulting from lossless, isentropic expansion

In an under-expanded or over-expanded nozzle flow, the nozzle pressure ratio ($\text{NPR} \equiv p_{t7}/p_0$) and the exit pressure ratio (p_0/p_9) quantify the static pressure mismatch at the exit plane:

1. Under-Expanded ($p_9 > p_0$): The nozzle expansion area ratio (A_9/A_8) is too small, preventing the fluid from expanding fully to ambient static pressure before exiting the duct.
2. Over-Expanded **(**$p_9 < p_0$ **):** The nozzle expansion area ratio (A_9/A_8) is excessively large, causing the fluid to expand past ambient static pressure inside the duct.

For a perfectly expanded nozzle, the exit static pressure precisely matches the ambient atmospheric pressure ($p_9 = p_0$). Under this condition, the nozzle adiabatic efficiency (η_n) simplifies directly to:

$$\eta_n = \frac{\text{NPR}^{\frac{k-1}{k}} - \pi_n^{-\frac{k-1}{k}}}{\text{NPR}^{\frac{K-1}{k}} - 1}$$

where: NPR is nozzle Pressure Ratio (p_{t7}/p_0), π_n is nozzle total pressure ratio (p_{t9}/p_{t7}), reflecting internal total pressure losses ($\pi_n \leq 1.0$), k is ratio of specific heats (c_p/c_v)

This page titled 4.1: Gas Generator Components is shared under a CC BY 4.0 license and was authored, remixed, and/or curated by Haifa El-Sadi.

4.2: On/Off Design Analysis

In general, on design is the process used to size and create engine component. It is used to determine component dimensions, mass flow rates, pressure ratios, and geometry. It occurs at a single, chosen to set of flight conditions (Mach number M_0, altitude h, and ambient conditions) and maximum operating limits (such as turbine inlet temperature T_{t4}). The physical size and internal engine components (e.g., compressor inlet area A_2, turbine nozzle blade angles, nozzle exit area A_8/A_9) are not fixed beforehand. Instead, they are calculated to meet specific performance requirements (such as achieving the required thrust or optimizing specific fuel consumption). To determine the required airflow, physical component sizes, and baseline cycle parameters needed to satisfy mission requirements at a critical flight condition (often cruise or takeoff).

Off-Design analysis is the process of taking a fixed, already-designed geometry (from the on-design) and simulating how it behaves when operating under *different* conditions. Off-design analysis evaluates how an engine behaves when operating away from its design point—such as during different flight phases (climb, loiter, descent, idle), changing Mach numbers, varying altitudes, or throttled-back power settings. The physical component sizes and geometry determined during on-design analysis are now fixed (or varied dynamically if using variable-geometry hardware, like variable inlet guide vanes). To predict engine performance (thrust, fuel consumption, spool (rotating assembly of turbine, compressor or fan and the shaft connected compressor to turbine) speeds, component efficiencies, and mass flow rates) across the full flight envelope given a fixed hardware configuration.

Example: Concorde Turbojet Engine

Example to show the difference between on/off design, by designing supersonic Concorde turbojet engine:

On Design: engineers chose Mach 2 and 50,000 ft, the physical geometry and baseline cycle parameters were calculated, so Concorde could efficiently travel faster than the speed of sound, a, so the needed physical sizes was calculated such as the precise cross sectional area of the intake, engine's core diameter and the nozzle expansion geometry to perform the optimal fuel burn and thrust while it is cruising at Ma =2. At this stage physically the engine was not set yet.

Off Design: Before spending millions of dollars building a physical prototype, engineers run off-design computer simulations using the fixed dimensions calculated in on design.

Concorde had to operate in real world but far from $Ma = 2$ cruise point. Concorde had to taxi on the tarmac at 15 knots, take off from London Heathrow at subsonic speeds, hold over airports in heavy air traffic, and fly over land at Mach 0.95 (due to noise regulations prohibiting sonic booms). Because the engine's physical core size and turbomachinery geometry were fixed by the design step, the engine control unit (and variable inlet ramps) had to adjust fuel flow and inlet airflow control to keep the engine running smoothly and safely without stalling or overheating. The engine hardware dimensions were fixed, and performance was calculated based on throttle adjustments and changing environmental conditions. Once the design passes both on-design and off-design computer simulations, the first physical prototype is manufactured.

This page titled 4.2: On/Off Design Analysis is shared under a CC BY 4.0 license and was authored, remixed, and/or curated by Haifa El-Sadi.

4.3: Turbojet

An ideal turbojet engine comprising the inlet, gas generator, and nozzle as shown in Figure 7) is thermodynamically equivalent to an ideal Brayton cycle. The classical Brayton cycle thermal efficiency (η_{th}) is expressed as:

$$\eta_{\text{th}} = 1 - \frac{T_0}{T_3}$$

where T_3 is the compressor discharges static temperature and 0 denotes ambient intake conditions.

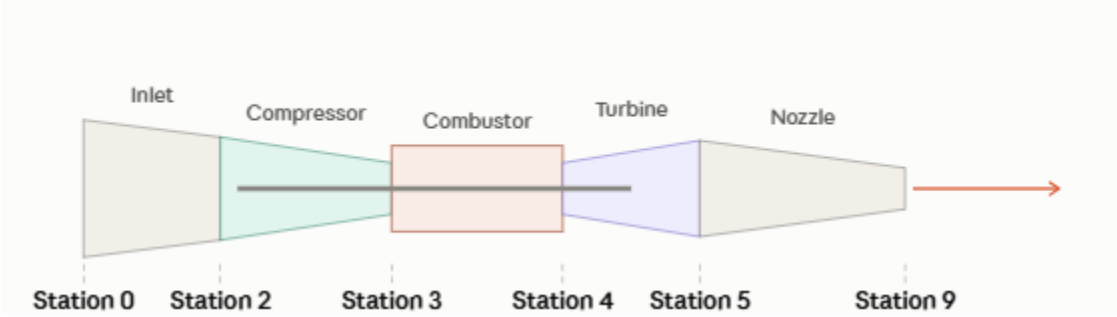


Figure 7. Turbojet components

Recasting the thermal efficiency in terms of the compressor temperature ratio ($\tau_c \equiv T_{t3}/T_{t2}$), ram temperature ratio ($\tau_r \equiv T_{t2}/T_0$), and compressor pressure ratio ($\pi_c \equiv p_{t3}/p_{t2}$):

$$\eta_{\text{th}} = 1 - \frac{1}{\frac{T_3}{T_0}} = 1 - \frac{1}{\left(\frac{T_{t3}}{T_{t2}}\right)\left(\frac{T_{t2}}{T_0}\right)} = 1 - \frac{1}{\tau_c \tau_r} = 1 - \frac{1}{\pi_c^{\frac{k-1}{k}}\left(1 + \frac{k-1}{2} Ma_0^2\right)}$$

For a fixed flight Mach number (Ma_0), the ram temperature ratio (τ_r) remains constant. Consequently, increasing the compressor pressure ratio (π_c) directly elevates thermal efficiency (η_{th}). While a higher π_c improves thermal performance, the resulting elevated compressor discharge temperature (T_{t3}) introduces severe structural and aerodynamic challenges for the high-pressure compressor (HPC). The advanced material requirements is standard titanium alloys reach thermal limits at high exit temperatures, forcing the use of nickel-based superalloys typically reserved for the turbine section. The active HPC cooling is extreme discharge temperatures may require active cooling schemes for the final compressor stages, such as regenerative fuel-cooling loops. The secondary flow & tip clearance losses are higher gas compression decreases fluid density, resulting in tiny blade heights and extremely narrow annular flow passages. Boundary layer displacement thickness and tip clearances consume a larger percentage of the flow path, significantly driving up secondary flow losses.

The relationship between flight Mach number, compressor pressure ratio, and cycle thermal efficiency is given by:

$$\eta_{\text{th}} = 1 - \frac{1}{\pi_c^{\frac{k-1}{k}}\left(1 + \frac{k-1}{2} Ma_0^2\right)}$$

For a fixed compressor pressure ratio (π_c), cycle thermal efficiency increases directly with flight Mach number (Ma_0). Higher flight speeds elevate the inlet total stagnation temperature (T_{t2}) via ram compression. When multiplied by a constant compressor pressure ratio (π_c), the overall compressor discharge temperature (T_{t3}) increases, raising the baseline thermodynamic efficiency of the cycle. Because $Ma_0 \approx 0$ during static takeoff, an engine operates at its lowest thermal efficiency at the start of flight. While thermal efficiency improves at higher airspeeds, flight Mach number is determined by aircraft mission profile requirements rather than an engine optimization variable.

Propulsive efficiency (η_p) measures how effectively the kinetic power produced by an engine is converted into useful propulsive power delivered to the aircraft:

\[η_p\equiv \dfrac{\mathrm{Thrust}~\mathrm{Power}}{Δ\mathrm{Kinetic}~\mathrm{Energy}~\mathrm{Rate}}=\dfrac{F\cdot V_0}

ParseError: invalid DekiScript (click for details)

```
Callstack:
    at (Bookshelves/Aerospace_Engineering/Aircraft_Engine:_Design_and_Analysis/
04:_Aircraft_Engine-_Gas_Turbine_Engine/4.04:_Turbojet), /content/body/p[11]/span, line 1,
column 1
```

\nonumber \]

To evaluate thrust power ($F \cdot V_0$), uninstalled or installed thrust values can be used. Calculating installed thrust is significantly more complex due to throttle-dependent inlet/exhaust drag and airframe integration effects.

To simplify analysis, uninstalled net thrust ($F_{n,\text{uninstalled}}$) is expressed in general form as:

$$F_{n,\text{uninstalled}} = \dot{m}_9 V_9 - \dot{m}_0 V_0 + (p_9 - p_0)\, A_9$$

Assuming a perfectly expanded nozzle ($p_9 = p_0$), the pressure thrust term vanishes. Further neglecting fuel mass contribution ($\dot{m}_f \ll \dot{m}_0 \Longrightarrow \dot{m}_9 \approx \dot{m}_0$), uninstalled net thrust simplifies to:

$$F_{n,\text{uninstalled}} \approx \dot{m}_0\,(V_9 - V_0)$$

Real engine components suffer from viscous losses, shocks, heat transfer, and mechanical friction rather than ideal isentropic behavior. At high supersonic speeds (e.g., $Ma_0 \geq 3$), external ram compression inside the inlet generates sufficient pressure rise on its own, eliminating the need for a mechanical compressor. Neglecting fuel mass addition ($\dot{m}_f \ll \dot{m}_a$), the net specific work output (w_c) of an ideal turbojet cycle is defined by the difference between total fluid expansion and compression:

$$w_c \approx (h_{t4} - h_9) - (h_{t3} - h_0)$$

$(h_{t4} - h_9)$ is specific work produced across the expansion leg (turbine and exhaust nozzle). $(h_{t3} - h_0)$ is specific work absorbed across the compression leg (inlet dynamic compression and compressor stage work).

Having determined the fuel-to-air ratio (f), exit velocity (V_9), ambient velocity (V_0), and exit static temperature (T_9), the specific thrust ($F_n/\dot{m}_0$) is expressed as:

$$\frac{F_n}{\dot{m}_0} = (1+f)\,V_9 - V_0 + \frac{RT_9\,(1+f)}{V_9}\left(1 - \frac{p_0}{p_9}\right)$$

The momentum terms $(1+f)\,V_9 - V_0$ provide the dominant contribution to specific thrust in an air-breathing engine. The pressure thrust term drops to zero under perfect expansion ($p_9 = p_0$) and remains small relative to the momentum component during off-design operation.

Multiplying the numerator and denominator of the pressure term by γ, and substituting $a_9^2 = kRT_9$ and $M_9^2 = V_9^2/a_9^2$, recasts the specific thrust into a more compact form:

$$\frac{F_n}{\dot{m}_0} = (1+f)\,V_9\left[1 + \frac{1}{\gamma M_9^2}\left(1 - \frac{p_0}{p_9}\right)\right] - V_0$$

Thrust Specific Fuel Consumption (TSFC) defines the fuel mass flow rate required per unit of net thrust generated:

$$\mathrm{TSFC} \equiv \frac{\dot{m}_f}{F_n} = \frac{f}{F_n/\dot{m}_0}$$

Combining the specific thrust and fuel-to-air ratio allows the engine's overall efficiency (η_o) to be expressed as a function of TSFC :

$$\eta_o = \frac{(F_n/\dot{m}_0)\,V_0}{fQ_R} = \frac{V_0/Q_R}{\mathrm{TSFC}}$$

where Q_R is the lower heating value of the fuel. This relationship demonstrates that overall engine efficiency is inversely

proportional to specific fuel consumption:

$$\eta_o \propto \frac{1}{\mathrm{TSFC}}$$

Lowering the engine's TSFC directly yields a higher overall thermodynamic and propulsive efficiency.

4.3.1 Turbojet Engine with Afterburner

To augment the net thrust of an aircraft gas turbine engine, an afterburner (or reheat system) can be integrated into the exhaust duct section as indicated in Figure 8. Widely utilized in military aircraft, this system offers an exceptionally simple and reliable mechanical solution for short-duration power boosts.

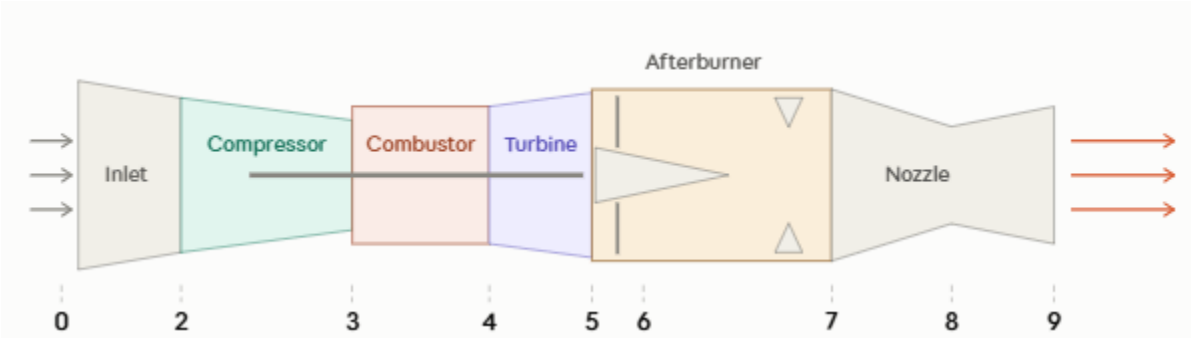


Figure 8. Turbojet with afterburner

The mass flow rate ($\dot{m}$) through a choked orifice is governed by the compressible flow continuity relation:

$$\dot{m} = \sqrt{\frac{k}{R}} \cdot \frac{p_t}{\sqrt{T_t}} \cdot A \cdot Ma\left(1 + \frac{k-1}{2} Ma^2\right)^{-\frac{k+1}{2\,(k-1)}}$$

Mass Flow Rate ($\dot{m}$) increases slightly due to auxiliary fuel addition ($\dot{m}_{f,\mathrm{AB}}$), roughly $3 - -4\%$, and total pressure (p_t) drops slightly across the burner due to combustion losses, roughly $5 - -8\%$.

Because $\dot{m}$, p_t, and gas properties undergo only minor fractional shifts, the required nozzle throat area (A_8) is predominantly driven by the total temperature (T_t). To prevent upstream pressure back-propagation, the variable-geometry throat (A_8) must open in direct proportion to the square root of the gas total temperature:

$$\frac{A_{8,\mathrm{AB-ON}}}{A_{8,\mathrm{AB-OFF}}} \approx \sqrt{\frac{T_{t8,\mathrm{AB-ON}}}{T_{t8,\mathrm{AB-OFF}}}}$$

An afterburner duct incorporates major structural systems to enable stable combustion, inlet diffuser decelerates incoming turbine exhaust gas to lower dynamic pressure, improving combustion efficiency and flame stability.

The addition of an afterburner modifies the inlet conditions to the exhaust nozzle in terms of mass flow rate, total pressure, and total temperature. The auxiliary fuel mass flow rate ($\dot{m}_{f,\mathrm{AB}}$) increases total mass flow, while combustion losses reduce total pressure (p_{t7}). The exit total temperature (T_{t7}) is bounded by thermal material limits. Consequently, nozzle expansion analysis follows standard compressible flow principles, using updated nozzle entry states.

The fundamental definitions for thermal efficiency (η_{th}) and propulsive efficiency (η_p) apply to afterburning turbojets, incorporating the additional heat energy input ($\dot{m}_{f,\mathrm{AB}} Q_{R,\mathrm{AB}}$):

\[η_{\mathrm{th}}\equiv \dfrac{Δ\dot{\mathrm{K}}\mathrm{E}}

ParseError: invalid DekiScript (click for details)

```
01 Callstack:
```

```
02     at (Bookshelves/Aerospace_Engineering/Aircraft_Engine:_Design_and_Analysis/
    04:_Aircraft_Engine-_Gas_Turbine_Engine/4.04:_Turbojet), /content/body/p[42]/span[1], line 1,
    column 1
```

=\dfrac{Δ\dot{\mathrm{K}}\mathrm{E}}
ParseError: invalid DekiScript (click for details)

```
01 Callstack:
02     at (Bookshelves/Aerospace_Engineering/Aircraft_Engine:_Design_and_Analysis/
    04:_Aircraft_Engine-_Gas_Turbine_Engine/4.04:_Turbojet), /content/body/p[42]/span[2], line 1,
    column 1
```

\nonumber \]

\[η_{\mathrm{th}}=\dfrac{\left({\dot{m}}_0+{\dot{m}}_f+{\dot{m}}_{f,\mathrm{AB}}\right)\dfrac{V^2_9}{2}-{\dot{m}}_0\
dfrac{V^2_0}{2}}

ParseError: invalid DekiScript (click for details)

```
01 Callstack:
02     at (Bookshelves/Aerospace_Engineering/Aircraft_Engine:_Design_and_Analysis/
    04:_Aircraft_Engine-_Gas_Turbine_Engine/4.04:_Turbojet), /content/body/p[43]/span, line 1,
    column 1
```

\nonumber \]

The Propulsive Efficiency (η_p)

\[η_p\equiv \dfrac{F\cdot V_0}{Δ\dot{\mathrm{K}}\mathrm{E}}=\dfrac{\left(\dfrac{F_n}

ParseError: invalid DekiScript (click for details)

```
01 Callstack:
02     at (Bookshelves/Aerospace_Engineering/Aircraft_Engine:_Design_and_Analysis/
    04:_Aircraft_Engine-_Gas_Turbine_Engine/4.04:_Turbojet), /content/body/p[45]/span, line 1,
    column 1
```

\right)\dfrac{V^2_9}{2}-\dfrac{V^2_0}{2}} \nonumber \]

where \(f\equiv \dfrac

ParseError: invalid DekiScript (click for details)

```
01 Callstack:
02     at (Bookshelves/Aerospace_Engineering/Aircraft_Engine:_Design_and_Analysis/
    04:_Aircraft_Engine-_Gas_Turbine_Engine/4.04:_Turbojet), /content/body/p[46]/span[1], line 1,
    column 1
```

\equiv \dfrac
ParseError: invalid DekiScript (click for details)

```
01 Callstack:
02     at (Bookshelves/Aerospace_Engineering/Aircraft_Engine:_Design_and_Analysis/
    04:_Aircraft_Engine-_Gas_Turbine_Engine/4.04:_Turbojet), /content/body/p[46]/span[2], line 1,
    column 1
```

{{\dot{m}}_0}\).

The total pressure ratio chain for an afterburning engine includes the pressure drop across the afterburner duct ($\pi_{\mathrm{AB}} \equiv p_{t7}/p_{t6}$).

Standard Turbojet Nozzle Pressure Ratio (π_n):

\[π_n={\left\

ParseError: invalid DekiScript (click for details)

```
01 Callstack:
02     at (Bookshelves/Aerospace_Engineering/Aircraft_Engine:_Design_and_Analysis/
04:_Aircraft_Engine-_Gas_Turbine_Engine/4.04:_Turbojet), /content/body/p[49]/span, line 1,
column 1
```

^{-\dfrac{k}{k-1}} \nonumber \]

Afterburning Turbojet (AB-TJ) Nozzle Pressure Ratio (π_n):

\[π_n={\left\

ParseError: invalid DekiScript (click for details)

```
01 Callstack:
02     at (Bookshelves/Aerospace_Engineering/Aircraft_Engine:_Design_and_Analysis/
04:_Aircraft_Engine-_Gas_Turbine_Engine/4.04:_Turbojet), /content/body/p[51]/span, line 1,
column 1
```

^{-\dfrac{k}{k-1}} \nonumber \]

By incorporating the afterburner total pressure ratio ($\pi_{\mathrm{AB}} \equiv p_{t7}/p_{t6}$) into the expansion chain, the nozzle exit Mach number (M_9) for an afterburning turbojet (AB-TJ) is expressed as:

$$M_9 = \sqrt{\frac{2}{\gamma-1}\left[\left(\pi_n\pi_{\mathrm{AB}}\pi_t\pi_b\pi_c\pi_d\pi_r\frac{p_0}{p_9}\right)^{\frac{k-1}{k}}-1\right]}$$

The corresponding exhaust exit velocity (V_9) is calculated using the exit Mach number and speed of sound (a_9), expressed in terms of the ambient speed of sound ($a_0 = \sqrt{kRT_0}$) and the burner temperature parameter ($\tau_{\lambda,\mathrm{AB}} \equiv T_{t7}/T_0$):

$$V_9 = Ma_9a_9 = Ma_9\sqrt{\frac{kRT_{t9}}{1+\frac{k-1}{2}Ma_9^2}} = Ma_9\sqrt{\frac{kRT_0\tau_{\lambda,\mathrm{AB}}}{1+\frac{k-1}{2}Ma_9^2}} = a_0Ma_9\sqrt{\frac{\tau_{\lambda,\mathrm{AB}}}{1+\frac{k-1}{2}Ma_9^2}}$$

Accounting for both primary combustor fuel (f) and afterburner fuel (f_{AB}), the specific thrust ($F_n/\dot{m}_0$) for an afterburning turbojet is derived as:

$$\frac{F_n}{\dot{m}_0} = \frac{\left(\dot{m}_0+\dot{m}_f+\dot{m}_{f,\mathrm{AB}}\right)V_9-\dot{m}_0V_0+\left(p_9-p_0\right)A_9}{\dot{m}_0}$$

Substituting $\dot{m}_9 = \rho_9V_9A_9$ and the ideal gas relation ($a_9^2 = kRT_9$) converts the pressure thrust component into nondimensional Mach form:

\[\dfrac{F_n}

ParseError: invalid DekiScript (click for details)

```
01 Callstack:
02     at (Bookshelves/Aerospace_Engineering/Aircraft_Engine:_Design_and_Analysis/
04:_Aircraft_Engine-_Gas_Turbine_Engine/4.04:_Turbojet), /content/body/p[59]/span, line 1,
column 1
```

\right)V_9-V_0+\left(1+f+f_{\mathrm{AB}}\right)\dfrac{p_9\left(1-\dfrac{p_0}{p_9}\right)A_9}{ρ_9V_9A_9} \nonumber \]

\[\dfrac{F_n}

ParseError: invalid DekiScript (click for details)

```
Callstack:
    at (Bookshelves/Aerospace_Engineering/Aircraft_Engine:_Design_and_Analysis/04:_Aircraft_Engine-_Gas_Turbine_Engine/4.04:_Turbojet), /content/body/p[60]/span, line 1, column 1
```

\right)V_9-V_0+\left(1+f+f_{\mathrm{AB}}\right)\dfrac{RT_9\left(1-\dfrac{p_0}{p_9}\right)}{V_9} \nonumber \]

\[\dfrac{F_n}

ParseError: invalid DekiScript (click for details)

```
Callstack:
    at (Bookshelves/Aerospace_Engineering/Aircraft_Engine:_Design_and_Analysis/04:_Aircraft_Engine-_Gas_Turbine_Engine/4.04:_Turbojet), /content/body/p[61]/span, line 1, column 1
```

\right)V_9\left[1+\dfrac{1-\dfrac{p_0}{p_9}}{\gM^2_9}\right]-V_0 \nonumber \]

The Thrust Specific Fuel Consumption (TSFC) accounts for the total fuel input across both combustion zones:

\[\mathrm{TSFC}\equiv \dfrac

ParseError: invalid DekiScript (click for details)

```
Callstack:
    at (Bookshelves/Aerospace_Engineering/Aircraft_Engine:_Design_and_Analysis/04:_Aircraft_Engine-_Gas_Turbine_Engine/4.04:_Turbojet), /content/body/p[63]/span, line 1, column 1
```

{F_n}=\dfrac{f+f_{\mathrm{AB}}}{F_n/{\dot{m}}_0} \nonumber \]

Multiplying specific thrust by average velocity [$\frac{1}{2}\left(V_0+V_9\right)$] yields the net specific work output (w_c) of the cycle:

$$w_c \approx \frac{V_9^2}{2}-\frac{V_0^2}{2}$$

For a given flight speed (V_0), maximizing specific cycle work requires maximizing exhaust kinetic energy ($\frac{1}{2}V_9^2$). The kinetic energy is governed by the total-to-static enthalpy drop across the exhaust nozzle:

$$\frac{V_9^2}{2} \equiv h_{t9}-h_9=h_{t9}\left(1-\frac{T_9}{T_{t9}}\right)=h_0\tau_{\lambda,\mathrm{AB}}\left[1-\frac{1}{1+\dfrac{k-1}{2}Ma_9^2}\right]$$

where $\tau_{\lambda,\mathrm{AB}} \equiv T_{t7}/T_0$.

For a fixed burner temperature parameter $(\tau_{\lambda,\mathrm{AB}})$ and ambient enthalpy (h_0), maximizing exit kinetic energy depends directly on maximizing the exit Mach number (Ma_9):

$$Ma_9^2=\frac{2}{k-1}\left[\left(\frac{p_{t9}}{p_9}\right)^{\dfrac{k-1}{k}}-1\right]$$

Maximizing Ma_9 requires maximizing the exit total-to-static pressure ratio (p_{t9}/p_9), expanded through the full component total pressure ratio chain:

$$\frac{p_{t9}}{p_9} = \left(\frac{p_{t9}}{p_{t7}}\right)\left(\frac{p_{t7}}{p_{t5}}\right)\left(\frac{p_{t5}}{p_{t4}}\right)\left(\frac{p_{t4}}{p_{t3}}\right)\left(\frac{p_{t3}}{p_{t2}}\right)\left(\frac{p_{t2}}{p_{t0}}\right)\left(\frac{p_{t0}}{p_0}\right)\left(\frac{p_0}{p_9}\right)$$

$$\frac{p_{t9}}{p_9} = \pi_n \pi_{\mathrm{AB}} \pi_t \pi_b \pi_c \pi_d \pi_r \left(\frac{p_0}{p_9}\right)$$

Assuming ideal components ($\pi_n = \pi_{\mathrm{AB}} = \pi_b = \pi_d = 1.0$), perfect expansion ($p_9 = p_0$), and substituting the ideal turbine temperature ratio ($\tau_t = 1 - \frac{\tau_r\left(\tau_c - 1\right)}{\tau_\lambda}$), the pressure ratio expression reduces to:

$$\frac{p_{t9}}{p_9} = 1 \cdot 1 \cdot \tau_t^{\frac{k}{k-1}} \cdot 1 \cdot \tau_c^{\frac{k}{k-1}} \cdot 1 \cdot \tau_r^{\frac{k}{k-1}} \cdot 1 \cdot 1 = \left[\tau_r \tau_c \left(1 - \frac{\tau_r\left(\tau_c - 1\right)}{\tau_\lambda}\right)\right]^{\frac{k}{k-1}}$$

This page titled 4.3: Turbojet is shared under a CC BY 4.0 license and was authored, remixed, and/or curated by Haifa El-Sadi.

4.4: Turbofan Engine

A turbofan engine is created by extending a core gas generator with additional low-pressure turbine stages. These stages extract thermal energy from the high-energy exhaust stream to provide mechanical shaft power to a forward fan.

From a thermodynamic standpoint, a fan behaves identically to a low-pressure compressor stage. It is characterized primarily by its total pressure ratio ($\pi_f \equiv p_{t13}/p_{t2}$), total temperature ratio ($\tau_f \equiv T_{t13}/T_{t2}$), and adiabatic fan efficiency (η_f).

The adiabatic fan efficiency (η_f) represents the ratio of ideal (isentropic) enthalpy rise to actual total enthalpy rise across the fan stage:

$$\eta_f \equiv \frac{h_{t13s} - h_{t2}}{h_{t13} - h_{t2}} = \frac{\Delta h_{t,\text{isentropic}}}{\Delta h_{t,\text{actual}}} = \frac{\text{Ideal Power}}{\text{Actual Power}}$$

Dividing the numerator and denominator by $h_{t2} = c_p T_{t2}$ expresses efficiency in terms of temperature and pressure ratios:

$$\eta_f = \frac{\frac{T_{t13s}}{T_{t2}} - 1}{\frac{T_{t13}}{T_{t2}} - 1} = \frac{\pi_f^{\frac{k-1}{k}} - 1}{\tau_f - 1}$$

Rearranging gives the explicit relations mapping fan temperature rise (τ_f) and pressure rise (π_f):

$$\tau_f = 1 + \frac{1}{\eta_f}\left(\pi_f^{\frac{k-1}{k}} - 1\right)$$

$$\pi_f = \left[1 + \eta_f\left(\tau_f - 1\right)\right]^{\frac{k}{k-1}}$$

In a turbofan engine, the power extracted by the turbine system must drive both the core high-pressure compressor and the low-pressure bypass fan:

$$\text{Turbine Power Delivered} = \text{Compressor Power Required} + \text{Fan Power Required}$$

Accounting for mechanical shaft transmission efficiency (η_m), primary combustor fuel addition ($f \equiv \dot{m}_f/\dot{m}_0$), and fan bypass ratio ($\alpha \equiv \dot{m}_{\text{fan}}/\dot{m}_0$), the energy balance equation is written as:

$$\eta_m \dot{m}_0 \left(1 + f\right)\left(h_{t4} - h_{t5}\right) = \dot{m}_0\left(h_{t3} - h_{t2}\right) + \alpha \dot{m}_0\left(h_{t13} - h_{t2}\right)$$

Dividing through by the primary air mass flow rate ($\dot{m}_0$) simplifies the expression to specific work terms:

$$\eta_m\left(1 + f\right) c_p\left(T_{t4} - T_{t5}\right) = c_p\left(T_{t3} - T_{t2}\right) + \alpha c_p\left(T_{t13} - T_{t2}\right)$$

Dividing the turbofan shaft power balance by core mass flow rate ($\dot{m}_0$) and non-dimensionalizing by flight static enthalpy ($h_0 = c_p T_0$) yields:

$$\eta_m\left(1 + f\right)\frac{h_{t4}}{h_0}\left(1 - \tau_t\right) = \frac{h_{t2}}{h_0}\left[\left(\tau_c - 1\right) + \alpha\left(\tau_f - 1\right)\right]$$

Substituting the burner temperature parameter ($\tau_\lambda \equiv h_{t4}/h_0 = T_{t4}/T_0$), ram temperature ratio ($\tau_r \equiv h_{t2}/h_0 = T_{t2}/T_0$), compressor temperature ratio (τ_c), and fan temperature ratio (τ_f) allows the turbine temperature ratio ($\tau_t \equiv T_{t5}/T_{t4}$) to be isolated:

$$\tau_t = 1 - \frac{\tau_r\left[\left(\tau_c - 1\right) + \alpha\left(\tau_f - 1\right)\right]}{\eta_m\left(1 + f\right)\tau_\lambda}$$

The primary burner fuel-to-air ratio ($f \equiv \dot{m}_f/\dot{m}_0$) is determined strictly by an energy balance across the main combustion chamber, making it independent of bypass ratio (α):

$$f = \frac{\tau_\lambda - \tau_r \tau_c}{\frac{Q_R \eta_b}{h_0} - \tau_\lambda}$$

where Q_R is the lower heating value of the fuel and η_b is the burner efficiency.

Analyzing the turbine expansion temperature ratio (τ_t) reveals its strong dependency on both the fan bypass ratio (α) and the compressor pressure ratio (π_c), as the total shaft power required for air compression is drawn directly from the turbine system.

To evaluate physical work limits, τ_t can be decomposed into two distinct loading components:

$$\tau_t = 1 - \frac{\tau_r (\tau_c - 1)}{\eta_m (1+f) \tau_\lambda} - \frac{\tau_r \alpha (\tau_f - 1)}{\eta_m (1+f) \tau_\lambda} = 1 - A - B$$

Nondimensionalizing the turbofan specific thrust is accomplished by dividing the specific thrust expression ($F_n/\dot{m}_0$) by the ambient speed of sound ($a_0 = \sqrt{\gamma R T_0}$):

\[\dfrac{F_n}

ParseError: invalid DekiScript (click for details)

```
01 Callstack:
02     at (Bookshelves/Aerospace_Engineering/Aircraft_Engine:_Design_and_Analysis/
   04:_Aircraft_Engine-_Gas_Turbine_Engine/4.05:_Turbofan_Engine), /content/body/p[27]/span,
   line 1, column 1
```

{a_0} \nonumber \]

Applying the general definition of Thrust Specific Fuel Consumption (TSFC) to a turbofan cycle, the fuel mass flow rate ($\dot{m}_f$) is scaled against the net uninstalled thrust (F_n):

$$\mathrm{TSFC} \equiv \frac{\dot{m}_f}{F_n} = \frac{f}{F_n/\dot{m}_0}$$

where $f \equiv \dot{m}_f/\dot{m}_0$ is the core fuel-to-air ratio.

Alternatively, expressing both fuel ratio and specific thrust on a total engine airflow basis ($\dot{m}_{\text{total}} = \dot{m}_0 + \dot{m}_{\text{fan}} = (1+\alpha)\dot{m}_0$) yields the equivalent form:

$$\mathrm{TSFC} = \frac{\frac{f}{1+\alpha}}{\frac{F_n}{(1+\alpha)\dot{m}_0}}$$

For an ideal turbofan engine, the cycle thermal efficiency (η_{th}) is identical to that of an ideal turbojet operating at the same overall pressure ratio (π_c), as the fan work transfer is entirely reversible:

$$\eta_{\text{th}} = 1 - \frac{1}{\tau_r \tau_c} = 1 - \frac{1}{\left(1 + \frac{k-1}{2} Ma_0^2\right) \pi_c^{\frac{k-1}{k}}}$$

For a real (non-ideal) turbofan engine, thermal efficiency is derived directly from the ratio of net kinetic energy generation rate ($\Delta\dot{\mathrm{KE}}$) to the total thermal power supplied by the fuel ($\dot{m}_f Q_R$):

\[η_{\mathrm{th}}\equiv \dfrac{Δ\dot{\mathrm{K}}\mathrm{E}}

ParseError: invalid DekiScript (click for details)

```
01 Callstack:
```

```
02     at (Bookshelves/Aerospace_Engineering/Aircraft_Engine:_Design_and_Analysis/
    04:_Aircraft_Engine-_Gas_Turbine_Engine/4.05:_Turbofan_Engine), /content/body/p[36]/span,
    line 1, column 1
```

{{\dot{m}}_fQ_R} \nonumber \]

Dividing the numerator and denominator by $\dot{m}_0$ expresses efficiency in terms of core and bypass velocity contributions:

$$\eta_{\text{th}} = \frac{\alpha V_{19}^2 + (1+f)\,V_9^2 - (1+\alpha)\,V_0^2}{2fQ_R}$$

Decomposing the kinetic energy output into core and bypass components yields:

$$\eta_{\text{th}} = \frac{(1+f)\,V_9^2 - V_0^2}{2fQ_R} + \alpha\left[\frac{V_{19}^2 - V_0^2}{2fQ_R}\right]$$

where: V_9 **:** Core exhaust exit velocity, V_{19} **:** Bypass nozzle exit velocity, V_0 **:** Flight inlet velocity, $f = \dfrac{\dot{m}_f}{\dot{m}_0}$ **:** Core fuel-to-air ratio.

The propulsive efficiency (η_p) of a turbofan engine is a strong function of the bypass ratio (α). It measures how effectively the net kinetic energy generated across both the core and bypass streams is converted into propulsive thrust power:

$$\eta_p \equiv \frac{F_n V_0}{\Delta\dot{\text{KE}}} = \frac{[(1+f)\,V_9 + \alpha V_{19} - (1+\alpha)\,V_0 + (p_9 - p_0)\,A_9 + (p_{19} - p_0)\,A_{19}]\,V_0}{(1+f)\,\dfrac{V_{9,\text{eff}}^2}{2} + \alpha\dfrac{V_{19,\text{eff}}^2}{2} - (1+\alpha)\,\dfrac{V_0^2}{2}}$$

Assuming both the core nozzle ($p_9 = p_0$) and bypass nozzle ($p_{19} = p_0$) are perfectly expanded, and neglecting the small core fuel contribution ($f \ll 1$), the propulsive efficiency simplifies to:

$$\eta_p \approx \frac{2V_0\,[V_9 + \alpha V_{19} - (1+\alpha)\,V_0]}{V_9^2 + \alpha V_{19}^2 - (1+\alpha)\,V_0^2}$$

4.4.1 Mixed exhaust turbofan with an after burner

A mixed exhaust turbofan is an engine configuration where the bypass duct extends all the way to the rear. The cold bypass air and hot core gases combine in an internal forced mixer section (typically featuring a lobed nozzle) before discharging together through a single exhaust nozzle. Figure 9 shows afterburner in mixed exhaust turbofan.

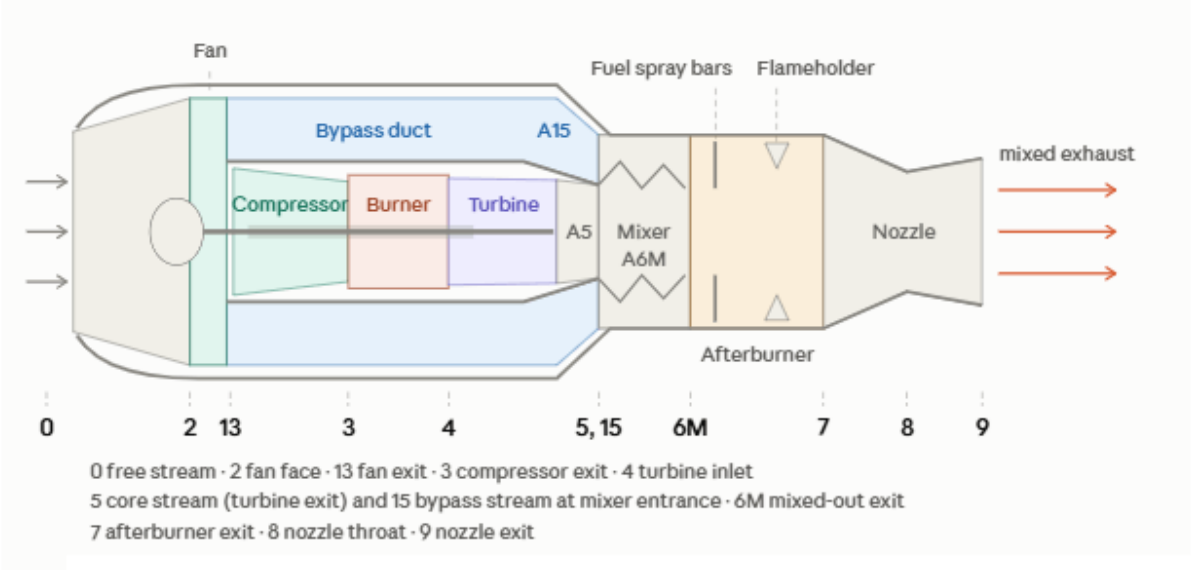


Figure 9. Mixed turbofan with afterburner

To analyze a constant-area mixer, we apply the fundamental conservation laws of mass, momentum, and energy alongside mixture gas laws to determine the mixed-out properties at the exit. Applying the conservation of energy to an insulated mixer yield:

$$\dot{m}_5 h_{t5} + \dot{m}_{15} h_{t15} = \dot{m}_{6M} h_{t6M}$$

Given known inlet conditions, the only unknown in Equation 4.144 is the mixed-out total enthalpy, h_{t6M}:

$$h_{t6M} = \frac{(1+f)\, h_{t5} + \alpha h_{t15}}{1+\alpha+f}$$

Expressing this relationship in terms of non-dimensional engine parameters gives:

$$h_{t6M} = h_0 \cdot \frac{(1+f)\, \tau_t \tau_\lambda + \alpha \tau_r \tau_f}{1+\alpha+f}$$

To determine the mixed-out exit pressure p_{6M}, we apply conservation of x -momentum along the streamwise direction (Figure 4.49). For steady, uniform flow, the momentum rate is expressed as $\dot{m}V_x$. Applying this to the mixer control volume:

$$\dot{m}_{6M} V_{6M} - (\dot{m}_5 V_5 + \dot{m}_{15} V_{15}) = \sum F_x$$

The term $\sum F_x$ represents the net external force acting on the control volume in the x -direction, comprised of integrated pressure forces and wall shear stresses over the wetted surface:

$$\sum F_x = p_5 A_5 + p_{15} A_{15} - p_{6M} A_{6M} - \int \tau_w dA_{\text{wetted}}$$

where the surface integral represents the internal wall friction drag, $D_{f,\text{mixer}}$.

Per the Kutta condition, the static pressures at the core and fan duct inlets are equal:

$$p_5 = p_{15}$$

Additionally, for a constant-area mixer:

$$A_{6M} = A_5 + A_{15}$$

Combing the above equations yields:

$$(\dot{m}_{6M} V_{6M} + p_{6M} A_{6M}) - (\dot{m}_5 V_5 + p_5 A_5) - (\dot{m}_{15} V_{15} + p_{15} A_{15}) = -D_{f,\text{mixer}}$$

Each grouped quantity $(\dot{m}V + pA)$ represents the flow impulse, I, at stations $6M$, 5, and 15, respectively. Consequently, the exit impulse is reduced relative to the sum of the inlet impulses due to wall friction.

Energy conservation for an insulated mixer is written as:

$$\dot{m}_5 h_{t5} + \dot{m}_{15} h_{t15} = \dot{m}_{6M} h_{t6M}$$

Solving for the mixed-out total enthalpy h_{t6M} in terms of inlet variables:

$$h_{t6M} = \frac{(1+f)\, h_{t5} + \alpha h_{t15}}{1+\alpha+f}$$

In non-dimensional form, becomes:

$$h_{t6M} = h_0 \left[\frac{(1+f)\, \tau_t \tau_\lambda + \alpha \tau_r \tau_f}{1+\alpha+f} \right]$$

To find the exit pressure p_{6M}, we apply x -momentum conservation along the flow axis. Assuming steady, 1D flow where momentum flux is $\dot{m}V_x$:

$$\dot{m}_{6M} V_{6M} - (\dot{m}_5 V_5 + \dot{m}_{15} V_{15}) = \sum F_x$$

The net axial force $\sum F_x$ accounts for pressure forces and wetted wall shear stress:

$$\sum F_x = p_5 A_5 + p_{15} A_{15} - p_{6M} A_{6M} - D_{f,\text{mixer}}$$

where $D_{f,\text{mixer}} = \int \tau_w dA_{\text{wetted}}$ is the mixer friction drag.

Assuming equal inlet static pressures ($p_5 = p_{15}$, via the Kutta condition) and a constant cross-sectional area ($A_{6M} = A_5 + A_{15}$), yields:

$$(\dot{m}_{6M} V_{6M} + p_{6M} A_{6M}) - (\dot{m}_5 V_5 + p_5 A_5) - (\dot{m}_{15} V_{15} + p_{15} A_{15}) = -D_{f,\text{mixer}}$$

Recognizing the term $(\dot{m}V + pA)$ as the flow impulse function I, If wall friction is neglected, impulse conservation simplifies to:

$$I_{6M} = I_5 + I_{15}$$

We make this inviscid assumption to obtain a closed-form analytical solution for the exit state, later introducing an empirical correction factor for total pressure friction losses.

Using $a^2 = kp/\rho$, the impulse I is recast in Mach number form:

The frictionless impulse equation:

$$p_{6M} A_{6M} \left(1 + k_{6M} M a_{6M}^2\right) - p_5 A_5 \left(1 + k_5 M a_5^2\right) - p_{15} A_{15} \left(1 + k_{15} M a_{15}^2\right) = 0$$

Nondimensionalizing by A_5 removes geometric scale:

$$p_{6M} \left(1 + k_{6M} M a_{6M}^2\right) \left(1 + \frac{A_{15}}{A_5}\right) = p_5 \left[\left(1 + k_5 M a_5^2\right) + \frac{A_{15}}{A_5} \left(1 + k_{15} M a_{15}^2\right)\right]$$

Determining the two remaining unknowns (p_{6M} and M_{6M}) requires the continuity equation, written in terms of static pressure, Mach number, and total temperature:

$$\dot{m} = \frac{kpAMa}{\sqrt{kRT_t}} \sqrt{1 + \frac{k-1}{2} Ma^2}$$

Applying mass conservation across the mixer yields:

$$\frac{p_{6M} M a_{6M} \sqrt{1 + \frac{k_{6M} - 1}{2} M a_{6M}^2}}{\sqrt{k_{6M} R_{6M} T_{t6M}}} \left(1 + \frac{A_{15}}{A_5}\right) = \frac{p_5 M a_5 \sqrt{1 + \frac{k_5 - 1}{2} M a_5^2}}{\sqrt{k_5 R_5 T_{t5}}} + \frac{p_{15} M a_{15} \sqrt{1 + \frac{k_{15} - 1}{2} M a_{15}^2}}{\sqrt{k_{15} R_{15} T_{t15}}} \left(\frac{A_{15}}{A_5}\right)$$

This page titled 4.4: Turbofan Engine is shared under a CC BY 4.0 license and was authored, remixed, and/or curated by Haifa El-Sadi.

4.5: Turboprop Engine

While the core turbine provides the necessary shaft power to run the compressor, the gas exiting station 5 remains highly energetic (p_{t5}, T_{t5}). By expanding this gas through an additional "power" turbine, shaft power is extracted and delivered through a reduction gearbox (GB) to drive the propeller as seen in Figure 10. Compared to a turbofan, the key benefit of a turboprop engine is its ability to operate at an extraordinarily large bypass ratio, typically between 30 and 100. Propellers convert mechanical shaft power (torque) into propulsive thrust for vehicle motion. Although this text focuses primarily on aircraft propulsion, the underlying aerodynamic and hydrodynamic principles apply equally to marine applications, including surface ships and submarines.

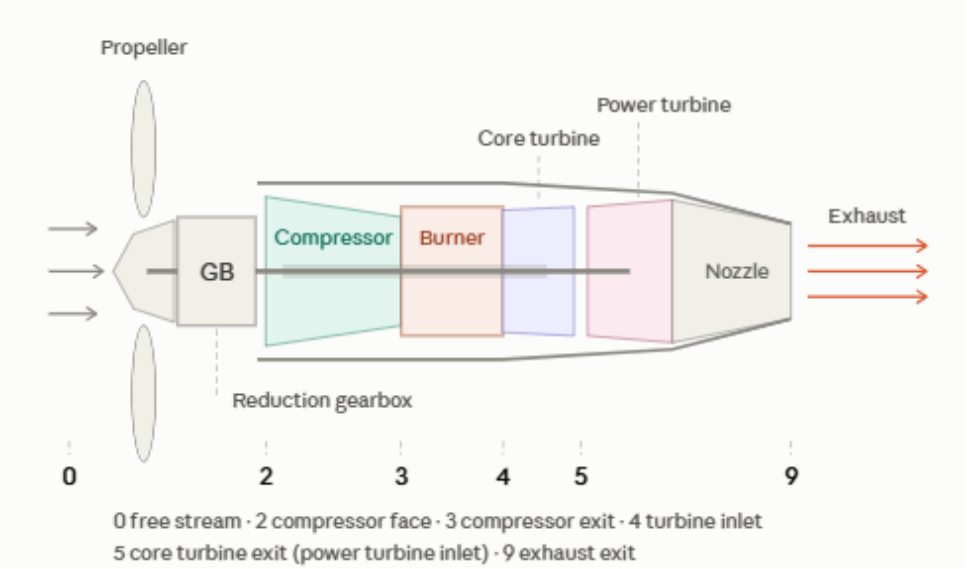


Figure 10: Turboprop Engine

Two primary aerodynamic methodologies govern propeller performance analysis: Momentum (Actuator Disk) Theory and Blade Element Theory. Momentum theory takes a macroscopic approach, treating the propeller as an infinitely thin disk that creates an instantaneous pressure jump within a fluid control volume. By applying global mass, momentum, and energy conservation, it yields fundamental estimates for ideal thrust, power requirements, and slipstream velocities without requiring details about blade geometry. In contrast, Blade Element Theory adopts a local, microscopic approach by dividing each blade into a series of 2D airfoil cross-sections along its radius. We will focus on momentum theory.

Consider an axisymmetric propeller disk in a uniform, incompressible stream ($\rho = \rho_0$). The incoming flow has zero swirl, but immediately downstream of the disk, a uniform tangential velocity $V_{\theta p'}$ is imparted. Far downstream (Station 1), the flow relaxes to ambient static pressure p_0 with axial velocity V_1 and swirl velocity $V_{\theta 1}$. The known parameters: Flight conditions: V_0, p_0, ρ_0, Disk area: A_p, Shaft power: $\mathcal{P}_p$, Shaft angular speed: ω, unknown variables**:** $A_0, A_1, V_p, V_{\theta p'}, V_1, V_{\theta 1}, p_p, p_{p'}$

Governing equations are constructed using fundamental conservation laws:

1. Continuity:
2. Upstream Bernoulli Equation (ignoring radial velocity):
3. Downstream Bernoulli Equation (including swirl component $V_{\theta p'}$):

$V_{\theta p'}$ is the tangential (swirl) velocity imparted by the rotating blades directly behind the disk, and $\frac{1}{2}\rho_0 V_{\theta p'}^2$ measures the corresponding swirl kinetic energy per unit volume. V_θ is the tangential (swirl) velocity of the air, measuring its rotational speed around the propeller axis rather than its axial motion along it.

1. Axial Linear Momentum Balance:

Here are two ways to rewrite the passage, formatted cleanly with standardized mathematical notation and clear technical transitions.

The static pressure jump across the disk generates propeller thrust acting in the $-z$ direction, with an equal and opposite reaction force applied to the fluid in the $+z$ direction. Equation 4.2.1 assumes that the streamwise integrals of static pressure along the captured streamtube boundaries (upstream and downstream of the disk) are negligible compared to the net propeller thrust. For a more detailed treatment of the underlying assumptions leading to Equation 4.2.1, see von Mises (1959).

The shaft power absorbed by the propeller ($\mathcal{P}_p$) converts into useful thrust power plus the net rate of kinetic energy imparted to the slipstream between Stations 0 and 1:

$$\mathcal{P}_p = F_{\text{prop}} V_0 + \dot{m}_p \left(\frac{V_1^2}{2} + \frac{V_{\theta 1}^2}{2} - \frac{V_0^2}{2} \right)$$

where the ideal net thrust is defined by the pressure jump across the disk:

$$F_{\text{prop}} = \left(p_{p'} - p_p \right) A_p$$

Applying conservation of angular momentum between the disk outlet and far downstream yields two equivalent expressions for shaft torque (τ_{prop}) and absorbed shaft power:

$$\mathcal{P}_p = \omega \cdot \tau_{\text{prop}} = \omega \int_0^{r_1} (r V_\theta) \rho_0 V_1 \left(2\pi r dr \right) = \frac{2}{3} \dot{m}_p \omega \overline{V}_{\theta 1} r_1$$

$$\mathcal{P}_p = \omega \cdot \tau_{\text{prop}} = \omega \int_0^{r_p} (r V_{\theta p'}) \rho_0 V_p \left(2\pi r dr \right) = \frac{2}{3} \dot{m}_p \omega \overline{V}_{\theta p'} r_p$$

Here, $\overline{V}_{\theta 1}$ and $\overline{V}_{\theta p'}$ represent the torque-weighted mean swirl velocities far downstream and immediately behind the disk, respectively.

Together, these fundamental conservation principles establish a closed system of eight coupled non-linear equations for the eight flow unknowns. Following Rankine, we can introduce two simplifying approximations to derive an analytical solution:

1. Neglect the swirl kinetic energy term in the downstream Bernoulli relation
2. Omit the swirl kinetic energy contribution in the global power balance, retaining only axial kinetic energy changes.

The simplified governing equations then reduce to:

$$p_{p'} + \frac{1}{2} \rho_0 V_p^2 \approx p_0 + \frac{1}{2} \rho_0 V_1^2$$

$$\mathcal{P}_p \approx F_{\text{prop}} V_0 + \dot{m}_p \left(\frac{V_1^2}{2} - \frac{V_0^2}{2} \right)$$

$$F_{\text{prop}} \approx \rho_0 V_p A_p \left(V_1 - V_0 \right) \qquad (\text{acting in the } -z \text{ forward thrust direction})$$

Subtracting the upstream Bernoulli relation from the simplified downstream relation yields:

$$p_{p'} - p_p \approx \frac{1}{2} \rho_0 \left(V_1^2 - V_0^2 \right) = \frac{F_{\text{prop}}}{A_p}$$

Substituting F_{prop} / A_p yields:

$$V_p \approx \frac{1}{2} \left(V_0 + V_1 \right)$$

Under Rankine's idealizations, the axial flow speed at the propeller plane (V_p) is simply the arithmetic average of the freestream flight speed (V_0) and the far-downstream slipstream speed (V_1). Next, substituting the thrust expression into the energy balance gives:

$$\mathcal{P}_p \approx \rho_0 V_p A_p \left(V_1 - V_0 \right) V_0 + \rho_0 V_p A_p \left(\frac{V_1^2 - V_0^2}{2} \right)$$

Substituting V_p will reduce the formulation to a single unknown, V_1. Expressing this relationship in terms of the velocity ratio V_1 / V_0

yields a cubic equation:

$$\frac{\mathcal{P}_p}{\left(\frac{1}{2}\rho_0 V_0^2\right) V_0 A_p} = \frac{1}{2}\left(\frac{V_1}{V_0}\right)^3 + \frac{3}{2}\left(\frac{V_1}{V_0}\right)^2 - \frac{1}{2}\left(\frac{V_1}{V_0}\right) - \frac{3}{2}$$

The non-dimensional parameter on the left-hand side composed of known operating values is defined as the propeller power coefficient or power loading, C_P. As expected, the required shaft power vanishes when the velocity ratio V_1/V_0 approaches unity (i.e., when no thrust is produced).

Finally, propeller efficiency (η_{prop}) is defined as the ratio of useful thrust power delivered to the total shaft power absorbed:

$$\eta_{\text{prop}} \equiv \frac{F_{\text{prop}} V_0}{\mathcal{P}_p}$$

Applying the ideal kinetic energy balance across the streamtube yields the classic Froude propulsive efficiency relation:

$$\eta_p \equiv \frac{F_{\text{prop}} V_0}{\dot{m}_p \left(\frac{V_1^2 - V_0^2}{2}\right)} \approx \frac{2V_0}{V_0 + V_1}$$

Note that propeller efficiency (η_{prop}) and ideal propulsive efficiency (η_p) are directly related. In fact, propulsive efficiency represents the theoretical upper limit of propeller efficiency, expressed as:

$$\eta_{\text{prop}} \equiv \frac{F_{\text{prop}} V_0}{\mathcal{P}_p} = \left[\frac{F_{\text{prop}} V_0}{\dot{m}_p \left(\frac{V_1^2 - V_0^2}{2}\right)}\right]\left[\frac{\dot{m}_p \left(\frac{V_1^2 - V_0^2}{2}\right)}{\mathcal{P}_p}\right] = \eta_p \cdot \eta_L$$

where η_L is the internal (loss) efficiency factor, defined as the ratio of actual kinetic energy added to the fluid stream relative to the absorbed shaft power:

$$\eta_L \equiv \frac{\dot{m}_p \left(\frac{V_1^2 - V_0^2}{2}\right)}{\mathcal{P}_p}$$

This factor η_L represents the internal efficiency of the propeller in converting absorbed shaft power into useful kinetic power within the fluid stream.

This page titled 4.5: Turboprop Engine is shared under a CC BY 4.0 license and was authored, remixed, and/or curated by Haifa El-Sadi.

4.6: Problems and References

Problem#1

A multistage axial-flow compressor processes a mass flow rate of $60\ \mathrm{kg/s}$ with an overall total pressure ratio of 40. The compressor operates with a polytropic efficiency of $e_c = 0.88$. At the compressor inlet, the total temperature and total pressure are $T_{t2} = 295\ \mathrm{K}$ and $p_{t2} = 101.3\ \mathrm{kPa}$, respectively. Assuming steady, adiabatic flow and constant fluid properties throughout the compression process ($k = 1.40$ and $c_p = 1004.5\ \mathrm{J/(kg \cdot K)}$), determine:

1. The compressor exits total temperature, T_{t3} (K)
2. The overall compressor adiabatic (isentropic) efficiency, η_c
3. The required compressor shaft power, $\mathcal{P}_c$ (MW)

Problem#2

A gas turbine combustor operates with an inlet total temperature of $T_{t3} = 1150\ ^\circ\mathrm{R}$ and an inlet total pressure of $p_{t3} = 450\ \mathrm{psia}$. The incoming air mass flow rate is $\dot{m}_a = 220\ \mathrm{lbm/s}$, with inlet fluid properties of $k_3 = 1.40$ and $c_{p3} = 0.240\ \mathrm{Btu/(lbm \cdot ^\circ R)}$. A hydrocarbon fuel with a lower heating value of $Q_R = 18,500\ \mathrm{Btu/lbm}$ is injected into the burner at a rate of $\dot{m}_f = 4.4\ \mathrm{lbm/s}$. The combustor operates with a burner efficiency of $\eta_b = 0.98$, and fluid friction/heat addition results in a 4% total pressure loss across the burner ($p_{t4} = 0.96 p_{t3}$). The working fluid properties at the combustor exit are $k_4 = 1.33$ and $c_{p4} = 0.276\ \mathrm{Btu/(lbm \cdot ^\circ R)}$.

Calculate:

1. The fuel-to-air ratio, f
2. The combustor exit total pressure, p_{t4} (psia)
3. The combustor exit total temperature, T_{t4} (R)

Problem#3

An uncooled turbine receives working fluid at its inlet with conditions matching the combustor exit: $T_{t4} = 1450\ \mathrm{K}$, $p_{t4} = 3.0\ \mathrm{MPa}$, and total mass flow rate $\dot{m} = 105\ \mathrm{kg/s}$. The turbine operates with an adiabatic efficiency of $\eta_t = 0.88$. The total power extracted by the turbine to drive the compressor and engine accessories is $\mathcal{P}_t = 65\ \mathrm{MW}$.

Assuming the fluid properties remain constant across the turbine stage at $k = 1.33$ and $c_p = 1150\ \mathrm{J/(kg \cdot K)}$, calculate:

1. The turbine exit total temperature, T_{t5} (K)
2. The turbine stage polytropic efficiency, e_t
3. The turbine exit total pressure, p_{t5} (kPa)
4. The required total temperature drop across the turbine, $\Delta T_t = T_{t4} - T_{t5}$ (K)

Problem#4

Consider a supersonic convergent–divergent (CD) exhaust nozzle operating at a nozzle pressure ratio of $\mathrm{NPR} = 12$. The working fluid maintains constant gas properties throughout the expansion, given by $k = 1.30$ and $c_p = 1240\ \mathrm{J/(kg \cdot K)}$. The nozzle's adiabatic expansion efficiency is $\eta_n = 0.96$.

Determine:

1. The nozzle total pressure recovery ratio (π_n).
2. The area ratio of the exit to the throat (A_9/A_8) for a perfectly expanded condition.
3. The nozzle exit Mach number (Ma_9) under perfectly expanded operation

Problem#5

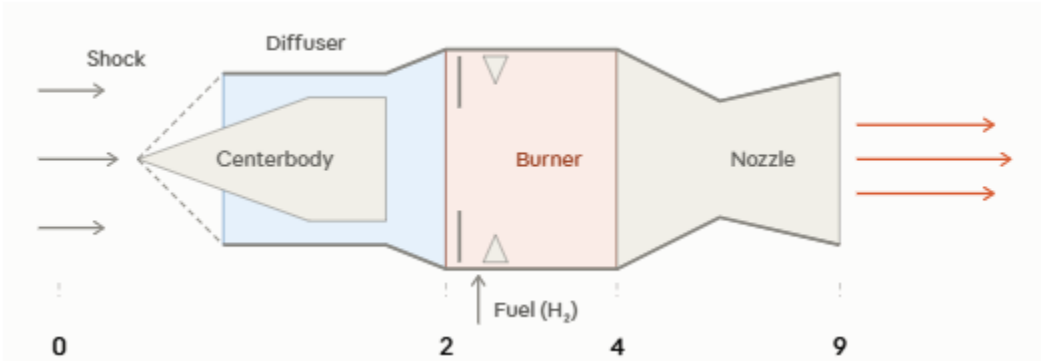
A ramjet flies at a flight Mach number of $Ma_0 = 3.2$ in an altitude ambient environment where $T_0 = 390^\circ\mathrm{R}$ ($p_0 = 1.6$ psia). The inlet diffuser has a total pressure recovery of $\pi_d = 0.88$. The combustor burns hydrogen fuel with a lower heating value of $Q_R = 50,500\ \mathrm{Btu/lbm}$ at a burner efficiency of $\eta_b = 0.96$, raising the total temperature at the burner exit to $T_{t4} = 3800^\circ\mathrm{R}$. The nozzle expands the gas perfectly back to ambient pressure ($p_9 = p_0$) but experiences a total pressure loss fraction of $\pi_n = 0.94$.

Assume standard gas properties throughout the engine:

- Air/Unburned Fluid (Inlet & Diffuser): $k_0 = 1.40$, $c_{pc} = 0.240\ \mathrm{Btu/(lbm \cdot {}^\circ R)}$
- Burner & Exhaust Fluid: $k_g = 1.33$, $c_{pg} = 0.276\ \mathrm{Btu/(lbm \cdot {}^\circ R)}$

Calculate:

1. Fuel-to-air ratio, f
2. Nozzle exit Mach number, Ma_9
3. Specific net thrust, $F_n/\dot{m}_0$ ($\mathrm{lbf/\,(lbm/s)}$)
4. Thermal efficiency, η_{th}
5. Propulsive efficiency, η_p



Problem#6

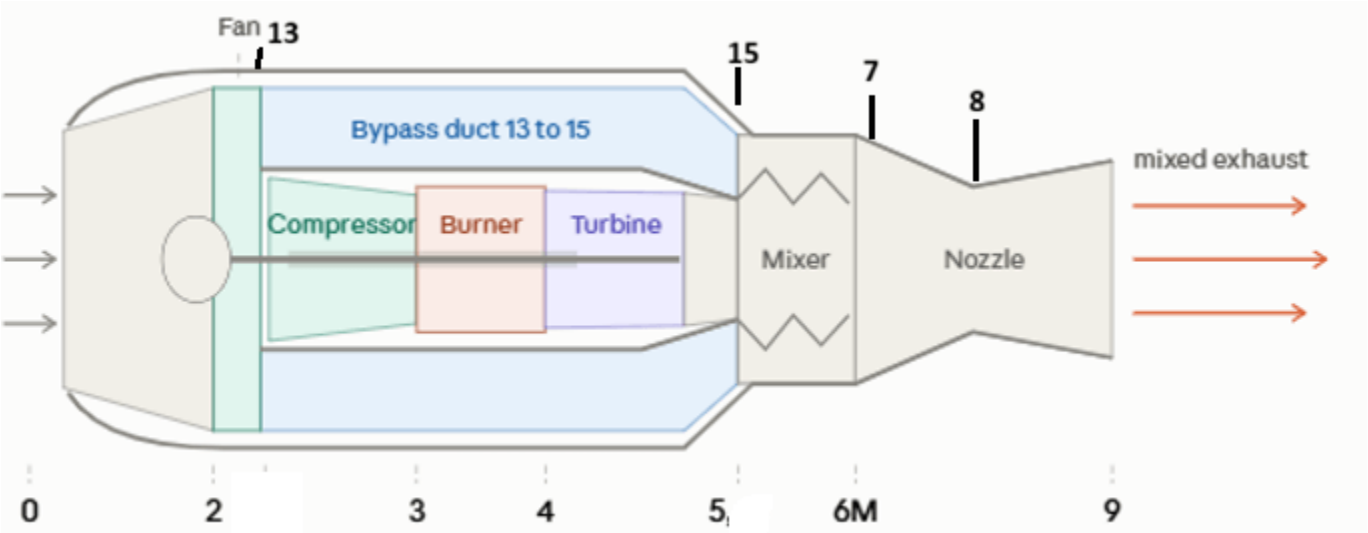
A non-afterburning mixed-flow turbofan engine operates under the following design and limit parameters at high-altitude supersonic flight:

- Flight Conditions: Flight Mach number $Ma_0 = 2.0$, ambient static pressure $p_0 = 12\ \mathrm{kPa}$, ambient static temperature $T_0 = 220\ \mathrm{K}$ ($-53.15^\circ\mathrm{C}$). Gas constant $R = 287\ \mathrm{J/(kg \cdot K)}$ and specific heat ratio $k = 1.40$ ($c_p = 1004.5\ \mathrm{J/(kg \cdot K)}$) throughout the engine.
- Inlet & Mass Flow: Total engine mass flow rate $\dot{m}_0 = (1+\alpha)\,\dot{m}_{\mathrm{core}} = 30\ \mathrm{kg/s}$, inlet total pressure recovery $\pi_d = 0.88$.
- Fan & Compressor: Fan pressure ratio $\pi_f = 1.6$, fan polytropic efficiency $e_f = 0.89$. Overall compressor pressure ratio $\pi_c = 18$, compressor polytropic efficiency $e_c = 0.89$.
- Combustor: Combustor total pressure ratio $\pi_b = 0.94$, burner efficiency $\eta_b = 0.98$, fuel lower heating value $Q_R = 43,000\ \mathrm{kJ/kg}$, turbine inlet total temperature $T_{t4} = 1723.15\ \mathrm{K}$ ($1450^\circ\mathrm{C}$).
- Turbine & Mechanical Transmission: Turbine polytropic efficiency $e_t = 0.90$, mechanical transmission efficiency $\eta_m = 0.97$, Mach number at turbine exit Station 5 $Ma_5 = 0.45$.
- Mixer & Duct: Fan duct (Stations 13 to 15) is frictionless and adiabatic ($p_{t15} = p_{t13}, T_{t15} = T_{t13}$). Total pressure ratio across fan side of mixer $\pi_{M,f} = 0.97$. Equal static pressure constraint applies at mixer entry ($p_{15} = p_6$).
- Exhaust Nozzle: Nozzle total pressure ratio $\pi_n = 0.92$, nozzle exit static pressure matches ambient ($p_9 = p_0$).

Calculate:

1. Ram drag, D_R (kN)
2. Inlet exit/Fan inlet stagnation properties: p_{t2} (kPa) and T_{t2} (K)
3. Compressor exit stagnation properties: p_{t3} (kPa) and T_{t3} (K)

4. Fan duct exit stagnation properties: p_{t13} (kPa) and T_{t13} (K)
5. Burner exit total pressure p_{t4} (kPa) and turbine exit total temperature T_{t5} (K)
6. Fuel-to-air ratio, f
7. Bypass ratio α, core mass flow rate $\dot{m}_{\text{core}}$ (kg/s), and fan duct mass flow rate $\dot{m}_{\text{fan}}$ (kg/s)
8. Mixed total temperature T_{t6M} (K)
9. Nozzle inlet stagnation properties: p_{t9} (kPa) and T_{t9} (K)
10. Nozzle exit Mach number M_9 and exit velocity V_9 (m/s)
11. Gross thrust F_g (kN) and net thrust F_n (kN)
12. Thrust-specific fuel consumption (TSFC) (mg/s/N)



Problem#7

A single-spool turbojet engine operates under the following on-design (sea-level static) conditions:

- Flight Conditions: $Ma_0 = 0$, $p_0 = 101.325$ kPa, $T_0 = 288.15$ K, $k = 1.40$, and $c_p = 1.0045$ kJ/(kg · K).
- Inlet: Total pressure recovery ratio $\pi_d = 0.98$.
- Compressor: Overall total pressure ratio $\pi_c = 25$, polytropic efficiency $e_c = 0.88$.
- Combustor: Burner efficiency $\eta_b = 0.98$, burner total pressure ratio $\pi_b = 0.94$, fuel lower heating value $Q_R = 43,000$ kJ/kg, and burner temperature ratio limit parameter $\tau_\lambda = \dfrac{T_{t4}}{T_0} = 6.2$.
- Turbine: Polytropic efficiency $e_t = 0.89$, mechanical transmission efficiency $\eta_m = 0.96$.
- Nozzle: Total pressure ratio $\pi_n = 0.97$, perfectly expanded ($p_9/p_0 = 1.0$).

Calculate for the on-design condition:

1. Compressors exit total pressure p_{t3} (kPa) and compressor temperature ratio $\tau_c = T_{t3}/T_{t2}$.
2. Fuel-to-air ratio f and combustor exit total pressure p_{t4} (kPa).
3. Turbine temperature ratio $\tau_t = T_{t5}/T_{t4}$.

   For the off-design condition ($M_0 = 0.80$ at an altitude of 11 km, where $T_{0,\text{off}} = 216.65$ K, $p_{0,\text{off}} = 22.63$ kPa), the engine throttle is adjusted such that $T_{t4,\text{off}} = 0.92 T_{t4,\text{design}}$. Assuming constant turbine temperature ratio ($\tau_{t,\text{off}} = \tau_{t,\text{design}}$) and choked turbine nozzle conditions:

4. Calculate the off-design compressor total pressure ratio, $\pi_{c,\text{off}}$.

Problem#8

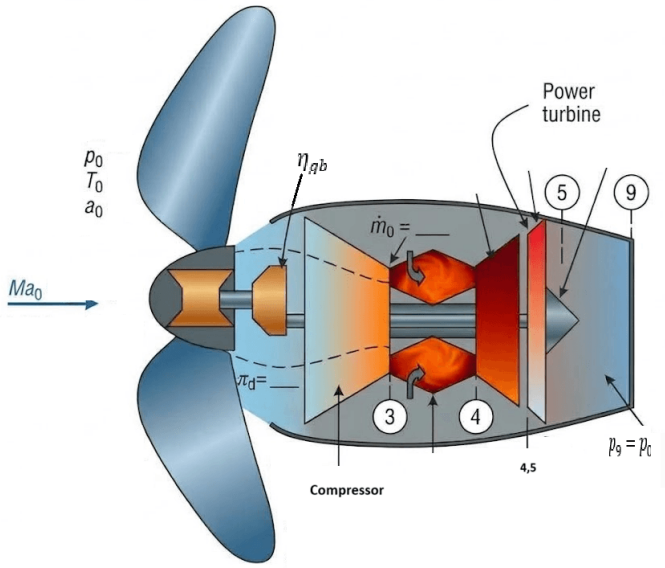
An advanced turboprop engine flies at a cruise Mach number of $Ma_0 = 0.70$ at a standard flight altitude of $35,000$ ft ($T_0 = 394.1$ °R , $p_0 = 3.468$ psia, $a_0 = 973.1$ ft/s). The core mass flow rate is $\dot{m}_{\text{core}} = 45$ lbm/s.

The design and operating component parameters are as follows:

- Diffuser: Total pressure recovery ratio $\pi_d = 0.98$
- Compressor: Overall pressure ratio $\pi_c = 20$, polytropic efficiency $e_c = 0.90$
- Combustor: Total pressure ratio $\pi_b = 0.95$, burner efficiency $\eta_b = 0.98$, fuel heating value $Q_R = 18,500$ Btu/lbm, turbine inlet total temperature $T_{t4} = 3000$ °R
- Compressor Turbine: Drives the compressor with mechanical efficiency $\eta_{m1} = 0.99$ and polytropic efficiency $e_{t1} = 0.90$
- Power Turbine: Drives the propeller through a reduction gearbox ($\eta_{gb} = 0.98$) with mechanical efficiency $\eta_{m2} = 0.98$ and polytropic efficiency $e_{t2} = 0.90$
- Propeller: Propeller efficiency $\eta_{\text{prop}} = 0.83$
- Exhaust Nozzle: Total pressure ratio $\pi_n = 0.96$, expanding to ambient pressure
- Fluid Properties: $k = 1.40$, $c_p = 0.240$ Btu/(lbm ·°R) throughout the engine.

Assuming an optimum power split fraction (α_{opt}) that maximizes total net thrust, calculate:

1. Core net thrust, $F_{n,\text{core}}$ (lbf)
2. Propeller net thrust, $F_{n,\text{prop}}$ (lbf)
3. Overall thrust-specific fuel consumption, TSFC (lbm/(h · lbf))
4. Overall engine thermal efficiency (η_{th}) and overall efficiency (η_o)



Problem#9

A military supersonic jet powered by a augmented (afterburning) turbojet engine operates at a cruise Mach number of $Ma_0 = 2.2$ at an altitude where the static pressure is $p_0 = 12$ kPa and ambient static temperature is $T_0 = -50°\text{C}$ (223.15 K).

The cold-section gas properties are $k_c = 1.4$ and $c_{pc} = 1005$ J/(kg · K). The engine component performance characteristics are:

- Inlet Diffuser: Total pressure recovery ratio $\pi_d = 0.90$
- Compressor: Overall pressure ratio $\pi_c = 15$, polytropic efficiency $e_c = 0.89$
- Main Combustor: Non-dimensional enthalpy limit $\tau_\lambda = 8.5$, fuel heating value $Q_R = 43,000$ kJ/kg, burner efficiency $\eta_b = 0.98$, pressure ratio $\pi_b = 0.96$
- Turbine: Hot-gas properties $k_t = 1.33$ and $c_{pt} = 1150$ J/(kg · K), polytropic efficiency $e_t = 0.84$, mechanical transmission

efficiency $\eta_m = 0.99$
- Afterburner: Non-dimensional enthalpy limit $\tau_{\lambda\mathrm{AB}} = 11.5$, fuel heating value $Q_{R\mathrm{AB}} = 43,000\ \mathrm{kJ/kg}$, combustion efficiency $\eta_{\mathrm{AB}} = 0.97$, pressure ratio $\pi_{\mathrm{AB}} = 0.94$, gas properties $k_{\mathrm{AB}} = 1.30$ and $c_{p\mathrm{AB}} = 1240\ \mathrm{J/(kg \cdot K)}$
- Exhaust Nozzle: Pressure ratio $\pi_n = 0.95$, expanding to ambient pressure ($p_9 = p_0$)

Determine:

1. Stagnation pressures (p_t) and temperatures (T_t) at all major engine stations, along with main burner (f) and afterburner (f_{AB}) fuel-to-air ratios.
2. Non-dimensional specific thrust $\dfrac{F_n}{\dot{m}_0 a_0}$.
3. Thrust Specific Fuel Consumption (TSFC) expressed in $\mathrm{mg/(s \cdot N)}$.
4. Overall thermal efficiency (η_{th}) and propulsive efficiency (η_p).

References

Mattingly, J. D. (1996). *Elements of Gas Turbine Propulsion*. McGraw-Hill Education.

(2nd Edition: Mattingly, J. D., & Boyer, K. M. (2014). American Institute of Aeronautics and Astronautics).

Mattingly, J. D., Heiser, W. H., & Pratt, D. T. (2002). *Aircraft Engine Design* (2nd ed.). American Institute of Aeronautics and Astronautics (AIAA).

Farokhi, S. (2014). *Aircraft Propulsion* (2nd ed.). John Wiley & Sons.

Kerrebrock, J. L. (1992). *Aircraft Engines and Gas Turbines* (2nd ed.). The MIT Press

This page titled 4.6: Problems and References is shared under a CC BY 4.0 license and was authored, remixed, and/or curated by Haifa El-Sadi.

5: COMPRESSOR AND TURBINES

5.0: Introduction
5.1: Axial-Flow Turbomachinery
5.2: Radial / Centrifugal Turbomachinery
5.4: Problems and References

This page titled 5: Compressor and Turbines is shared under a CC BY 4.0 license and was authored, remixed, and/or curated by Haifa El-Sadi.

5.0: Introduction

The integration of a compressor and turbine into a self-sustaining aircraft engine was achieved almost simultaneously in the late 1930s by two independent inventors: Sir Frank Whittle in Great Britain and Hans von Ohain in Germany. While serving as a Royal Air Force pilot, Whittle patented the concept of linking a compressor to a gas-driven turbine in 1930, successfully running his first experimental engine on a test stand by April 1937. Unaware of Whittle's work, German physicist Hans von Ohain developed his own turbojet design and secured backing from industrialist Ernst Heinkel, which led to his engine powering the Heinkel He 178 on August 27, 1939—marking the first flight of a jet-powered aircraft in history. Whittle's engine later made its flight debut aboard the Gloster E.28/39 in May 1941. Shortly thereafter, German engineer Anselm Franz advanced the technology by designing the Junkers Jumo 004, the first mass-produced jet engine to feature an axial compressor and turbine setup, which powered the Messerschmitt Me 262 fighter jet [1].

Gas turbine engines rely on turbomachinery to pressurize air and extract energy. These components are broadly classified into two major aerodynamic categories: axial-flow and radial-flow (centrifugal).

This page titled 5.0: Introduction is shared under a CC BY 4.0 license and was authored, remixed, and/or curated by Haifa El-Sadi.

5.1: Axial-Flow Turbomachinery

In axial-flow compressors and turbines, fluid flows parallel to the engine's central axis of rotation. Axial compressors consist of alternating rows of rotating blades (rotors) and stationary blades (stators). Rotors add kinetic energy to the air, while stators convert that velocity into static pressure. On the other hand, axial compressor offers high mass flow rates, small frontal areas (reducing aerodynamic drag), and high-pressure ratios across multiple stages. The axial compressor is used for modern commercial jetliners and military fighters where high thrust and high aerodynamic efficiency are critical.

For an axial turbine, high-energy gas enters stationary nozzles (vanes) that accelerate the flow and direct it onto rotating turbine blades, transferring mechanical torque to the drive shaft. The axial turbine is highly efficient at handling large mass flows and can be designed with multiple stages (such as Low-Pressure and High-Pressure turbines) to drive different spools. It is used in all large aviation engines to power the compressor stages, intake fans, and external propellers or rotors. Figure 1 shows the axial compressor blade row.

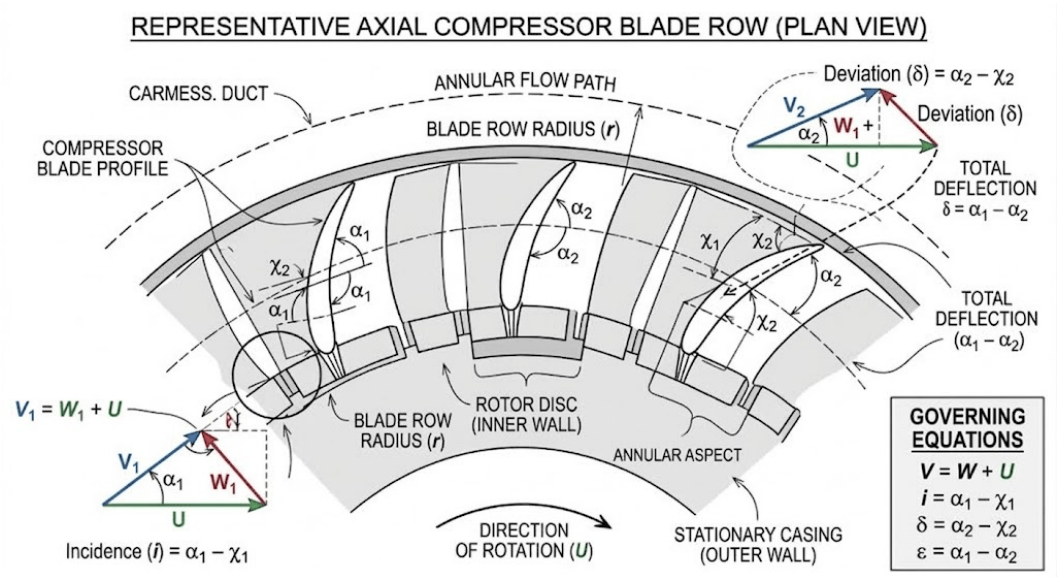


Figure 1. Axial compressor blade row (AI creation)

Velocity Angles (Measured relative to the axial direction):

- α: Absolute gas angle either into or out of the blades
- χ: blade metal angle

The total flow deflection (ϵ) produced by a blade row and it is the total turn bend the air stream undergoes as it passes through the blade row. It is the difference between the gas inlet angle and the gas outlet angle ($\epsilon = \alpha_1 - \alpha_2$).

The incidence angle (i) is defined as the difference between the gas inlet angle and the blade metal inlet angle ($i = \alpha_1 - \chi_1$). The incidence measures how accurately the incoming air stream aligns with the physical leading edge of the blade.

Conversely, the difference between the gas outlet angle and the blade metal outlet angle is defined as the deviation angle ($\delta = \alpha_2 - \chi_2$). Deviation measures the failure of the gas flow to leave the blade row perfectly parallel to the physical trailing edge metal angle. Deviation depends primarily on blade row geometry, inlet Mach number (Ma), and incidence (i).

An axial compressor stage consists of a rotating Rotor followed by a stationary Stator. The passage between compressor rotor blades acts as a diffusing channel (expanding area relative to flow).

Core Vector Velocity Equations

1.

2.
3.

where:

1. $\mathbf{V}$ = Absolute fluid velocity vector
2. $\mathbf{W}$ = Relative fluid velocity vector
3. $\mathbf{U}$ = Tangential blade speed vector

Axial Velocity Components (V_a)

The relative flow angles are $\beta_1 = \chi + i$ at inlet and $\beta_2 = \chi + \delta$ at outlet, taking V_a as the axial velocity component perpendicular to the tangential blade speed U:

1. $$V_{a1} = V_1 \cos\alpha_1 = W_1 \cos\beta_1$$
2. $$V_{a2} = V_2 \cos\alpha_2 = W_2 \cos\beta_2$$

(For ideal continuous flow across a constant-area annulus, $V_{a1} = V_{a2} = V_a$.)

Tangential Velocity Components (V_θ, W_θ)

1. $$V_{\theta 1} = V_1 \sin\alpha_1 = V_{a1} \tan\alpha_1$$
2. $$W_{\theta 1} = W_1 \sin\beta_1 = V_{a1} \tan\beta_1$$
3. $$V_{\theta 2} = V_2 \sin\alpha_2 = V_{a2} \tan\alpha_2$$
4. $$W_{\theta 2} = W_2 \sin\beta_2 = V_{a2} \tan\beta_2$$

Tangential Velocity Sums & Blade Speed (U)

From the geometry of the inlet and outlet velocity triangles:

1. $$U_1 = V_{\theta 1} + W_{\theta 1} = V_{a1} \left(\tan\alpha_1 + \tan\beta_1\right)$$
2. $$U_2 = V_{\theta 2} + W_{\theta 2} = V_{a2} \left(\tan\alpha_2 + \tan\beta_2\right)$$

Absolute and Relative Magnitudes

1. $$V_1 = \sqrt{V_{a1}^2 + V_{\theta 1}^2} = \frac{V_{a1}}{\cos\alpha_{\ 1}}$$
   $$V_2 = \sqrt{V_{a2}^2 + V_{\theta 2}^2} = \frac{V_{a2}}{\cos\alpha_{\ 2}}$$
2. $$W_1 = \sqrt{V_{a1}^2 + W_{\theta 1}^2} = \frac{V_{a1}}{\cos\beta_{\ 1}}$$
   $$W_2 = \sqrt{V_{a2}^2 + W_{\theta 2}^2} = \frac{V_{a2}}{\cos\beta_{\ 2}}$$

The specific torque per unit mass flow rate ($\tau/\dot{m}$) acting on or by the rotor is given by as shown in Figure 2:

$$\tau = \dot{m} \left(r_2 V_{\theta 2} - r_1 V_{\theta 1}\right)$$

- $\dot{m}$: Mass flow rate of the fluid ($\mathrm{kg/s}$)
- r_1, r_2: Radius at the inlet and outlet stations (m)
- $V_{\theta 1}, V_{\theta 2}$: Tangential (whirl) velocity components at inlet and outlet ($\mathrm{m/s}$)

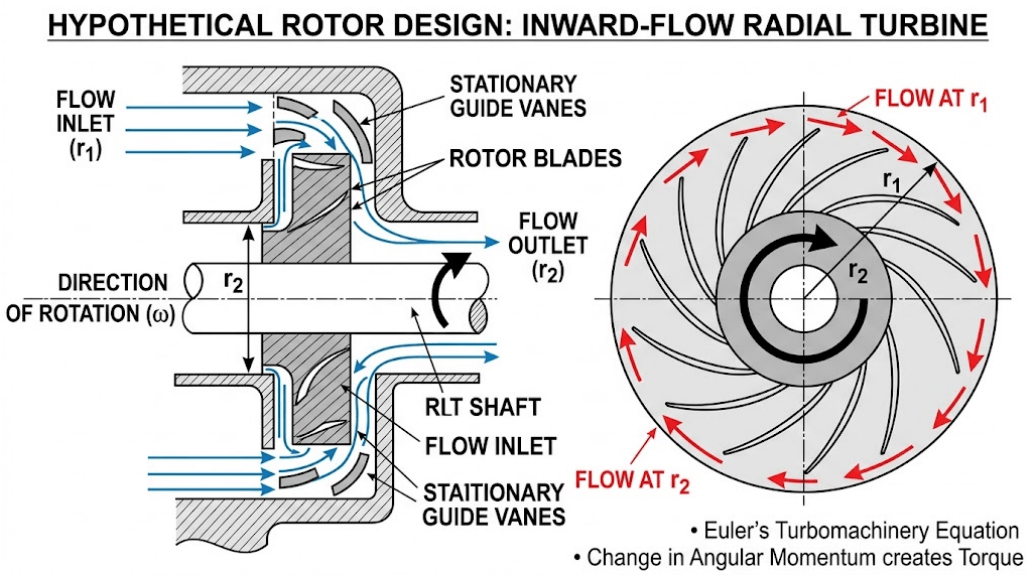


Figure 2. hypothetical rotor design (AI creation)

The power equation is

$$P = \tau \cdot \omega$$

where:

- P = Shaft power
- τ = Mechanical torque generated
- ω = Rotational speed $(\mathrm{rad/s})$

For adiabatic systems with no heat loss ($q = 0$), the First Law of Thermodynamics dictates that the energy extracted from the fluid must equal the shaft power. Combining this with Euler's turbomachinery equation gives:

$$\Delta h_0 = U_2 V_{\theta 2} - U_1 V_{\theta 1}$$

In an axial compressor stage, the fluid moves primarily in the direction parallel to the shaft axis. For a given blade stage, the mean inlet radius equals the mean outlet radius ($r_1 \approx r_2$), which means $U_1 = U_2 = U$

In this case, Euler's power equation simplifies to:

$P = \dot{m} U \left(V_{\theta 2} - V_{\theta 1}\right)$ where $\Delta h_0 = \ U \left(V_{\theta 2} - V_{\theta 1}\right)$

(As gas expands across the turbine rotor passage, relative flow accelerates and is turned sharply toward the axial direction, exerting a driving force on the blade).

4. Specific Work (Euler Turbomachinery Equation)

The specific work (w) transferred between the fluid and the drive shaft is dictated by the change in absolute tangential momentum across the rotor:

$$w = U \cdot \left(C_{\theta 2} - C_{\theta 1}\right)$$

1. **For Compressors ($w > 0$):** Energy is added to the fluid. $C_{\theta 2} > C_{\theta 1}$, turning the gas flow in the direction of rotor motion.
2. **For Turbines ($w < 0$):** Energy is extracted from the fluid. $C_{\theta 1} > C_{\theta 2}$, turning the gas flow against the direction of motion to produce torque.

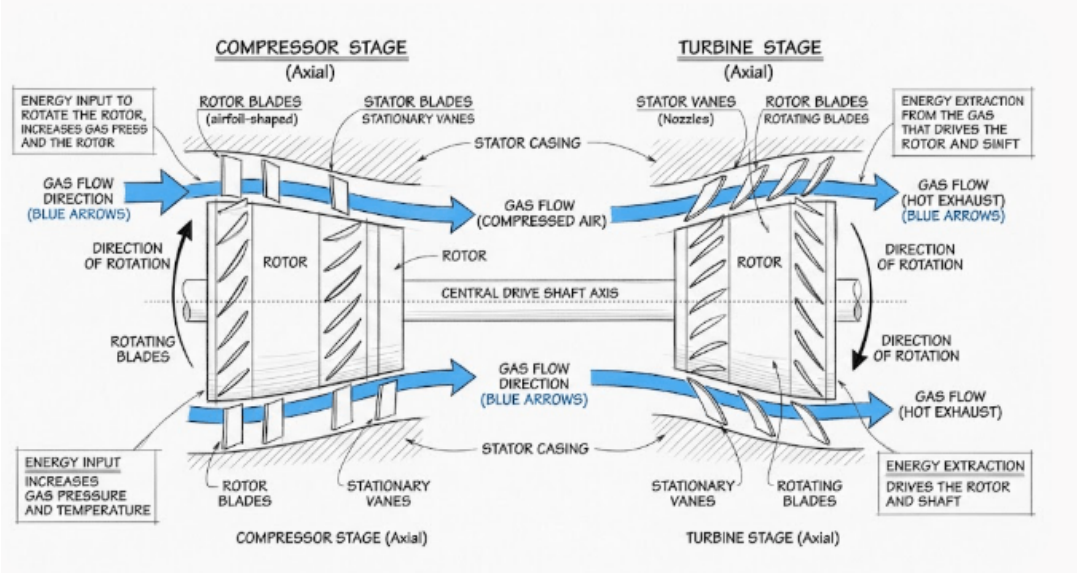


Figure 1. compressor and turbine stages-AI creation

This page titled 5.1: Axial-Flow Turbomachinery is shared under a CC BY 4.0 license and was authored, remixed, and/or curated by Haifa El-Sadi.

5.2: Radial / Centrifugal Turbomachinery

In radial-flow systems, fluid flow moves perpendicular to the rotational axis, directed outward from or inward toward the center.

Centrifugal (Radial) Compressors

For radial compressors, air enters axially at the intake ("impeller eye") and is accelerated outward radially by a high-speed rotating impeller, then slowed down in a stationary diffuser to build static pressure. It achieves a high-pressure ratio in a single stage and is robust against foreign object damage (FOD), but features a larger frontal cross-section. Radial compressors are common in smaller aircraft engines (turboprops, auxiliary power units [APUs], helicopters) and engine starters.

Radial Turbines

For a radial turbine, hot exhaust gas enters radially around the outer diameter and flows inward toward the axis, expanding as it turns to exit axially. It has a simple design, is compact, and is effective for low mass flow applications, though less efficient at high flow rates compared to axial counterparts. It is widely used in automotive turbochargers, small gas turbine APUs, and industrial microturbines.

Mixed-Flow Configurations

Mixed flow combines features of both axial and radial machinery, where the flow exits at an angle between 0° (axial) and 90° (radial). It offers a compromise—higher flow capacity than a purely radial design with a higher pressure rise per stage than a single axial stage. It is used in selected specialized small turboshaft or turboprop engines seeking high efficiency in compact spaces.

This page titled 5.2: Radial / Centrifugal Turbomachinery is shared under a CC BY 4.0 license and was authored, remixed, and/or curated by Haifa El-Sadi.

5.4: Problems and References

Problem 1

a. The engine intake decelerates the airflow during cruise. The axial flow entering the fan has an axial Mach number of $M_{a1} = 0.50$. Assuming this value, determine the static temperature (T_1) and the speed of sound (a_1) at the fan inlet when the aircraft is cruising at $M_\infty = 0.82$ at an altitude of $36,000$ ft (where ambient static temperature $T_\infty = 216.65$ K, $\gamma = 1.4$, and $R = 287$ J/(kg · K)).

b. The engine total mass flow rate at cruise is $\dot{m}_{\text{total}} = 400$ kg/s with a bypass ratio $B = 10.0$ (so core mass flow rate $\dot{m}_{\text{core}} = 36.36$ kg/s). With a fan pressure ratio of 1.6, the required fan outer tip diameter is $D_{\text{tip}} = 2.80$ m (tip radius $r_t = 1.40$ m). Assuming a relative tip Mach number of $M_{\text{a}} = 1.35$, calculate the blade tip velocity (U_t) and the rotational speed of the fan (Ω_{LP} in rad/s). *(Note:* $V_{\text{rel, tip}} = \sqrt{U_t^2 + V_x^2}$*).*

c. The average stagnation pressure ratio across the fan rotor for the core stream is $\pi_f = 1.50$, with an isentropic efficiency of $\eta_f = 0.88$. Find the total (stagnation) pressure (P_{02}) and total (stagnation) temperature (T_{02}) entering the booster (LP compressor).

Problem 2

a. The hub radius increases through the fan and stator downstream of the fan. At the booster inlet, the hub radius r_h and tip radius r_t are 0.48 and 0.56 times the tip radius of the fan ($r_{\text{fan, tip}} = 1.40$ m), making the mean radius of the booster $r_m = 0.52 \cdot r_{\text{fan, tip}} = 0.728$ m. This means radius is constant from inlet to exit. The stators after the fan leave the flow direction at mid-radius inclined at 25° from axial. The effective flow area at booster inlet is $\pi\left(r_t^2 - r_h^2\right)\cos\left(25^\circ\right)$. The core mass flow rate is $\dot{m}_{\text{core}} = 35.0$ kg/s. The stagnation properties entering the booster are $T_{02} = 280.11$ K and $P_{02} = 52.98$ kPa, yielding a speed of sound at mid-span of $a \approx 320$ m/s. The axial Mach number is approximately $M_x \approx 0.42$. Find the resultant velocity V at mid-span, the axial velocity V_x, and the ratio of axial velocity to mean blade speed (V_x/U_m) for the booster, assuming $\Omega_{\text{LP}} = 274.67$ rad/s.

b. Find the stagnation temperature (T_{03}) and pressure (P_{03}) at the outlet of the booster if the overall pressure ratio across the fan and booster combined is 2.8 and the overall efficiency is 88%. Assuming the axial velocity V_x remains constant through the booster, find the static temperature (T_3), static pressure (P_3), and air density (ρ_3) at the booster exit. Hence, calculate the flow area at the exit (A_{exit}) and the corresponding exit blade height (h) where $A_{\text{exit}} \approx 2\pi r_m h$.

c. The pressure ratio across the fan for core flow is 1.5, so the required pressure ratio across the booster alone is $\pi_b = 2.8/1.5 = 1.867$. The stage loading coefficient $\psi = \Delta h_0/U_m^2$ for the booster is not to exceed 0.38. Find the minimum number of stages required and the resulting value of the stage loading coefficient, assuming it is equal across all stages.

Problem 3

a. The fan and LP compressor (booster) combined provide a total pressure ratio of 2.8 to the core stream entering the HP compressor, with an overall efficiency of 88%. The flow at entry to the HP compressor is purely axial with a velocity of $V_x = 160$ m/s. The inlet ambient total temperature is $T_{01} = 245.8$ K and total pressure is $P_{01} = 35.32$ kPa. Find the static temperature (T_{21}), static pressure (P_{21}), air density (ρ_{21}), and Mach number (Ma_{21}) at HP compressor entry. Supposing the hub-to-tip radius ratio at entry is $r_h/r_t = 0.65$ and the core mass flow rate is $\dot{m}_{\text{core}} = 35.0$ kg/s, find the mean radius (r_m), tip radius (r_t), and hub radius (r_h).

b. Throughout the HP compressor, $V_x/U_m = 0.50$, where U_m is the mid-span blade speed. For the first stage, the hub radius is 0.65 times the tip radius ($r_h = 0.65 r_t$). Assuming the relative Mach number at the first stage tip is $\text{Ma} = 1.25$, find the relative velocity ($V_{\text{rel, tip}}$), tip speed (U_t), rotational speed of the HP shaft (Ω_{HP} in rev/s), and the actual axial velocity (V_x).

Problem 4

a. At the HP compressor exit, the flow is purely axial and the mean radius is constant at $r_m = 0.30$ m. The HP compressor operates with a pressure ratio of $\Pi_{\text{HP}} = 15.0$ and an isentropic efficiency of $\eta_{\text{HP}} = 0.88$. The stagnation conditions entering the HP compressor are $T_{021} = 330$ K and $P_{021} = 90.0$ kPa, and the axial velocity is held constant at $V_x = 165$ m/s throughout. For a core mass flow rate of $\dot{m}_{\text{core}} = 32.0$ kg/s, determine the static temperature (T_3), static pressure (P_3), and air density (ρ_3)

at the compressor exit. From these, calculate the required exit cross-sectional area (A_{exit}) and the corresponding exit blade height (h), assuming $A_{\text{exit}} \approx 2\pi r_m h$.

b. If the stage loading coefficient for the HP compressor is constrained to $\psi = \frac{\Delta h_0}{U_m^2} \leq 0.40$ (where $U_m = 350\ \text{m/s}$ is the mean blade speed), determine the minimum number of stages (N) required and the resulting actual stage loading coefficient across all stages.

References

Mattingly, J. D., Heiser, W. H., & Pratt, D. T. (2002). *Aircraft Engine Design* (2nd ed.). American Institute of Aeronautics and Astronautics (AIAA).

"The Design of High-Efficiency Turbomachinery and Gas Turbines" by David Gordon Wilson and Theodosios Korakianitis.

This page titled 5.4: Problems and References is shared under a CC BY 4.0 license and was authored, remixed, and/or curated by Haifa El-Sadi.

6: COMBUSTOR- WORKING FLUID AND MODELS OF ENGINE CYCLES

6.0: Working Fluid Dynamics
6.1: Thermodynamic and Chemical Evolution of Working Fluids
6.2: Thermodynamics Relations for Engine Process
6.3: Problems and References

This page titled 6: Combustor- Working Fluid and Models of Engine Cycles is shared under a CC BY 4.0 license and was authored, remixed, and/or curated by Haifa El-Sadi.

6.0: Working Fluid Dynamics

In internal combustion engines, the working fluid is not a static, idealized medium, but rather a dynamic thermodynamic substance whose chemical composition, phase, and physical properties evolve continuously throughout the engine cycle. This transformation begins during the intake stroke, where the fresh unburned mixture is drawn into the cylinder, mixed with residual combustion gases, and subjected to complex phase-change and thermodynamic interactions. Before entering the cylinder, ambient air is mixed with fuel in the induction system via a carburetor, port fuel injector, or direct cylinder injector. The fresh charge consists primarily of standard atmospheric air and vaporized or atomized hydrocarbon fuel.

In gas turbine engines (turbofans, turbojets, and turboprops), the working fluid flows continuously through the engine, undergoing continuous changes in temperature, pressure, phase, chemical composition, and thermodynamic properties as it moves from the ambient air intake to the exhaust nozzle. Unlike piston engines—where fuel is mixed with air during or prior to the intake stroke—a gas turbine inducts and compresses pure atmospheric air before any fuel is introduced. In an aircraft piston engine, the working fluid undergoes a complete chemical and thermodynamic conversion across the four distinct strokes of the cycle. Unlike gas turbine engines, which compress pure air and burn lean in a continuous flow, the aircraft piston engine processes discrete batches of a near-stoichiometric fuel-air mixture that reacts periodically under high pressure and temperature.

Aircraft piston engines and gas turbine engines differ fundamentally in their operational, thermodynamic, and physical characteristics. In a piston engine, fuel is inducted or injected before combustion and burned in an intermittent batch process following the constant-volume Otto cycle near a stoichiometric equivalence ratio ($\phi \approx 0.9 - 1.1$), relying on a mechanical volume compression ratio typically restricted to $7:1 - 9:1$. In contrast, gas turbine engines inject fuel directly after full compression, operating as a continuous, steady-flow process under the constant-pressure Brayton cycle; they function with a highly lean overall equivalence ratio ($\phi \approx 0.2 - 0.4$) and achieve significantly higher-pressure compression ratios ranging from $15:1$ to over $40:1$. Consequently, while the specific heat ratio (γ) of the expanded exhaust gas in a piston engine drops to approximately $1.25 - 1.28$ due to rich triatomic combustion products at high temperatures, the excess air in a gas turbine yields a slightly higher expanded gas γ of approximately $1.30 - 1.33$.

The ideal working fluid for both engines is evaluated using air-standard cycle models, but their governing compression mechanisms and heat addition processes differ fundamentally:

1. **Piston Engine (Constant-Volume Otto Cycle):** Heat addition occurs instantaneously at Top Dead Center (TDC) under constant volume ($V = \text{constant}$). Thermal efficiency (η_{Otto}) is governed by the volumetric compression ratio $r = V_{\max}/V_{\min}$:
2. **Gas Turbine Engine (Constant-Pressure Brayton Cycle):** Heat addition occurs continuously at constant pressure ($P = \text{constant}$). Thermal efficiency (η_{Brayton}) is governed by the pressure compression ratio $r_p = P_2/P_1$:

The equivalence Ratio (ϕ) & Mass Fuel-Air Ratio

The chemical composition of the working fluid during and after combustion is dictated by the equivalence ratio (ϕ), defined as:

Missing superscript or subscript argument

1. **Piston Engine ($\phi \approx 0.9 - 1.1$):** Operates near stoichiometric conditions ($F/A \approx 0.067$). The working fluid transitions entirely into combustion products:
2. **Gas Turbine Engine ($\phi \approx 0.2 - 0.4$):** Operates highly lean overall ($F/A \approx 0.015 - 0.025$) to restrict turbine inlet temperatures (T_4). Consequently, the hot working fluid is a mixture of combustion products heavily diluted by unreacted excess air:

This page titled 6.0: Working Fluid Dynamics is shared under a CC BY 4.0 license and was authored, remixed, and/or curated by Haifa El-Sadi.

6.1: Thermodynamic and Chemical Evolution of Working Fluids

The thermodynamic and state relationships connecting the unburned mixture (subscript u **)** and the burned mixture (subscript b) are defined using a two-zone thermodynamic framework.

1. Mass and Mass Fraction Conservation

At any point during the combustion process (or across the flame front), the total cylinder mass m is divided into unburned and burned masses:

$$m = m_u + m_b$$

Defining the burned mass fraction as $x = \frac{m_b}{m}$ and the unburned mass fraction as

$$(1 - x) = \frac{m_u}{m}$$

$$m_u = (1 - x)\, m \qquad \text{and} \qquad m_b = xm$$

If residual exhaust gas from the previous cycle is present, the initial unburned mixture mass fraction is further related to the residual mass fraction x_r (or f_r):

$$x_r = \frac{m_r}{m}$$

$$m_u = m_{\text{fresh}} + m_r = (1 - x_r)\, m + x_r m$$

2. Volume, Specific Volume, and Density Relations

The total instantaneous cylinder volume $V(\theta)$ at crank angle θ is the sum of the partial volumes of the two zones:

$$V = V_u + V_b = m_u v_u + m_b v_b$$

Dividing by total mass m gives the overall average specific volume v:

$$v = (1 - x)\, v_u + x v_b$$

Expressed in terms of densities ($\rho_u = 1/v_u$ and $\rho_b = 1/v_b$):

$$\frac{1}{\rho} = \frac{1 - x}{\rho_u} + \frac{x}{\rho_b}$$

3. Ideal Gas State Equations across the Pressure-Uniform Boundary

Heywood assumes that pressure P is uniform throughout the combustion chamber at any given instant ($P_u = P_b = P$). The state equations for both unburned and burned gas zones are:

$$P v_u = R_u T_u = \left(\frac{R_u}{M_u}\right) T_u$$

$$P v_b = R_b T_b = \left(\frac{R_u}{M_b}\right) T_b$$

Where M_u and M_b are the molecular weights of the unburned and burned gases, and R_u is the universal gas constant.

Dividing the two equations yields the density/volume transformation ratio across the unburned and burned zones:

$$\frac{v_b}{v_u} = \frac{\rho_u}{\rho_b} = \left(\frac{M_u}{M_b}\right)\left(\frac{T_b}{T_u}\right)$$

4. Unburned and Burned Mixture Enthalpy and Internal Energy

The total internal energy U and total enthalpy H of the two-zone cylinder contents are weighted by mass fraction:

$$U = m_u u_u\left(T_u\right) + m_b u_b\left(T_b\right) = m\left[\left(1-x\right)u_u\left(T_u\right) + x u_b\left(T_b\right)\right]$$

$$H = m_u h_u\left(T_u\right) + m_b h_b\left(T_b\right) = m\left[\left(1-x\right)h_u\left(T_u\right) + x h_b\left(T_b\right)\right]$$

Heywood defines absolute specific enthalpy $h\left(T\right)$ and absolute specific internal energy $u\left(T\right)$ by including the standard enthalpy/internal energy of formation at reference temperature $T_0 = 298.15\ \mathrm{K}$:

$$h_u\left(T_u\right) = h^\circ_{f,u} + \int_{T_0}^{T_u} c_{p,u}\left(T\right)dT$$

$$h_b\left(T_b\right) = h^\circ_{f,b} + \int_{T_0}^{T_b} c_{p,b}\left(T\right)dT$$

Where:

1. $h^\circ_{f,u}$ = Mass-weighted enthalpy of formation of the unburned mixture (air + fuel + residual gas).
2. $h^\circ_{f,b}$ = Mass-weighted enthalpy of formation of the burned equilibrium products.

5. First-Law Differential Conservation Equation (Two-Zone Model)

For an engine cylinder undergoing progressive combustion with work $dW = PdV$ and heat loss to the walls dQ, Heywood formulates the First Law energy equation as:

$$dU = dQ - dW$$

$$d\left[m_u u_u + m_b u_b\right] = dQ - PdV$$

Expanding $d\left(m_u u_u + m_b u_b\right)$ with $dm_b = -dm_u = mdx$:

$$m\left(1-x\right)du_u + mxdu_b + m\left(u_b - u_u\right)dx = dQ - PdV$$

This equation directly ties the rate of mass burning (dx) to the energy shift between the unburned state u_u and burned state u_b.

6. Adiabatic Flame Temperature Relation ($T_{b,\mathrm{adiabatic}}$)

For complete, constant-volume adiabatic combustion ($dV = 0, dQ = 0$) of an unburned charge at T_u converting entirely into burned gas ($x = 1$):

$$u_b\left(T_b\right) = u_u\left(T_u\right)$$

$$h^\circ_{f,b} + \int_{T_0}^{T_b} c_{v,b}\left(T\right)dT - R_b T_b = h^\circ_{f,u} + \int_{T_0}^{T_u} c_{v,u}\left(T\right)dT - R_u T_u$$

Solving this equation implicitly yields the adiabatic flame temperature T_b of the burned mixture from the initial unburned temperature T_u.

This page titled 6.1: Thermodynamic and Chemical Evolution of Working Fluids is shared under a CC BY 4.0 license and was authored, remixed, and/or curated by Haifa El-Sadi.

6.2: Thermodynamics Relations for Engine Process

The overall engine operating parameters of greatest interest which can be determined from a thermodynamic analysis of the engine operating cycle are:

The indicated fuel conversion efficiency $\eta_{f,i}$:

$$\eta_{f,i} = \frac{W_{c,i}}{m_f Q_{\text{LHV}}}$$

(which, since the combustion efficiency is unity, is equal to the indicated thermal conversion efficiency $\eta_{t,i}$)

The indicated mean effective pressure ($imep$):

$$imep = \frac{W_{c,i}}{V_d} = \frac{m_f Q_{\text{LHV}} \eta_{f,i}}{V_d}$$

$W_{c,i}$, the indicated work per cycle, is the sum of the compression stroke work and the expansion stroke work:

$$W_{c,i} = W_C + W_E$$

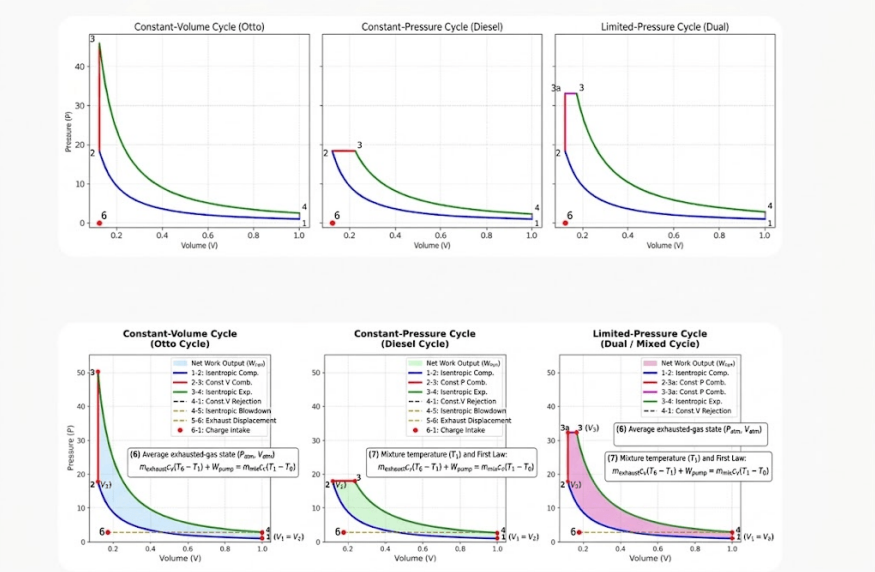


Figure 1. The $P-V$ diagrams representing the Constant-Volume (Otto), Constant-Pressure (Diesel), and Limited-Pressure (Dual)- AI creation

The following relationships (Figure 1) are obtained by applying the first and second laws of thermodynamics to the cylinder contents:

Compression stroke:

$$\frac{v_1}{v_2} = r_c$$

Since the process is adiabatic and reversible:

$$s_2 = s_1$$

The compression work is:

$$W_C = U_1 - U_2 = m\,(u_1 - u_2)$$

Combustion process:

For the constant-volume cycle:

$$v_3 = v_2, \qquad u_3 - u_2 = 0$$

For the constant-pressure cycle:

$$p_3 = p_2, \qquad h_3 - h_2 = 0$$

For the limited-pressure cycle:

$$v_{3a} = v_2, \qquad p_{3b} = p_{3a}$$

and

$$u_{3a} - u_2 = 0, \qquad h_{3b} - h_{3a} = 0$$

Expansion stroke:

For the constant-volume cycle:

$$\frac{v_4}{v_3} = r_c, \qquad s_4 = s_3$$

and the expansion work is:

$$W_E = U_3 - U_4 = m\,(u_3 - u_4)$$

For the constant-pressure cycle:

$$p_3 = p_2, \qquad \frac{v_4}{v_2} = r_c, \qquad s_4 = s_3$$

and the expansion work is:

$$W_E = U_3 - U_4 + p_2(V_3 - V_2)$$
$$= m\,(u_3 - u_4) + p_2(v_3 - v_2)$$

For the limited-pressure cycle:

$$\frac{v_4}{v_{3a}} = r_c, \qquad p_{3b} = p_{3a}, \qquad s_4 = s_{3b}$$

and the expansion work is: $W_E = m[(h_{3b} - h_4) + p_4 v_4 - p_3 v_{3a}]$

The indicated fuel conversion efficiency is:

1. For the constant-volume cycle:
2. For the constant-pressure cycle:
3. For the limited-pressure cycle:

The state of the mixture at point 1 in the cycle depends on the intake mixture properties and the residual gas properties at the end of the exhaust stroke.

When the exhaust valve opens at point 4, the cylinder pressure is above the exhaust manifold pressure and a blowdown process occurs. In the ideal exhaust process model, this blowdown occurs with the piston stationary at BC. During this blowdown process, the gas which remains inside the cylinder expands isentropically. The gases escaping from the cylinder undergo an unrestrained expansion or throttling process which is irreversible. It is assumed that the kinetic energy acquired by each gas element as it is accelerated through the exhaust valve is dissipated in a turbulent mixing process in the exhaust port into internal energy and flow work. Since it is also assumed that no heat transfer occurs, the enthalpy of each element of gas after it leaves the cylinder remains constant.

The gas remaining in the cylinder expands isentropically along the line 4–5. The first element of gas which leaves the cylinder at point 4 enters the exhaust manifold at state a on the pressure $= p_e$ line. An element that leaves the cylinder at an intermediate state b on the expansion line 4–5 would enter the exhaust manifold at state c. At the end of the blowdown process the gas in the cylinder and the last gas to leave have the same state—5. There is, therefore, a gradient in temperature within the exhausted gas. The temperature of the first element exhausted, T_a, is slightly less than T_4 ; the temperature of the last element exhausted is T_5.

A displacement of gas out of the cylinder follows the blowdown process as the piston moves from BC to TC. If heat-transfer and kinetic energy dissipation effects are neglected, no change in thermodynamic state of the gas occurs. In this displacement process, the mass of gas within the cylinder at the end of the blowdown process is further decreased by the ratio V_5/V_6.

The mass of residual gas m_r in the cylinder at point 6 in the cycle is obtained by first determining the state of the gas (T_5, v_5) at the end of the blowdown process following an isentropic expansion from p_4 to p_e and then by reducing the cylinder volume to the clearance volume V_6. The residual mass fraction is thus given by:

$$\frac{m_r}{m} = x_r = \frac{v_4/v_5}{r_c} = \frac{v_2}{v_5}$$

The average state of the exhausted gas can be determined by considering the open system defined by the piston face, cylinder walls, and cylinder head, shown in Fig. 5-4. Applying the first law of thermodynamics for an open system gives:

$$U_6 - U_4 = p_e\left(V_4 - V_6\right) - H_e$$

where H_e is the enthalpy of the mass of gas exhausted from the cylinder. The average specific exhaust enthalpy is, therefore:

$$\overline{h}_e = \frac{m_4 u_4 - m_6 u_6 + p_e V_d}{m_4 - m_6}$$

which, with $p = p_e$, defines the average exhausted-gas state.

The mixture temperature at the end of the intake stroke and at the start of the compression stroke (point 1 in Fig. 1) can now be determined. Application of the first law between points 6 and 1 gives:

$$U_1 - U_6 = -p_i\left(V_1 - V_6\right) + \left(m_1 - m_6\right) h_i$$

or

$$m_1 u_1 - m_6 u_6 = -p_i\left(V_1 - V_6\right) + \left(m_1 - m_6\right) h_i$$

or

$$m_1 h_1 = m_6 h_6 + \left(m_1 - m_6\right) h_i + V_2\left(p_i - p_e\right)$$

where h_i is the specific enthalpy of the inlet mixture and $p_1 = p_i$.

Note that when $p_i < p_e$, part of the residual gas in the cylinder at the end of the exhaust stroke will flow into the intake system when the intake valve opens. This flow will cease when the cylinder pressure equals p_i. However, provided no heat transfer occurs, this backflow will not affect Eqs. [GrindEQ__5_19_] above, since the flow of residual through the intake valve is a constant enthalpy process.

In many engines, the closing of the exhaust valve and the opening of the intake valve overlap. Flow of exhausted gases from the exhaust system through the cylinder into the intake system can then occur.

In the four-stroke engine cycle, work is done on the piston during the intake and the exhaust processes. The work done by the cylinder gases on the piston during exhaust is:

$$W_e = p_e\left(V_2 - V_1\right)$$

The work done by the cylinder gases on the piston during intake is:

$$W_i = p_i\left(V_1 - V_2\right)$$

The net work to the piston over the exhaust and intake strokes, the pumping work, is:

$$W_p = (p_i - p_e)(V_1 - V_2)$$

which, for the cylinder gas system, is negative for $p_i < p_e$ and positive for $p_i > p_e$.

The pumping mean effective pressure ($pmep$) is usually defined as a positive quantity. Thus:

1. For $p_i < p_e$:
2. For $p_i > p_e$:

The net and gross indicated mean effective pressures are related by:

$$imep_n = imep_g - (p_e - p_i)$$

The net indicated fuel conversion efficiency is related to the gross indicated fuel conversion efficiency by:

$$\eta_{f,in} = \eta_{f,ig}\left(1 - \frac{p_e - p_i}{imep_g}\right)$$

If the working fluid in these ideal cycles is assumed to be an ideal gas, with c_v and c_p constant throughout the engine operating cycle, the equations developed in the previous section which describe engine performance and efficiency can be further simplified. We will use the notation of Fig. 1.

Constant-Volume Cycle:

The compression work becomes:

$$W_C = mc_v(T_1 - T_2)$$

The expansion work becomes:

$$W_E = mc_v(T_3 - T_4)$$

The $m_f Q_{\mathrm{LHV}}$, can be related to the temperature rise during combustion. For the working fluid model under consideration, the $U(T)$ lines for the reactants and products on a U -T diagram such as Fig. 2 are parallel and have equal slopes, of magnitude c_v. Hence, for a constant-volume adiabatic combustion process:

$$mc_v(T_3 - T_2) = m_f Q_{\mathrm{LHV}}$$

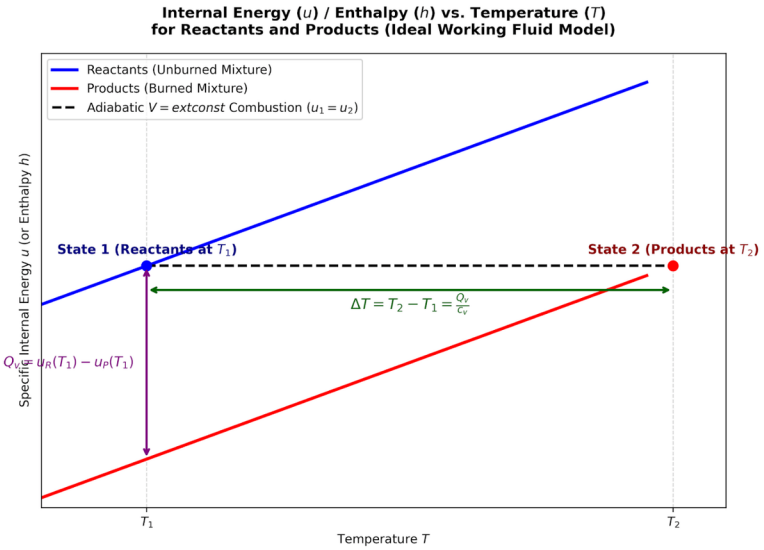


Figure 2. The $u - T$ (or $h - T$) thermodynamic diagram- AIA creation

If insufficient air is available for complete combustion of the fuel. The right-hand side of the equation should then be $\eta_c m_f Q_{\mathrm{LHV}}$ *, where* η_c *is the combustion efficiency:*

$$\eta_c = \frac{H_R - H_P}{m_f Q_{HV}}$$

Note that the heating values at constant volume and constant pressure are the same for this working fluid. For convenience we will define:

$$Q^* = \frac{m_f Q_{\mathrm{LHV}}}{m}$$

Q^* is the specific internal energy (and enthalpy) decrease, during isothermal combustion, per unit mass of working fluid.

The relation for indicated fuel conversion efficiency becomes:

$$\eta_{f,i} = \frac{(T_3 - T_4) - (T_2 - T_1)}{T_3 - T_2} = 1 - \frac{T_4 - T_1}{T_3 - T_2}$$

Since 1–2 and 3–4 are isentropic processes between the same volumes, V_1 and V_2:

$$\frac{T_2}{T_1} = \left(\frac{V_1}{V_2}\right)^{k-1} = r_c^{\gamma-1} = \left(\frac{V_4}{V_3}\right)^{k-1} = \frac{T_3}{T_4}$$

where $\gamma = c_p/c_v$. Hence:

$$\frac{T_4}{T_1} = \frac{T_3}{T_2}$$

and Eq. [GrindEQ__5_30_] can be rearranged as:

$$\eta_{f,i} = 1 - \frac{1}{r_c^{k-1}}$$

The indicated fuel conversion efficiency increases with increasing compression ratio and decreases as k decreases.

The indicated mean effective pressure becomes:

$$\frac{imep}{p_1} = \left(\frac{Q^*}{c_v T_1}\right)\left(\frac{1}{k-1}\right)\left(\frac{r_c}{r_c - 1}\right)\left(1 - \frac{1}{r_c^{k-1}}\right)$$

The dimensionless numbers r_c, k, and $Q^*/(c_v T_1)$ are sufficient to describe the characteristics of the constant-volume ideal gas standard cycle, relative to its initial conditions p_1, T_1.

It is useful to compare the $imep$ —a measure of the effectiveness with which the displaced volume of the engine is used to produce work—and the maximum pressure in the cycle, p_3. The ratio p_3/p_1 can be determined from the ideal gas law applied at points 2 and 3, and the relation:

$$\frac{T_3}{T_2} = 1 + \frac{Q^*}{c_v T_1 r_c^{k-1}}$$

Then give:

$$\frac{imep}{p_3} = \frac{1}{(k-1)\, r_c^k}\left(\frac{r_c}{r_c - 1}\right)\frac{1 - 1/r_c^{k-1}}{c_v T_1/Q^* + 1/r_c^{k-1}}$$

A high value of $imep/p_3$ is desirable. Engine weight will increase with increasing p_3 to withstand the increasing stresses in components.

The indicated fuel conversion efficiency and the ratios $imep/p_1$ and $imep/p_3$ for this ideal cycle model do not depend on whether the cycle is throttled or supercharged. However, the relationships between the working fluid properties at points 1 and 6 do depend on the degree of throttling or supercharging. For throttled engine operation, the residual gas mass fraction x_r can be determined as follows. Since state 5 corresponds to an isentropic expansion from state 4 to $p = p_e$, x_r is given by:

\[x_r=\dfrac

ParseError: invalid DekiScript (click for details)

```
Callstack:
    at (Bookshelves/Aerospace_Engineering/Aircraft_Engine:_Design_and_Analysis/06:_Combustor-_Working_Fluid_and_Models_of_Engine_Cycles/
6.03:_Thermodynamics_Relations_for_Engine_Process), /content/body/p[102]/span[1], line 1,
column 1
```

{r_c}=\dfrac
ParseError: invalid DekiScript (click for details)

```
Callstack:
    at (Bookshelves/Aerospace_Engineering/Aircraft_Engine:_Design_and_Analysis/06:_Combustor-_Working_Fluid_and_Models_of_Engine_Cycles/
6.03:_Thermodynamics_Relations_for_Engine_Process), /content/body/p[102]/span[2], line 1,
column 1
```

{r_c} \nonumber \]

Since

$$\frac{p_1}{p_4} = \frac{p_1}{p_2}\frac{p_2}{p_3}\frac{p_3}{p_4} = \frac{1}{r_c^k}\frac{T_2}{T_3}r_c^k = \left(1 + \frac{Q^*}{c_v T_1 r_c^{k-1}}\right)^{-1}$$

it follows that

\[x_r=\dfrac{1}{r_c}\dfrac

ParseError: invalid DekiScript (click for details)

```
Callstack:
    at (Bookshelves/Aerospace_Engineering/Aircraft_Engine:_Design_and_Analysis/06:_Combustor-_Working_Fluid_and_Models_of_Engine_Cycles/
6.03:_Thermodynamics_Relations_for_Engine_Process), /content/body/p[106]/span[1], line 1,
column 1
```

ParseError: invalid DekiScript (click for details)

```
Callstack:
    at (Bookshelves/Aerospace_Engineering/Aircraft_Engine:_Design_and_Analysis/06:_Combustor-_Working_Fluid_and_Models_of_Engine_Cycles/
6.03:_Thermodynamics_Relations_for_Engine_Process), /content/body/p[106]/span[2], line 1,
column 1
```

\nonumber \]

The residual mass fraction increases as p_i decreases below p_e, decreases as r_c increases, and decreases as $Q^*/\left(c_v T_1\right)$ increases.

Through a similar analysis, the temperature of the residual gas T_6 can be determined:

$$\frac{T_6}{T_1} = \left(\frac{p_e}{p_i}\right)^{(k-1)/k}\left(1 + \frac{Q^*}{c_v T_1 r_c^{k-1}}\right)^{1/k}$$

The mixture temperature at point 1 in the cycle can be related to the inlet mixture temperature, T_i, For a working fluid with c_v and c_p constant, this equation becomes:

$$c_p T_1 = x_r c_p T_6 + \left(1 - x_r\right) c_p T_i - \frac{R T_1}{r_c}\left(\frac{p_e}{p_i} - 1\right)$$

leads to the relation:

$$\frac{T_1}{T_i} = \frac{1 - x_r}{1 - 1/(kr_c)\left[p_e/p_i + (k-1)\right]}$$

Extensive results for the constant-volume cycle with $k = 1.4$ can be found in Taylor.

Limited- and Constant-Pressure Cycles

The constant-pressure cycle is a limited-pressure cycle with $p_3 = p_2$. For the limited-pressure cycle, the compression work remains:

$$W_C = mc_v\left(T_1 - T_2\right)$$

The expansion work becomes:

$$W_E = m\left[c_v\left(T_{3b} - T_4\right) + p_3\left(v_{3b} - v_{3a}\right)\right]$$

For the combustion process give:

$$m_{f,2-3a}Q_{\text{LHV}} = mc_v\left(T_{3a} - T_2\right)$$

$$m_{f,3a-3b}Q_{\text{LHV}} = mc_p\left(T_{3b} - T_{3a}\right)$$

or

$$m_f Q_{\text{LHV}} = m\left[c_v\left(T_{3a} - T_2\right) + c_p\left(T_{3b} - T_{3a}\right)\right]$$

for a working fluid with c_v and c_p constant throughout the cycle.

Then :

$$\eta_{f,i} = 1 - \frac{T_4 - T_1}{\left(T_{3a} - T_2\right) + \gamma\left(T_{3b} - T_{3a}\right)}$$

Use of the isentropic relationships for the working fluid along 1–2 and 3b–4, with the substitutions:

$$\alpha = \frac{p_3}{p_2}, \qquad \beta = \frac{V_{3b}}{V_{3a}}$$

leads to the result:

$$\eta_{f,i} = 1 - \frac{1}{r_c^{k-1}}\left[\frac{\alpha\beta^k - 1}{\alpha k\left(\beta - 1\right) + \alpha - 1}\right]$$

For $\beta = 1$ this result becomes the constant-volume cycle efficiency. For $\alpha = 1$, this result gives the constant-pressure cycle efficiency as a special case.

The mean effective pressure is related to p_1 and p_3 via:

$$\frac{imep}{p_1} = \frac{Q^*}{c_v T_1\left(-1\right)}\left(\frac{r_c}{r_c - 1}\right)\eta_{f,i}$$

$$\frac{imep}{p_3} = \frac{1}{\alpha r_c^k}\left(\frac{Q^*}{c_v T_1}\right)\left(\frac{1}{k-1}\right)\left(\frac{r_c}{r_c - 1}\right)\eta_{f,i}$$

Cycle Comparison:

The above expressions are most useful if values for k and $Q^*/\left(c_v T_1\right)$ are chosen to match real working fluid properties. The average values of k_u and k_b were determined which match real working fluid properties over the compression and expansion strokes, respectively. Values for a stoichiometric mixture appropriate to an SI engine are $k_u \approx 1.3$, $k_b \approx 1.2$. However, analysis of pressure-volume data for real engine cycles indicates that pV^n, where $n \approx 1.3$, is a good fit to the expansion stroke p -V data.

Heat transfer from the burned gases increases the exponent above the value corresponding to k_b. A value of k $= 1.3$ for the entire cycle is thus a reasonable compromise.

Q^* is the enthalpy decrease during isothermal combustion per unit mass of working fluid. Hence:

$$Q^* = \left(\frac{m_f}{m_a}\right) Q_{\text{LHV}} \left(\frac{m_a}{m}\right)$$

A simple approximation for (m_a/m) is $(r_c - 1)/r_c$; i.e., fresh air fills the displaced volume and the residual gas fills the clearance volume at the same density. Then, for isooctane fuel, for a stoichiometric mixture, Q^* is given by $2.92 \times 10^6 (r_c - 1)/r_c$ J/kg air. For $k = 1.3$ and an average molecular weight $M = 29.3$, $c_v = 946$ J/kg · K. For $T_1 = 333$ K, $Q^*/(c_v T_1)$ becomes $9.3 (r_c - 1)/r_c$. For this value of $Q^*/(c_v T_1)$ all cycles would be burning a stoichiometric mixture with an appropriate residual gas fraction.

For all cases $k = 1.3$ and $Q^*/(c_v T_1) = 9.3 (r_c - 1)/r_c$. At any given r_c, the constant-volume cycle has the highest efficiency and lowest $imep/p_3$. For a given maximum pressure p_3, the constant-pressure cycle has the highest efficiency (and the highest compression ratio). For the limited-pressure cycle, at constant p_3/p_1, there is little improvement in efficiency and $imep$ above a compression ratio of about 8 to 10 as r_c is increased.

FUEL-AIR CYCLE ANALYSIS:

A more accurate representation of the properties of the working fluid inside the engine cylinder is to treat the unburned mixture as frozen in composition and the burned gas mixture as in equilibrium. Values for thermodynamic properties for these working fluid models can be obtained with the charts for unburned and burned gas mixtures, or the computer codes (EES). When these working fluid models are combined with the ideal engine process models, the resulting cycles are called fuel-air cycles. The sequence of processes and assumptions are (with the notation of Fig. 1):

1. 1–2: Reversible adiabatic compression of a mixture of air, fuel vapor, and residual gas without change in chemical composition.
2. 2–3: Complete combustion (at constant volume or limited pressure or constant pressure), without heat loss, to burned gases in chemical equilibrium.
3. 3–4: Reversible adiabatic expansion of the burned gases which remain in chemical equilibrium.
4. 4–5–6: Ideal adiabatic exhaust blowdown and displacement processes with the burned gases fixed in chemical composition.
5. 6–7–1: Ideal intake process with adiabatic mixing between residual gas and fresh mixture, both of which are fixed in chemical composition.

This page titled 6.2: Thermodynamics Relations for Engine Process is shared under a CC BY 4.0 license and was authored, remixed, and/or curated by Haifa El-Sadi.

6.3: Problems and References

Problem#1

Inside an aircraft piston engine cylinder, a turbulent flame front propagates through a compressed mixture of air, Avgas vapor, and residual gas. Just prior to local ignition, the unburned mixture is at a temperature of $T_u = 720\ \mathrm{K}$ and a pressure of $P = 18\ \mathrm{bar}$. After passing through the flame zone, the local burned gas reaches an equilibrium temperature of $T_b = 2650\ \mathrm{K}$. Assuming the mean molecular weight of the unburned gas is $M_u = 29.5\ \mathrm{kg/kmol}$ and for the burned gas is $M_b = 28.2\ \mathrm{kg/kmol}$ due to high-temperature dissociation, calculate:

1. The specific volume ratio (v_b/v_u) across the flame front.
2. The density of the unburned mixture (ρ_u) and the burned gas mixture (ρ_b).

Problem#2

An engine inducts a fresh air-fuel charge with a mass-specific enthalpy of $h_{\mathrm{fresh}} = -150\ \mathrm{kJ/kg}$ at $T_{\mathrm{fresh}} = 310\ \mathrm{K}$. At the end of the intake stroke, the total charge in the cylinder is mixed with a residual gas fraction of $x_r = 0.07$ (7% by mass) remaining in the clearance volume from the previous exhaust stroke. The residual gas has an enthalpy of $h_r = +680\ \mathrm{kJ/kg}$ at $T_r = 950\ \mathrm{K}$.

Determine the mass-specific enthalpy of the resulting unburned mixture (h_u) before compression.

Problem#3

An unburned fuel-air mixture operates at a stoichiometric fuel-air equivalence ratio ($\phi = 1.0$) and is diluted with a residual burned gas fraction of $x_b = 0.08$ (8% residual gases by mass). The mixture is compressed inside an internal combustion chamber to a state corresponding to the end of the compression stroke, defined by:

- Unburned mixture temperature: $T_1 = 650\ \mathrm{K}$
- Unburned mixture pressure: $P_1 = 1.57\ \mathrm{MPa}$
- Unburned specific internal energy: $u_{s,u} = 300\ \mathrm{kJ/kg\ air}$
- Unburned specific volume: $v_u = 0.13\ \mathrm{m^3/kg\ air}$

Assuming complete adiabatic combustion, calculate the final equilibrium mixture temperature (T_2) and pressure (P_2) for two distinct thermodynamic heat addition modes:

1. Constant-Volume Adiabatic Combustion at Top Dead Center (Otto Cycle).
2. Constant-Pressure Adiabatic Combustion

Problem#4

Utilize a chemical equilibrium calculation program (such as NASA CEA or Cantera) to determine the equilibrium state, thermodynamic properties, and species mole fractions for the following combustion conditions:

Part (a): Equilibrium Product Composition

Plot the variation of specific heat (c_p), ratio of specific heats (γ), average molecular weight (M), and equilibrium species concentrations ($\mathrm{N_2}$, $\mathrm{CO_2}$, $\mathrm{H_2O}$, CO, $\mathrm{H_2}$, $\mathrm{O_2}$, OH, O, H, and NO) across equivalence ratios ranging from $\phi = 0.3$ to 1.5.

1. Fuel: n-Heptane vapor ($\mathrm{C_7H_{16}}$) combusted with air
2. Conditions: Constant pressure $P = 35\ \mathrm{atm}$ and constant temperature $T = 2400\ \mathrm{K}$
3. Plotting Requirement: Display all mole fractions on a single logarithmic vertical axis versus equivalence ratio ϕ.

Part (b): Constant Pressure and Constant Volume Combustion

An unburned reactant mixture of n-heptane vapor and air at $T_1 = 650\ \mathrm{K}$ and $P_1 = 15\ \mathrm{atm}$ undergoes two separate combustion processes: one at constant pressure and one at constant volume.

1. Unburned Mixture Evaluation:
    1. Calculate the molar enthalpy ($\overline{h}$) and molar internal energy ($\overline{u}$) of n-heptane vapor at $650\ \mathrm{K}$ in $\mathrm{cal/gmol}$.
    2. Calculate the specific volume of the reactant mixture (v_{mix}) in $\mathrm{cm^3/g}$ for equivalence ratios $\phi = 0.3, 0.5, 0.7, 0.9, 1.1, 1.3, 1.5$.
2. Adiabatic Flame Conditions:
    1. Using the equilibrium solver, determine the adiabatic flame temperature reached during constant-pressure combustion.
    2. Determine the peak temperature and peak pressure achieved following constant-volume combustion.
    3. Plot these resulting temperatures and pressures as a function of ϕ.

Reference Data: Thermodynamic Properties of n-Heptane Vapor ($\mathrm{C_7H_{16}}$)

T (K)	c¯p (cal/mol· K)	h¯ − h¯298 (kcal/mol)	△ h¯f,298◦ (kcal/mol)
298	43.98	0.00	−44.89
650	76.42	22.15	−53.12

Problem#5

A gas engine running on a gaseous mixture of butane ($\mathrm{C_4H_{10}}$) and air has the following conditions in the cylinder prior to constant-volume adiabatic combustion:

- Initial Pressure (P_1): $93.98\ \mathrm{psia}$ ($6.48 \times 10^5\ \mathrm{N/m^2}$)
- Initial Temperature (T_1): $1080\ ^\circ\mathrm{R}$ ($600\ \mathrm{K}$)
- Charge Composition: Air plus 50% of the stoichiometric quantity of butane fuel ($\phi = 0.50$).

Calculate the pressure and temperature at the end of combustion using the data given below.

Thermodynamic Data

1. Reactant Internal Energies ($\overline{u}$ in $\mathrm{Btu/lbmol}$):

Species	T=536.4 ◦ R (298 K)	T=1080 ◦ R (600 K)
Air	$2,649\ \mathrm{Btu/lbmol}$	$5,415\ \mathrm{Btu/lbmol}$
Butane ($\mathrm{C_4H_{10}}$)	$-33.1\ \mathrm{Btu/lbmol}$	$16,519\ \mathrm{Btu/lbmol}$

2. Combustion Reaction Data:

1. Internal energy of combustion of butane at $536.4\ ^\circ\mathrm{R}$ ($298\ \mathrm{K}$):

3. Product Internal Energies ($\overline{u}$ per lbmol of products at $\phi = 0.50$):

Temperature T (◦ R)	u¯ (Btu/lbmol)
$536.4\ ^\circ\mathrm{R}$	$2,705.7\ \mathrm{Btu/lbmol}$
$3735.0\ ^\circ\mathrm{R}$	$23,313.4\ \mathrm{Btu/lbmol}$
$3744.0\ ^\circ\mathrm{R}$	$23,379.2\ \mathrm{Btu/lbmol}$

Problem#6

For $k = 1.3$, compression ratio $r_c = 6$, and a stoichiometric mixture with intake temperature $300\ \mathrm{K}$, find the residual gas fraction, residual gas temperature, and mixture temperature at point 1 in the constant-volume cycle for $p_e/p_i = 1$ (unthrottled operation) and 2 (throttled operation).

For a stoichiometric mixture, for isooctane:

$$Q^* = \frac{m_f}{m} Q_{\mathrm{LHV}} = \left(\frac{m_f}{m_i}\right)\left(\frac{m_i}{m}\right) Q_{\mathrm{LHV}} = \frac{44.38}{16.14}\,(1 - x_r) = 2.75\,(1 - x_r)\ \ \mathrm{MJ/kg}$$

For $k = 1.3$, $c_v = 946\ \mathrm{J/kg \cdot K}$ and

$$\frac{Q^*}{c_v T_1} = \frac{2.75 \times 10^6}{946 T_1}\,(1 - x_r) = \frac{2910}{T_1}\,(1 - x_r)$$

For $r_c = 6$ and $k = 1.3$, become:

\[x_r=\dfrac{1}{6}\dfrac

ParseError: invalid DekiScript (click for details)

```
01 Callstack:
02     at (Bookshelves/Aerospace_Engineering/Aircraft_Engine:_Design_and_Analysis/06:_Combustor-_Working_Fluid_and_Models_of_Engine_Cycles/6.04:_Problems_and_References), /content/body/div[6]/p[7]/span[1], line 1, column 1
```

ParseError: invalid DekiScript (click for details)

```
01 Callstack:
02     at (Bookshelves/Aerospace_Engineering/Aircraft_Engine:_Design_and_Analysis/06:_Combustor-_Working_Fluid_and_Models_of_Engine_Cycles/6.04:_Problems_and_References), /content/body/div[6]/p[7]/span[2], line 1, column 1
```

\nonumber \]

$$\frac{T_r}{T_1} = \left(\frac{p_e}{p_i}\right)^{0.23}\left(1 + \frac{Q^*}{c_v T_1 \times 6^{0.3}}\right)^{0.769}$$

$$\frac{T_1}{300} = \frac{1 - x_r}{1 - [1/(1.3 \times 6)]\,(p_e/p_i + 0.3)}$$

A trial-and-error solution is required. It is easiest to estimate x_r, solve for T_1 from (d), evaluate $Q^*/(c_v T_1)$ from (a), and check the value of x_r assumed with that given by (b).

For $(p_e/p_i) = 1$ (unthrottled operation):

$$x_r = 0.044, \qquad T_1 = 344\ \mathrm{K}, \qquad \frac{Q^*}{c_v T_1} = 8.1, \qquad T_r = 1316\ \mathrm{K}$$

For $(p_e/p_i) = 2$ (throttled operation):

$$x_r = 0.082, \qquad T_1 = 391\ \mathrm{K}, \qquad \frac{Q^*}{c_v T_1} = 6.8, \qquad T_r = 1580\ \mathrm{K}$$

Problem#7

Calculate the performance characteristics of the constant-volume fuel-air cycle. The compression ratio is 8; the fuel is isooctane and the mixture is stoichiometric; the pressure and temperature inside the cylinder at the start of compression are $1\ \mathrm{atm}$ and

350 K, respectively. Use the notation of Fig. 1 to define the states at the beginning and end of each process.

The compression process:

$$T_1 = 350 \text{ K}, \qquad p_1 = 101.3 \text{ kPa}, \qquad v_1 = 1 \text{ m}^3/\text{kg air}, \qquad u_{s1} = 40 \text{ kJ/kg air}$$

$$T_2 = 682 \text{ K}, \qquad p_2 = 1.57 \text{ MPa}, \qquad v_2 = 0.125 \text{ m}^3/\text{kg air}, \qquad u_{s2} = 350 \text{ kJ/kg air}$$

$$W_{1-2} = W_C = -310 \text{ kJ/kg air}$$

The constant-volume adiabatic combustion process *(it was assumed that the residual gas fraction was 0.08)*:

$$u_{b3} = u_{s2} + \Delta u^{\circ}_{f,u} = -5 \text{ kJ/kg air}, \qquad s_3 = 9.33 \text{ kJ/kg air} \cdot \text{K}$$

$$v_3 = v_2 = 0.125 \text{ m}^3/\text{kg air}, \qquad T_3 = 2825 \text{ K}, \qquad p_3 = 7100 \text{ kPa}$$

$$T_4 = 1840 \text{ K}, \qquad p_4 = 570 \text{ kPa}, \qquad u_4 = -1540 \text{ kJ/kg air}$$

$$W_{3-4} = W_E = 1535 \text{ kJ/kg air}$$

Problem#8

It is desired to increase the output of a spark-ignition engine by either [GrindEQ__1_] raising the compression ratio from 8 to 10 or [GrindEQ__2_] increasing the inlet pressure from 1.0 atm to 1.5 atm. Using the constant-volume cycle as a model for engine operation, which procedure will give:

a. The highest pressure of the cycle?
b. The highest efficiency?
c. The highest mep?

Assume $k = 1.3$ and $\left(m_f Q_{\text{HV}}\right) / \left(m c_v T_1\right) = 9.3 \left(r_c - 1\right) / r_c$.

Problem#9

A spark-ignition engine is throttled when operating at part load (the inlet pressure is reduced) while the fuel/air ratio is held essentially constant. The inlet air is at pressure p_1, the exhaust pressure is atmospheric p_a, and the ambient temperature is T_a. Derive an expression for the *decrease* in net indicated fuel conversion efficiency due to throttling from the ideal constant-volume cycle efficiency and show that it is proportional to $(p_a/p_1 - 1)$. Assume mass fuel $\ll$ mass air.

References

J. B. Heywood, *Internal Combustion Engine Fundamentals*. New York, NY, USA: McGraw-Hill, 1988.

Charles Fayette Taylor, *The Internal Combustion Engine in Theory and Practice* (Volumes 1 & 2), MIT Press

This page titled 6.3: Problems and References is shared under a CC BY 4.0 license and was authored, remixed, and/or curated by Haifa El-Sadi.

7: ENGINE HEAT TRANSFER

7.0: Introduction
7.1: Heat transfer and Engine energy balance
7.2: Convective heat transfer
7.3: Radiative Heat Transfer
7.4: Problems and References

This page titled 7: Engine Heat Transfer is shared under a CC BY 4.0 license and was authored, remixed, and/or curated by Haifa El-Sadi.

7.0: Introduction

Heat transfer is one of the focal factors determining the performance, efficiency, durability and emissions of an internal combustion engine. During combustion, burned gas temperatures reach 2,500 K or more, far above what the cylinder head, piston, liner and valves can resist. These parts survive only because a large share of the heat released by the fuel is removed through the walls to the coolant and oil. Normally, 20 to 35 percent of the fuel energy ends up as wall heat loss, and a similar share leaves with the exhaust. Only about a quarter to a third is transformed into useful work.

Heat transfer significantly impacts engine performance, efficiency, and design across multiple operational areas. Heat lost from in-cylinder gases during compression, combustion, and expansion reduces cylinder pressures, directly lowering work output and thermodynamic efficiency, a penalty that is particularly pronounced at part-load operation in spark-ignition engines where wall heat loss represents a large fraction of total fuel energy. Simultaneously, heat transfer to the incoming charge reduces charge density, decreasing volumetric efficiency while raising end-gas temperatures and the propensity for engine knock. Combustion chamber wall temperatures must be carefully balanced to protect structural materials and lubricating oil films while remaining high enough to limit unburned hydrocarbon emissions resulting from flame quenching. Furthermore, exhaust system heat losses dictate available energy for turbocharging and determine operating temperatures for catalysts or particulate traps, while the engine cooling system must be sized to manage total heat rejection under peak thermal loading conditions.

In-cylinder heat transfer encompasses all three fundamental transport modes, dominated by highly intense, spatially non-uniform, and unsteady gas-to-wall convection driven by rapid cycle-resolved changes in pressure, temperature, and velocity. Radiation originates from hot burned gases and soot particles in diesel flames—where it accounts for 20 to 35 percent of total heat transfer—while conduction transports heat through the cylinder walls to the coolant. Due to these complex, dynamic interactions, engine thermal analysis relies on empirical correlations, such as those developed by Annand and Woschni, rather than first-principles modeling.

This page titled 7.0: Introduction is shared under a CC BY 4.0 license and was authored, remixed, and/or curated by Haifa El-Sadi.

7.1: Heat transfer and Engine energy balance

Applying the First Law of Thermodynamics to a control volume surrounding a steady-state engine yield:

$$\dot{m}_a h_a + \dot{m}_f h_f = P_b + \dot{Q}_{\text{loss}} + \dot{Q}_{misc} + (m_{\text{f}} + \dot{m}_a) h_e$$

Where P_b is the brake power, $\dot{Q}_{\text{loss}}$ is the heat transfer rate to the cooling media, $\dot{Q}_{misc}$ is the heat rejected to the oil + convection+ radiation from engines to external, h_e is the exhaust enthalpy

Expressed on a fuel-energy basis:

$$\dot{m}_f Q_{\text{LHV}} = P_b + \dot{Q}_{\text{loss}} + \dot{Q}_{\text{misc}} + \dot{H}_{\text{e,ic}} + h_{e,s}\dot{m}$$

Where $\dot{H}_{\text{e,ic}}$ represents the exhaust enthalpy loss due to incomplete combustion, $\dot{m}_f \cdot Q_{\text{LHV}}$ is fuel energy input (total rate of energy released by fuel combustion), $P_b = 2\pi NT$ = is useful work rate, N in rev/s, T =torque, (brake power), $\dot{Q}_{loss} = \dot{m}_c \cdot c_{p,c} \cdot (T_{c,\text{out}} - T_{c,\text{in}})$ is rate of heat rejection to the cooling fluid

Brake thermal efficiency represents the useful fraction of fuel energy converted to power:

$$\eta_f = \frac{P_b}{\dot{m}_f Q_{\text{LHV}}}$$

Typical full-load energy distribution:

- Brake Work: 25–35% (higher values expected in diesel engines)
- Coolant Loss: 20–30%
- Exhaust Loss: 30–40%
- Friction, Radiation & Unburned Fuel: Remaining few percent

Indicated power is given by:

$$P_i = \text{imep} \cdot V_d \cdot N \cdot \left(\frac{1}{n_R}\right)$$

Where n_R is the number of crank revolutions per power stroke ($n = 2$ for a four-stroke cycle, where one power stroke occurs every two crankshaft revolutions, and $n = 1$ for a two-stroke cycle, where one power stroke occurs every single crankshaft revolution), N is the engine crankshaft speed (the rotational speed of the crankshaft), V_d is the displaced volume or engine displacement, which is the total volume swept by the piston as it travels from Top Dead Center (TDC) to Bottom Dead Center (BDC) calculated for a single cylinder of bore B and stroke S as $V_d = \frac{\pi}{4} B^2 S$ and IMEP is the indicated mean effective pressure, which is a fictitious constant pressure that, if applied to the piston during the power stroke, would produce the same net indicated work per cycle (W_i) as the actual fluctuating cylinder pressure profile. The relationship between indicated power, brake power, and friction power is expressed through mean effective pressure (mep):

$$\text{bmep} = \text{imep}_n - \text{rfmep} - amep$$

Where bmep is the brake mean effective pressure, imep is net indicated mean effective pressure, and amep is auxiliary (or accessory) mean effective pressure. Heywood defines total engine friction ($tfmep$) as the sum of mechanical rubbing friction (rfmep), pumping losses (pmep), and accessory/auxiliary losses (amep):

$$\text{tfmep} = \text{rfmep} + \text{pmep} + \text{amep}$$

For specified engine geometry, $tfmep$ is frequently expressed as a quadratic function of crankshaft rotational speed N:

$$\text{tfmep} = C_1 + C_2 \left(\frac{N}{1000}\right) + C_3 \left(\frac{N}{1000}\right)^2$$

This page titled 7.1: Heat transfer and Engine energy balance is shared under a CC BY 4.0 license and was authored, remixed, and/or curated by Haifa El-Sadi.

7.2: Convective heat transfer

The calculation of instantaneous heat flux $q(\theta)$ across the engine cycle relies on a quasi-steady assumption. The gas-side convective heat transfer coefficient h_c is determined by engine geometry (bore B, length ratios), gas properties (k, μ, c_p, ρ), flow field parameters (v), chemical energy release rate $\dot{q}_{ch}$, engine speed N, and crank angle θ:

$$f\left(h_c, B, z, y_1, \ldots, y_m, v, u_1, \ldots, u_n, k, \mu, c_p, \rho, \dot{q}_{ch}, N, \theta\right) = 0$$

Applying dimensional analysis yields four fewer nondimensional groups, incorporating the Nusselt (Nu), Reynolds (Re), and Prandtl (Pr) numbers:

$$\Phi\left(\frac{h_c B}{k}, \frac{\rho S_p B}{\mu}, \frac{c_p \mu}{k}, \frac{B}{L}, \frac{\dot{q}_{ch}}{\rho c_p N T}, r_c, R, y_1, \ldots, y_m, \theta, u_1, \ldots, u_n\right) = 0$$

where mean piston speed $S_p = 2LN$ is chosen as the characteristic velocity v. Correlations generally adopt the classical turbulent boundary-layer form, Nusselt number:

$$\mathrm{Nu} = a\mathrm{Re}^m \mathrm{Pr}^n$$

Taylor and Toong defined an effective mean gas temperature $T_{g,a}$ such that the cycle-integrated heat flow sums to zero:

$$\int A h_c \left(T - T_{g,a}\right) d\theta = 0$$

The overall gas-side heat transfer correlates against charge flow rate Reynolds number:

$$\mathrm{Nu} = \frac{\dot{Q} B}{\pi B^2/4 \left(T_{g,a} - T_c\right) k_g} = \frac{4\dot{Q}}{\pi B k_g \left(T_{g,a} - T_c\right)}$$

$$\mathrm{Re} = \frac{\dot{m} B}{\mu_g \left(\pi B^2/4\right)} = \frac{4\dot{m}}{\pi \mu_g B}$$

Annand observed that diesel engine correlations yield approximately 25% higher Nusselt numbers than SI engines at equivalent Reynolds numbers, primarily due to soot radiation.

Annand developed the following correlation and evaluates the cylinder-average charge temperature $\overline{T}_g = \frac{pVM}{m\overline{R}}$:

$$\left(\frac{h_c B}{k}\right) = a\left(\frac{\rho S_p B}{\mu}\right)^b$$

Parameter range: $b = 0.7$, and $0.35 \leq a \leq 0.8$, scaling proportionally with the intensity of in-cylinder charge motion.

Woschni assumes $\mathrm{Nu} = 0.035\mathrm{Re}^m$ with $m = 0.8$, Woschni correlation with exponent can be summarized as:

$$h_c = 3.26 B[\mathrm{m}]^{-0.2} p[\mathrm{kPa}]^{0.8} T[\mathrm{K}]^{-0.55} w[\mathrm{m/s}]^{0.8}$$

The effective local gas velocity w accounts for a four stroke, water-cooled, four valve direct injection CI engine without swirl was expressed as:

$$w = \left[C_1 \overline{S}_p + C_2 \frac{V_d T_r}{p_r V_r}\left(p - p_m\right)\right]$$

The effective local gas velocity w accounts for piston motion and combustion-induced density change:

Operating Period	C_1 (No Swirl)	C_1 (With Swirl)	C_2
Gas Exchange	6.18	$6.18 + 0.417\frac{v_s}{\overline{S}_p}$	0

Operating Period	C_1 (No Swirl)	C_1 (With Swirl)	C_2
Compression	2.28	$2.28 + 0.308\frac{v_s}{\overline{S}_p}$	0
Combustion & Expansion	2.28	$2.28 + 0.308\frac{v_s}{\overline{S}_p}$	$3.24 \times 10^{-3}\ \mathrm{m/(s \cdot K)}$

(Note: Swirl speed $v_s = \frac{B\omega_p}{2}$, where ω_p is the paddle-wheel rotation speed. p_m denotes the motored cylinder pressure).

Boundary-Layer Flat-Plate Models

Applied to swirling flows in Direct-Injection (DI) diesel engines at radius r:

$$\dot{q}(r) = 0.023\frac{k}{r}\left(\frac{\omega r^2}{\nu}\right)^{0.8}\left[\overline{T}_g(r) - T_w(r)\right]$$

Two-Zone Models (SI Engines) separate the cylinder into unburned (u) and burned (b) zones:

$$\dot{Q}_u = A_{u,w}h_{c,u}(T_u - T_w), \qquad \dot{Q}_b = A_{b,w}h_{c,b}(T_b - T_w)$$

Thermal Boundary-Layer Models divide the burned gas region into an adiabatic core (T_{ac}) and a thermal boundary layer of thickness δ:

$$\dot{q} = \frac{k_e(T_{ac} - T_w)}{\delta}$$

Boundary layer growth: $\delta \propto t^{0.5}$ (laminar regime); $\delta \propto t^{0.8}$ (turbulent regime).

Intake Manifold modeled via steady, turbulent internal pipe flow correlations. Liquid fuel evaporation introduces two-phase heat transfer complexity. For exhaust system & valves, exhaust heat transfer exhibits the highest heat flux rates in the operating cycle due to high-velocity blowdown gases. For valve open period ($L_v/D_v \leq 0.2$ - Jet Regimes):

$$\mathrm{Nu} = K\mathrm{Re}_j^n$$

where

$$\mathrm{Re}_j = \frac{v_j D_v}{\nu}$$

Standard pipe flow based on port velocity v_p and diameter D_p.

For valve closed period, the correlation:

$$\mathrm{Nu} = 0.022\overline{\mathrm{Re}}_D^{0.8}$$

For downstream exhaust pipe:

$$\mathrm{Nu} = 0.0483\mathrm{Re}^{0.783}$$

(Note: Pulsating flow increases heat transfer rates to roughly twice those predicted by steady-flow turbulent pipe correlations).

This page titled 7.2: Convective heat transfer is shared under a CC BY 4.0 license and was authored, remixed, and/or curated by Haifa El-Sadi.

7.3: Radiative Heat Transfer

Radiative contributions differ fundamentally by engine category:

- **SI Engines:** Radiation originates from non-luminous gaseous products (CO_2, H_2O) and represents $< 5\%$ of peak convective heat flux (cycle-integrated gas radiation is negligible).
- **CI (Diesel) Engines:** Highly luminous turbulent diffusion flames generate incandescent soot particles. Radiant flux accounts for 20–35% of total heat transfer.

Gas emissivity depends on component partial pressures p_i, path length l, and gas temperature T_g:

$$\varepsilon_g = f\left(T_g, p_1 l, \ldots, p_n l\right)$$

The mean beam path length l for volume V and surface area A is:

$$l = 0.9\left(\frac{4V}{A}\right)$$

Peak gas emissivity reach $\varepsilon_g \approx 0.1$ with peak radiative heat fluxes of $\sim 0.2\ \mathrm{MW/m^2}$. Because gas radiation scales with T_g^4, it decays rapidly during expansion.

For flame radiation, soot particle radiation exhibits continuous spectral emission. Monochromatic emissivity ε_λ follows the empirical dispersion relation:

$$\varepsilon_\lambda = 1 - \exp\left(-\frac{kl}{\lambda^{0.95}}\right)$$

Combining ε_λ with Planck's blackbody law yields the apparent radiation temperature T_R and apparent grey-body emissivity ε_a:

$$e_{b,\lambda} = \frac{2\pi K_1}{\lambda^5\left(e^{K_2/\lambda T_R} - 1\right)}, \qquad \varepsilon_a = \frac{\int \varepsilon_\lambda e_{b,\lambda} d\lambda}{\int e_{b,\lambda} d\lambda}$$

(where $K_1 = 0.59548 \times 10^{-16}\ \mathrm{W \cdot m^2}$ and $K_2 = 1.43879\ \mathrm{cm \cdot K}$).

For soot monochromatic absorption coefficient, the absorption coefficient k_λ depends on soot mass concentration $c_s\ (\mathrm{kg/m^3})$ and soot density $\rho_s \approx 2 \times 10^3\ \mathrm{kg/m^3}$:

$$k_\lambda = 36\pi\left(\frac{c_s}{\rho_s}\right) f\left(\lambda, T\right)$$

Evaluating the emissive-power-weighted average yields the mean absorption coefficient k_a:

$$k_a = \frac{\int k_\lambda e_{b,\lambda} d\lambda}{\int e_{b,\lambda} d\lambda}$$

For blackbody radiation at $1800\ \mathrm{K}$, $k_a \approx 1300 c_s\ \mathrm{m^{-1}}$. Annand related flame emissivity to mean absorptivity via $\varepsilon_a = 1 - \exp\left(-k_a l\right)$. Peak emissions ($\varepsilon_a = 0.8$, $l \approx 0.07\ \mathrm{m}$) yield $k_a \approx 22\ \mathrm{m^{-1}}$ and in-cylinder soot loading $c_s \approx 16\ \mathrm{g/m^3}$.

Annand radiant correlation combines convective models with a bulk temperature radiative term:

$$\dot{q}_R = \beta\sigma\left(\overline{T}_g^4 - T_w^4\right)$$

Parameter β: $\beta \approx 0.6$ (initial estimate) to $\beta \approx 1.6$ (modified version). Because $\overline{T}_g$ represents mean gas temperature rather than local flame temperature, β acts as an empirical scaling factor rather than physical emissivity.

Flynn developed an empirical expression fit instantaneous radiant flux profiles using the crank angle at radiation onset (θ_s):

$$\dot{q}_R = 2\overline{q}_R b\,(a+1)\left(\frac{\theta-\theta_s}{360}\right)^a \exp\left[-\frac{(\theta-\theta_s)^{a+1}}{360}\right]$$

Parameters $\overline{q}_R$, a, b, and θ_s are correlated as functions of engine speed, manifold pressure, equivalence ratio, and injection timing.

This page titled 7.3: Radiative Heat Transfer is shared under a CC BY 4.0 license and was authored, remixed, and/or curated by Haifa El-Sadi.

7.4: Problems and References

Problem#1

Given that the average heat flux through a particular zone in a cast iron liner $8\ \mathrm{mm}$ thick is $0.25\ \mathrm{MW/m^2}$, the coolant temperature is $90^{\circ}\mathrm{C}$, and the coolant-side heat transfer coefficient is $8000\ \mathrm{W/m^2 \cdot K}$, find the average surface temperature on the combustion chamber and coolant sides of the liner at that zone.

Problem#2

Using dimensional analysis, compare the relative heat losses of two geometrically similar SI engines (same bore/stroke ratio, same connecting rod/stroke ratio) operating at the same imep and power. Engine A has three times the displacement per cylinder of Engine B. Assume that the wall temperature and the gas temperature for both engines are the same.

Problem#3

a. Using Woschni's correlation, evaluate the percentage increase in heat transfer expected from an engine with a mean piston speed of $12\ \mathrm{m/s}$ when the swirl ratio is raised from 0 to 4. Do your comparison for the intake process only. The engine bore is $0.12\ \mathrm{m}$ and the engine speed is $3000\ \mathrm{rev/min}$.
b. Explain how both the generation of swirl and the resulting change in heat transfer affect the volumetric efficiency of an engine.

Problem#4

The three main regimes of energy loss due to friction: boundary-regime friction, hydrodynamic (full fluid film) lubrication, and turbulent viscous dissipation. Calculate the approximate fractional breakdown of total per-cycle frictional work across these three regimes for a V8 passenger-car gasoline engine running at an engine speed of 3200 RPM.

Problem#5

Consider four-stroke, naturally aspirated multi-cylinder gasoline (SI) and diesel compression-ignition (CI) automotive powerplants operating under WOT (100% load) as well as 40% partial load at a intermediate rotational speed of 2500 RPM. Provide rough percentage distributions of the total friction mean effective pressure across the following three functional components: pumping mean effective pressure (pmep), mechanical rubbing mean effective pressure (rfmep), and auxiliary/accessory loss (amep). Clearly explain the methodology used to arrive at your estimates and list all components classified under auxiliary devices.

References

J. B. Heywood, *Internal Combustion Engine Fundamentals*, New York: McGraw-Hill Education, 1988

This page titled 7.4: Problems and References is shared under a CC BY 4.0 license and was authored, remixed, and/or curated by Haifa El-Sadi.

INDEX

A

absolute pressure
1.1: Ideal Gas Relations
absolute temperature
1.1: Ideal Gas Relations
adiabatic
1.3: Isentropic Relations
adiabatic efficiency
4.1: Gas Generator Components
adiabatic expansion
1.6: Problems and References
adiabatic process
6.3: Problems and References
aerodynamic
4.4: Turbofan Engine
aerodynamic principles
4.5: Turboprop Engine
aerodynamics
4.6: Problems and References
Aerospace_Engineering
5.1: Axial-Flow Turbomachinery
afterburners
2.0: Introduction
air transportation
4.1: Gas Generator Components
aircraft
3.1: Aircraft Piston Engine
3.3: Problems and References
5.0: Introduction
aircraft engines
3.0: Introduction
5.2: Radial / Centrifugal Turbomachinery
aircraft propulsion
4.5: Turboprop Engine
aircraft_cruise
5.4: Problems and References
Aircraft_Engine
5.1: Axial-Flow Turbomachinery
airflow requirements
4.2: On/Off Design Analysis
aviation
4.0: Introduction
aviation engines
3.1: Aircraft Piston Engine
aviation gasoline
3.3: Problems and References
axial Mach number
4.1: Gas Generator Components

B

blade_tip_velocity
5.4: Problems and References
brake horsepower
3.3: Problems and References
brake thermal efficiency
7.1: Heat transfer and Engine energy balance
Brayton cycle
4.0: Introduction
4.3: Turbojet
6.0: Working Fluid Dynamics
bypass ratio
4.5: Turboprop Engine
bypass_ratio
5.4: Problems and References

C

centrifugal compressors
5.2: Radial / Centrifugal Turbomachinery
Centrifugal Turbomachinery
5: Compressor and Turbines
CI engines
7.3: Radiative Heat Transfer
combustion
3.1: Aircraft Piston Engine
6.0: Working Fluid Dynamics
6.1: Thermodynamic and Chemical Evolution of Working Fluids
7.0: Introduction
7.1: Heat transfer and Engine energy balance
7.3: Radiative Heat Transfer
combustion chamber
2.3: Problems and References
7.0: Introduction
combustion chambers
2.2: Rayleigh flow
combustion efficiency
4.1: Gas Generator Components
combustion performance
4.0: Introduction
combustion process
6.2: Thermodynamics Relations for Engine Process
6.3: Problems and References
commercial jetliners
3.0: Introduction
component efficiencies
4.2: On/Off Design Analysis
components
4: Aircraft Engine- Gas Turbine Engine
compressible flow
1: Introduction to Compressible Flow
1.0: Fundamentals of Compressible Flow
1.5: Compressible Flow Relationships
2.0: Introduction
2.1: Subsonic, sonic and supersonic flow
compressible wave propagation
2.0: Introduction
compression ratio
6.3: Problems and References
Compressor
4.1: Gas Generator Components
5.0: Introduction
5.1: Axial-Flow Turbomachinery
compressor power input
1.6: Problems and References
compressor pressure ratio
4.3: Turbojet
conservation of energy
1.4: Integral Formulations via Reynolds Transport Theorem (RTT)
control volume
7.1: Heat transfer and Engine energy balance
convective heat transfer
7: Engine Heat Transfer
convective heat transfer coefficient
7.2: Convective heat transfer
convective models
7.3: Radiative Heat Transfer
converging duct
2.1: Subsonic, sonic and supersonic flow
coolant temperature
7.4: Problems and References
crankshaft speed
3.2: Volumetric Efficiency

D

density
6.1: Thermodynamic and Chemical Evolution of Working Fluids
density ratio
1.3: Isentropic Relations
design analysis
4: Aircraft Engine- Gas Turbine Engine
Design_and_Analysis
5.1: Axial-Flow Turbomachinery
diesel engine correlations
7.2: Convective heat transfer
diesel engines
7.3: Radiative Heat Transfer
diffuser
4.1: Gas Generator Components
diverging duct
2.1: Subsonic, sonic and supersonic flow

E

efficiency
4.4: Turbofan Engine
4.5: Turboprop Engine
electricity generation
4.0: Introduction
energy
1.2: Thermodynamic Entropy Relations (Tds Equations)
energy balance
2.2: Rayleigh flow
energy loss
7.4: Problems and References
engine
4.4: Turbofan Engine
4.6: Problems and References
5.0: Introduction
6.0: Working Fluid Dynamics
6.2: Thermodynamics Relations for Engine Process
7.3: Radiative Heat Transfer
engine cycle
7.2: Convective heat transfer
engine design
4.2: On/Off Design Analysis
engine displacement
7.4: Problems and References
engine energy balance
7: Engine Heat Transfer

engine geometry
7.1: Heat transfer and Engine energy balance

engine knock
7.0: Introduction

engine performance
1.5: Compressible Flow Relationships
3.1: Aircraft Piston Engine
3.3: Problems and References
7.0: Introduction
7.3: Radiative Heat Transfer

engine throttling
6.3: Problems and References

engineering
1: Introduction to Compressible Flow

EngineProcess
6: Combustor- Working Fluid and Models of Engine Cycles

enthalpy
1.2: Thermodynamic Entropy Relations (Tds Equations)
6.1: Thermodynamic and Chemical Evolution of Working Fluids

entropy
1: Introduction to Compressible Flow
1.2: Thermodynamic Entropy Relations (Tds Equations)
1.3: Isentropic Relations

entropy variation
2.2: Rayleigh flow

Eulerian viewpoint
1.4: Integral Formulations via Reynolds Transport Theorem (RTT)

exhaust heat transfer
7.2: Convective heat transfer

exhaust system
3.2: Volumetric Efficiency

exit velocity
1.6: Problems and References

F

fan_pressure_ratio
5.4: Problems and References

first law
1.2: Thermodynamic Entropy Relations (Tds Equations)
7.1: Heat transfer and Engine energy balance

First Law of Thermodynamics
1.4: Integral Formulations via Reynolds Transport Theorem (RTT)

flight conditions
4.2: On/Off Design Analysis

flight Mach number
4.3: Turbojet

flow process
1.3: Isentropic Relations

flow relationships
1: Introduction to Compressible Flow

fluid dynamics
1.4: Integral Formulations via Reynolds Transport Theorem (RTT)
1.5: Compressible Flow Relationships

fluid flow
5.2: Radial / Centrifugal Turbomachinery

fluid mechanics
1: Introduction to Compressible Flow
1.0: Fundamentals of Compressible Flow
1.4: Integral Formulations via Reynolds Transport Theorem (RTT)

Fluid_dynamics
5.1: Axial-Flow Turbomachinery

friction regimes
7.4: Problems and References

fuel air ratio
6.3: Problems and References

fuel combustion
6.3: Problems and References

fuel consumption
3.3: Problems and References
4.2: On/Off Design Analysis

fuel efficiency
4.6: Problems and References
6.2: Thermodynamics Relations for Engine Process

fuel energy
7.0: Introduction

fuel energy input
7.1: Heat transfer and Engine energy balance

fuel injection
6.0: Working Fluid Dynamics

fuel mass flow rate
1.6: Problems and References

G

gas constant
1.1: Ideal Gas Relations

gas dynamics
2.3: Problems and References

gas equation
1.1: Ideal Gas Relations

gas exchange
6.2: Thermodynamics Relations for Engine Process

gas generator
4: Aircraft Engine- Gas Turbine Engine

gas laws
1.2: Thermodynamic Entropy Relations (Tds Equations)

gas properties
7.2: Convective heat transfer

gas turbine
5.0: Introduction
5.2: Radial / Centrifugal Turbomachinery
6.0: Working Fluid Dynamics

gas turbine engine
4.0: Introduction

gas turbine engines
3.0: Introduction
4.1: Gas Generator Components

general aviation
3.0: Introduction
3.3: Problems and References

H

heat flux
7.4: Problems and References

heat transfer
2.2: Rayleigh flow
2.3: Problems and References
6.1: Thermodynamic and Chemical Evolution of Working Fluids
6.2: Thermodynamics Relations for Engine Process
7: Engine Heat Transfer
7.0: Introduction
7.1: Heat transfer and Engine energy balance
7.3: Radiative Heat Transfer

heat transfer coefficient
7.4: Problems and References

Heinkel He 178
5.0: Introduction

I

ideal gas
1: Introduction to Compressible Flow
1.1: Ideal Gas Relations
6.1: Thermodynamic and Chemical Evolution of Working Fluids

ideal gas behavior
1.0: Fundamentals of Compressible Flow

ideal gas law
2.2: Rayleigh flow

indicated fuel conversion efficiency
6.3: Problems and References

induction system
3.2: Volumetric Efficiency

instantaneous heat flux
7.2: Convective heat transfer

intake rate
3.2: Volumetric Efficiency

integration
5.0: Introduction

internal combustion
3.1: Aircraft Piston Engine
6.0: Working Fluid Dynamics

internal combustion engine
3.2: Volumetric Efficiency
4.0: Introduction
7.0: Introduction

internal energy
1.1: Ideal Gas Relations
6.1: Thermodynamic and Chemical Evolution of Working Fluids

Introduction
5: Compressor and Turbines

isentropic
1.3: Isentropic Relations

isentropic relations
1: Introduction to Compressible Flow

isentropic_efficiency
5.4: Problems and References

J

jet engine combustion
2.0: Introduction

L

Lagrangian viewpoint
1.4: Integral Formulations via Reynolds Transport Theorem (RTT)

linear momentum
1.4: Integral Formulations via Reynolds Transport Theorem (RTT)

M

Mach number
- 1.0: Fundamentals of Compressible Flow
- 1.5: Compressible Flow Relationships
- 2.1: Subsonic, sonic and supersonic flow
- 2.2: Rayleigh flow
- 2.3: Problems and References
- 4.2: On/Off Design Analysis

mass conservation
- 1.4: Integral Formulations via Reynolds Transport Theorem (RTT)
- 1.6: Problems and References
- 6.1: Thermodynamic and Chemical Evolution of Working Fluids

mass density
- 1.0: Fundamentals of Compressible Flow

mass flow applications
- 5.2: Radial / Centrifugal Turbomachinery

mass flow parameter
- 1.5: Compressible Flow Relationships

mass flow rate
- 2.1: Subsonic, sonic and supersonic flow
- 3.2: Volumetric Efficiency

mass_flow_rate
- 5.1: Axial-Flow Turbomachinery
- 5.4: Problems and References

mean effective pressure
- 6.2: Thermodynamics Relations for Engine Process

mechanical efficiency
- 3.3: Problems and References

mechanical friction
- 7.1: Heat transfer and Engine energy balance

mechanics
- 4.6: Problems and References

military aircraft
- 3.0: Introduction

molecular weight
- 1.1: Ideal Gas Relations

moles
- 1.1: Ideal Gas Relations

momentum theory
- 4.5: Turboprop Engine

N

Newton's Second Law
- 1.4: Integral Formulations via Reynolds Transport Theorem (RTT)

nozzle
- 2.1: Subsonic, sonic and supersonic flow

nozzle design
- 1.6: Problems and References

Nusselt number
- 7.2: Convective heat transfer

O

Otto cycle
- 6.0: Working Fluid Dynamics

P

perfect gas
- 2.2: Rayleigh flow

performance
- 4.6: Problems and References

performance characteristics
- 6.3: Problems and References

performance efficiency
- 5.2: Radial / Centrifugal Turbomachinery

performance evaluation
- 4.2: On/Off Design Analysis

physics
- 1: Introduction to Compressible Flow

piston engine
- 3.3: Problems and References
- 6.0: Working Fluid Dynamics

piston engines
- 3.0: Introduction
- 3.1: Aircraft Piston Engine

power balance
- 4.4: Turbofan Engine

power turbine
- 4.5: Turboprop Engine

Power_equation
- 5.1: Axial-Flow Turbomachinery

Prandtl number
- 7.2: Convective heat transfer

pressure
- 1.2: Thermodynamic Entropy Relations (Tds Equations)

pressure disturbances
- 2.1: Subsonic, sonic and supersonic flow

pressure drop
- 2.0: Introduction

pressure ratio
- 1.3: Isentropic Relations
- 4.4: Turbofan Engine
- 5.2: Radial / Centrifugal Turbomachinery

pressure uniformity
- 6.1: Thermodynamic and Chemical Evolution of Working Fluids

problems
- 4: Aircraft Engine- Gas Turbine Engine
- 5: Compressor and Turbines
- 7: Engine Heat Transfer

ProblemsReferences
- 6: Combustor- Working Fluid and Models of Engine Cycles

propeller performance
- 4.5: Turboprop Engine

propulsion
- 4.6: Problems and References

propulsion systems
- 1.5: Compressible Flow Relationships

propulsive efficiency
- 4.3: Turbojet

R

radial turbines
- 5.2: Radial / Centrifugal Turbomachinery

Radial Turbomachinery
- 5: Compressor and Turbines

radiant flux
- 7.3: Radiative Heat Transfer

radiative heat transfer
- 7: Engine Heat Transfer

Rayleigh flow
- 2.0: Introduction
- 2.2: Rayleigh flow
- 2.3: Problems and References

references
- 4: Aircraft Engine- Gas Turbine Engine
- 5: Compressor and Turbines
- 7: Engine Heat Transfer

reversible process
- 1.2: Thermodynamic Entropy Relations (Tds Equations)

Reynolds number
- 7.2: Convective heat transfer

Reynolds Transport Theorem
- 1: Introduction to Compressible Flow
- 1.4: Integral Formulations via Reynolds Transport Theorem (RTT)

rocket combustion
- 1.6: Problems and References

rotary machinery
- 5.2: Radial / Centrifugal Turbomachinery

rotational_speed
- 5.4: Problems and References

S

shaft power
- 4.5: Turboprop Engine

shock waves
- 4.1: Gas Generator Components

SI engines
- 7.3: Radiative Heat Transfer
- 7.4: Problems and References

sonic flow
- 2.1: Subsonic, sonic and supersonic flow

spark ignition
- 3.1: Aircraft Piston Engine

spark ignition engine
- 6.3: Problems and References

specific fuel consumption
- 4.4: Turbofan Engine

specific heat
- 1.3: Isentropic Relations

specific heat input
- 2.3: Problems and References

specific heat ratio
- 1.5: Compressible Flow Relationships
- 2.3: Problems and References

specific thrust
- 4.3: Turbojet
- 4.4: Turbofan Engine

specific volume
- 1.1: Ideal Gas Relations
- 6.1: Thermodynamic and Chemical Evolution of Working Fluids

Specific_Work
- 5.1: Axial-Flow Turbomachinery

speed of sound
- 1.0: Fundamentals of Compressible Flow

speed_of_sound
- 5.4: Problems and References

stagnation temperature
- 1.5: Compressible Flow Relationships

stagnation_pressure_ratio
- 5.4: Problems and References

state relations
- 1.3: Isentropic Relations

static bench testing
- 1.6: Problems and References

static_temperature
- 5.4: Problems and References

steady state
- 1.0: Fundamentals of Compressible Flow

subsonic compressors
- 4.1: Gas Generator Components

subsonic flow
2.1: Subsonic, sonic and supersonic flow
supersonic aircraft engines
2.0: Introduction
supersonic flow
2.1: Subsonic, sonic and supersonic flow
2.3: Problems and References
swirl ratio
7.4: Problems and References

T

temperature
1.2: Thermodynamic Entropy Relations (Tds Equations)
temperature ratio
1.3: Isentropic Relations
temperature rise
2.0: Introduction
thermal choking
2.2: Rayleigh flow
2.3: Problems and References
thermal efficiency
3.3: Problems and References
4.3: Turbojet
4.4: Turbofan Engine
6.0: Working Fluid Dynamics
6.2: Thermodynamics Relations for Engine Process
6.3: Problems and References
thermal radiation
7.3: Radiative Heat Transfer
thermodynamic cycle
4.0: Introduction
thermodynamic efficiency
7.0: Introduction
thermodynamic state relations
1.0: Fundamentals of Compressible Flow
ThermodynamicChemicalEvolution
6: Combustor- Working Fluid and Models of Engine Cycles
thermodynamics
1: Introduction to Compressible Flow
1.1: Ideal Gas Relations
1.2: Thermodynamic Entropy Relations (Tds Equations)
1.3: Isentropic Relations
1.5: Compressible Flow Relationships
4.6: Problems and References
6.0: Working Fluid Dynamics
6.1: Thermodynamic and Chemical Evolution of Working Fluids
6.2: Thermodynamics Relations for Engine Process
7.1: Heat transfer and Engine energy balance
ThermodynamicsRelations
6: Combustor- Working Fluid and Models of Engine Cycles
thrust
4.4: Turbofan Engine
4.6: Problems and References
thrust analysis
4.2: On/Off Design Analysis
thrust calculation
1.6: Problems and References
thrust power
4.3: Turbojet
4.5: Turboprop Engine
thrust specific fuel consumption
4.3: Turbojet
Torque
5.1: Axial-Flow Turbomachinery
total pressure
1.5: Compressible Flow Relationships
total pressure recovery
4.1: Gas Generator Components
turbine
5.0: Introduction
turbine blades
4.0: Introduction
Turbines
5.1: Axial-Flow Turbomachinery
turbochargers
5.2: Radial / Centrifugal Turbomachinery
turbofan
3.0: Introduction
4.0: Introduction
4.4: Turbofan Engine
turbofan engine
4: Aircraft Engine- Gas Turbine Engine
turbojet
3.0: Introduction
4: Aircraft Engine- Gas Turbine Engine
4.0: Introduction
4.3: Turbojet
4.6: Problems and References
5.0: Introduction
turbojet engine
1.6: Problems and References
4.2: On/Off Design Analysis
turbomachinery
5.0: Introduction
turboprop
3.0: Introduction
4.5: Turboprop Engine
4.6: Problems and References
turboprop engine
4: Aircraft Engine- Gas Turbine Engine
turboshaft
3.0: Introduction
turbulent flow
7.2: Convective heat transfer

U

uniform viscosity
1.0: Fundamentals of Compressible Flow

V

V8 engine
7.4: Problems and References
valve timing
3.2: Volumetric Efficiency
variable geometry
4.2: On/Off Design Analysis
volume
1.2: Thermodynamic Entropy Relations (Tds Equations)
volumetric efficiency
3.2: Volumetric Efficiency
7.4: Problems and References

W

wall heat loss
7.0: Introduction
work done
6.2: Thermodynamics Relations for Engine Process
WorkingFluidDynamics
6: Combustor- Working Fluid and Models of Engine Cycles

This page titled Index is shared under a CC BY 4.0 license and was authored, remixed, and/or curated by Haifa El-Sadi.

GLOSSARY

S

Sample Word 1 | Sample Definition 1

This page titled Glossary is shared under a CC BY 4.0 license and was authored, remixed, and/or curated by Haifa El-Sadi.

DETAILED LICENSING

Overview

Title: Aircraft Engine: Design and Analysis

Webpages: 52

All licenses found:

- CC BY 4.0: 100% (52 pages)

By Page

- Aircraft Engine: Design and Analysis - *CC BY 4.0*
  - Front Matter - *CC BY 4.0*
    - TitlePage - *CC BY 4.0*
    - InfoPage - *CC BY 4.0*
    - Table of Contents - *CC BY 4.0*
    - Licensing - *CC BY 4.0*
  - 1: Introduction to Compressible Flow - *CC BY 4.0*
    - 1.0: Fundamentals of Compressible Flow - *CC BY 4.0*
    - 1.1: Ideal Gas Relations - *CC BY 4.0*
    - 1.2: Thermodynamic Entropy Relations (Tds Equations) - *CC BY 4.0*
    - 1.3: Isentropic Relations - *CC BY 4.0*
    - 1.4: Integral Formulations via Reynolds Transport Theorem (RTT) - *CC BY 4.0*
    - 1.5: Compressible Flow Relationships - *CC BY 4.0*
    - 1.6: Problems and References - *CC BY 4.0*
  - 2: Compressible Flow With Heat Addition - *CC BY 4.0*
    - 2.0: Introduction - *CC BY 4.0*
    - 2.1: Subsonic, sonic and supersonic flow - *CC BY 4.0*
    - 2.2: Rayleigh flow - *CC BY 4.0*
    - 2.3: Problems and References - *CC BY 4.0*
  - 3: Aircraft Engines- Reciprocating Engine - *CC BY 4.0*
    - 3.0: Introduction - *CC BY 4.0*
    - 3.1: Aircraft Piston Engine - *CC BY 4.0*
    - 3.2: Volumetric Efficiency - *CC BY 4.0*
    - 3.3: Problems and References - *CC BY 4.0*
  - 4: Aircraft Engine- Gas Turbine Engine - *CC BY 4.0*
    - 4.0: Introduction - *CC BY 4.0*
    - 4.1: Gas Generator Components - *CC BY 4.0*
    - 4.2: On/Off Design Analysis - *CC BY 4.0*
    - 4.3: Turbojet - *CC BY 4.0*
    - 4.4: Turbofan Engine - *CC BY 4.0*
    - 4.5: Turboprop Engine - *CC BY 4.0*
    - 4.6: Problems and References - *CC BY 4.0*
  - 5: Compressor and Turbines - *CC BY 4.0*
    - 5.0: Introduction - *CC BY 4.0*
    - 5.1: Axial-Flow Turbomachinery - *CC BY 4.0*
    - 5.2: Radial / Centrifugal Turbomachinery - *CC BY 4.0*
    - 5.4: Problems and References - *CC BY 4.0*
  - 6: Combustor- Working Fluid and Models of Engine Cycles - *CC BY 4.0*
    - 6.0: Working Fluid Dynamics - *CC BY 4.0*
    - 6.1: Thermodynamic and Chemical Evolution of Working Fluids - *CC BY 4.0*
    - 6.2: Thermodynamics Relations for Engine Process - *CC BY 4.0*
    - 6.3: Problems and References - *CC BY 4.0*
  - 7: Engine Heat Transfer - *CC BY 4.0*
    - 7.0: Introduction - *CC BY 4.0*
    - 7.1: Heat transfer and Engine energy balance - *CC BY 4.0*
    - 7.2: Convective heat transfer - *CC BY 4.0*
    - 7.3: Radiative Heat Transfer - *CC BY 4.0*
    - 7.4: Problems and References - *CC BY 4.0*
  - Back Matter - *CC BY 4.0*
    - Index - *CC BY 4.0*
    - Glossary - *CC BY 4.0*
    - Detailed Licensing - *CC BY 4.0*

This page titled Aircraft Engine: Design and Analysis is shared under a CC BY 4.0 license and was authored, remixed, and/or curated by Haifa El-Sadi.